

LASER-INDUCED BREAKDOWN SPECTROSCOPY FOR THE DETERMINATION OF
CARBON IN SOIL

By

LYDIA EDWARDS

A DISSERTATION PRESENTED TO THE GRADUATE SCHOOL
OF THE UNIVERSITY OF FLORIDA IN PARTIAL FULFILLMENT
OF THE REQUIREMENTS FOR THE DEGREE OF
DOCTOR OF PHILOSOPHY

UNIVERSITY OF FLORIDA

2007

© 2007 Lydia Edwards

Dedicated to my Mum and my husband, Daniel

ACKNOWLEDGMENTS

I extend my deepest gratitude to my advisor, Dr. James D. Winefordner for his unwavering support and guidance during my four years in his research group. His knowledge and patience are legendary and have contributed to a research environment that fosters cooperation and mutual respect. I am incredibly proud to have been a member of his group, and even more honored to have been one of his last students before his retirement. I have great appreciation for Dr. Nicolo Omenetto and Dr. Ben Smith, who have nurtured my interest in applications of spectroscopy and provided countless insightful observations about this research. I also extend a special thank you to Dr. Igor Gornushkin, who was so patient with me and wrote data analysis programs that saved me from weeks, if not months, of incredibly tedious and repetitive data processing. Additionally I thank Dr. Andy Freedman and Dr. Joda Wormhoudt of Aerodyne Research, Inc, who initially proposed and provided funding for this research.

I thank all the past and present members of the Winefordner/Omenetto/Smith research group, who have become like a second family to me over the years. I have learned so much from each of them beyond chemistry and know that life-long friendships have been developed. I directly thank Mariela Rodriguez for understanding the frustrations involved in LIBS applications and for her many illuminating ideas, and also Benoit Lauly for his elucidation of plasma fundamentals. Past group members whom I acknowledge for significantly influencing my research include Dr. Galan Moore and Dr. Kirby Amponsah-Manager. No list of acknowledgements would be complete without thanking Jeanne Karably and Lori Clark for keeping the often forgotten paper-work in line.

I cannot begin to express that gratitude I owe to my family for their love and support during my time in both undergraduate and graduate school. I owe so much to my Mum, Kay, who is my inspiration and never lets me forget that anything can be accomplished. I especially

thank my step-father, Keith, my grandparents, Roy and Jean, and my brothers and sisters, Elliot, Yvonne and Daryll who are my motivation.

Finally, I would like to acknowledge my husband, Daniel, without whom none of this would be possible. Because of his love and support, seven years ago I took a chance and stayed in America while my family moved to England, and I'd like to think that none of this would have been possible if not for that.

TABLE OF CONTENTS

	<u>page</u>
ACKNOWLEDGMENTS	4
LIST OF TABLES	8
LIST OF FIGURES	9
ABSTRACT	13
CHAPTER	
1. INTRODUCTION TO LASER-INDUCED BREAKDOWN SPECTROSCOPY	15
Introduction.....	15
Characteristics of LIBS.....	16
Instrumentation	18
Laser	18
Spectral Resolution.....	19
Detectors.....	20
Advantages of LIBS	21
Sample Preparation.....	21
Micro-destructive Nature.....	22
Portable and Stand-off LIBS	22
Rapid Analysis.....	23
Challenges to LIBS.....	23
Precision	24
Matrix Effects.....	24
Applications of LIBS for Soil Analysis.....	26
Scope of Research.....	33
2. CARBON IN SOIL.....	39
Sequestration of Carbon in Soil.....	39
Current Methods for the Determination of Carbon in Soil.....	42
The Challenges of Soil Analysis.....	44
3. INSTRUMENTATION AND DATA ANALYSIS.....	52
Instrumental Components.....	52
Laser	52
Optics.....	53
Fiber Optics	53
Spectrometer.....	53
Software.....	54
Optimizing Instrumental Parameters.....	55

Laser Energy.....	55
Optimization of the Q-Switch Delay.....	56
Optimization of Fiber Probe Position.....	57
Optimization of Lens-to-Sample Distance.....	59
Data Analysis.....	60
4. SAMPLE PRESENTATION AND SAMPLING CHARACTERISTICS	72
Sample Presentation.....	72
Pressed Pellets vs. Mounting Tape.....	72
Analysis of Bare Mounting Tape	75
Grain Size.....	76
Sampling Characteristics	80
Number of Laser Shots.....	80
Repetitive Laser Shots.....	81
Conclusion.....	84
5. THE SPECTROSCOPY OF CARBON AND CALIBRATION CURVES WITH SIMULATED SOILS	99
The Spectroscopy of Carbon	99
Choice of Analytical Line	99
Curves of Growth	101
Experimental Calibration Curves	102
Silica and Aluminum Silicate Artificial Soils	102
Analysis of Powdered Soil Samples.....	103
6. LIBS MEASUREMENTS OF NATURAL SOILS: IS QUANTIFICATION POSSIBLE?.....	114
Introduction.....	114
CHN Analysis.....	114
LIBS Measurements of Natural Soils.....	115
High-Resolution LIBS Measurements of Soils	118
7. CONCLUSION AND FUTURE WORK.....	130
LIST OF REFERENCES.....	135
BIOGRAPHICAL SKETCH	140

LIST OF TABLES

<u>Table</u>		<u>page</u>
2-1	Techniques for measuring CO ₂ in combination with dry combustion or wet oxidation. Reproduced from ref. 72.....	49
2-2	The three major groups of soil size fractions are sand, silt and clay. These can be further subdivided into finer size fractions.....	50
3-1	Specifications for the Big Sky Ultra Nd:YAG pulsed laser.....	61
3-2	Mean pulse energies of the Big Sky laser measured with a power meter.....	66
4-1	Statistics for the analysis of quartz size fractions spiked with graphite.....	92
4-2	C247 statistics for intra-sample and inter-sample measurements.....	95
5-1	Carbon content of soil samples determined by CHN analysis.....	111
5-2	Predicted carbon content of soils using the applicable silica or aluminum silicate calibration curve.....	113
6-1	Results of dry combustion CHN analysis performed on a suite of natural soil samples.....	122

LIST OF FIGURES

<u>Figure</u>	<u>page</u>
1-1 Number of LIBS publications since 1960.....	35
1-2 Significant events during plasma formation.....	36
1-3 Temporal evolution of the LIBS plasma.....	37
1-4 Typical schematic of a LIBS set-up.....	38
2-1 Magnitudes of the reservoirs of actively cycling carbon in gigatons (Gt).	47
2-2 Carbon cycle.	48
2-3 Constituents of humus, the major contribution to soil organic carbon.....	51
3-1 Configuration of LIBS instrumentation.....	62
3-2 Ablation area produced on copper foil by a 50 mJ laser pulse and a 2.5 inch focal length lens.....	63
3-3 A soil spectrum that clearly shows the discontinuities between different spectrometer channels in the LIBS2000+ unit.	64
3-4 Arrangement of the individual fiber apertures in the fiber optic probe	65
3-5 Controlling the CCD emission acquisition delay time by manipulating the laser Q-switch.....	67
3-6 Results of changing the spectrometer delay times on soil spectra.....	68
3-7 Graphite pellet spectra	69
3-8 C247 signal intensity (the average of 10 shots) as a function of focal point offset.....	70
3-9 Calculation of intensity (I), background (B) and area (above the red line).....	71
4-1 An image of a pressed pellet and soil mounted on a microscope slide.....	86
4-2 C247 signal as a function of shot number on the same pellet spot for five different locations.....	87
4-3 Analysis of bare mounting tape.....	88
4-4 Microscope images (4X magnification) of the craters produced after the indicated shot number.....	89

4-5	Images of different quartz size fractions spiked with graphite (4X magnification).	90
4-6	C247 peak area as a function of carbon concentration (wt %) for different particle sizes of quartz matrix.	91
4-7	Microscope images of three soils to illustrate heterogeneity.	93
4-8	RSD of the C247 signal intensity as a function of the number of shots on separate spots.	94
4-9	C247 and Ca422 signal intensities as a function of shot number on the same spot.	96
4-10	Microscope images of soil after the indicated number of laser shots (4X magnification).	97
4-11	Proposed mechanism for the second shot signal enhancement on soil.	98
5-1	Full spectrum of carbon taken on a graphite pellet with prominent lines and bands identified.	106
5-2	C247 peak area as a function of spectrometer delay time. The integration time is fixed at 200 ns.	107
5-3	The CN molecule, with a band head at 388 nm, is barely detected in a soil sample.	108
5-4	Theoretical curves of growth for carbon in a silicon dioxide matrix at three different plasma temperatures.	109
5-5	Calibration curves produced from graphite in	110
5-6	Results of LIBS measurements on finely ground soil samples.	112
6-1	Microscope images of natural soil samples (3.5X magnified).	121
6-2	A histogram of the RSD's from LIBS C247 measurements on natural soils using the first shot and the second shot.	124
6-3	LIBS C247 peak area as a function of % carbon.	123
6-4	Normalizing the C247 peak area by soil surface density increases the correlation between LIBS signal and carbon concentration.	125
6-5	Extent of the iron spectral interference.	126
6-6	A soil spectrum produced using the Acton SpectraPro showing the resolved carbon and iron lines.	127
6-7	LIBS C247 peak area as a function of carbon concentration for measurements produced using a high resolution spectrometer.	128

6-8 A plot of the C247 peak area normalized by surface density vs. carbon content for measurements produced using a high resolution spectrometer.....129

LIST OF ABBREVIATIONS

AAS	Atomic absorption spectrometry
AES	Atomic emission spectrometry
CCD	Charge coupled device
COG	Curve of growth
FTSD	Fiber-to-sample distance
FWHM	Full-width at half-maximum
ICCD	Intensified charge coupled device
ICP	Inductively coupled plasma
LIBS	Laser-induced breakdown spectroscopy
LIF	Laser-induced fluorescence
LTE	Local thermal equilibrium
LTSD	Lens-to-sample distance
Nd:YAG	Neodymium doped yttrium-aluminum-garnet
OES	Optical emission spectroscopy
PSI	Pounds-per-square inch
RSD	Relative standard deviation
S/B	Signal-to-background ratio
SOM	Soil organic matter

Abstract of Dissertation Presented to the Graduate School
of the University of Florida in Partial Fulfillment of the
Requirements for the Degree of Doctor of Philosophy

LASER-INDUCED BREAKDOWN SPECTROSCOPY FOR THE DETERMINATION OF
CARBON IN SOIL

By

Lydia Edwards

December 2007

Chair: James D. Winefordner

Major: Chemistry

Laser-induced breakdown spectroscopy (LIBS) is a relatively young atomic emission technique that has found great utility in the elemental analyses of a variety of materials. In brief, LIBS is achieved by focusing a high-powered, short-pulse laser onto a sample surface to produce plasma that is rich in electrons, atoms and ions. The atoms and ions in the plasma emit radiation that is characteristic of the elemental composition of the sample. While LIBS has been extensively applied to soil analysis, its use as a means of determining carbon in soil has been lacking, limited to a few proof-of-principle demonstrations by research groups at Los Alamos and Oak Ridge National Laboratories. Since the sequestration of carbon in soil may offer a means of mitigating the effects of global warming, it is becoming increasingly urgent to develop a practical device that can accurately measure terrestrial carbon inventories in order to understand the status of the global carbon cycle. Due to the unique advantages of LIBS, including the potential for *in-situ* analysis, little-to-no sample preparation, simultaneous multi-element detection and relatively simple instrumentation, the technique has the potential to fulfill the requirements of an in-field carbon monitor. Before a field-based LIBS instrument can be designed there must be a laboratory-based demonstration of the capability to determine carbon in soil.

The purpose of our research was to investigate the potential of LIBS for carbon in soil determination with an emphasis on minimal sample preparation and the potential for *in-situ* analysis. While the quantification of carbon in soil by LIBS was not achieved in this study, an optimal soil sampling regime was established that increased sensitivity and measurement precision. The LIBS instrumentation was optimized specifically for soil samples, including the laser energy, optical configuration and spectrometer delay time. The sample presentation was extensively studied, including the effect of soil grain size on LIBS signal and the advantages of mounting the sample on tape as a thin monolayer rather than as a pressed pellet.

CHAPTER 1
INTRODUCTION TO LASER-INDUCED BREAKDOWN SPECTROSCOPY

Introduction

Laser-induced breakdown spectroscopy (LIBS), sometimes referred to as laser-induced plasma spectroscopy (LIPS), is a relatively young atomic emission technique that has found great utility in the elemental analyses of a variety of materials. In brief, LIBS is achieved by focusing a high-powered, short-pulse laser onto a sample target to produce plasma that is rich in electrons, atoms and ions. The atoms and ions in the plasma emit radiation that is characteristic of the elemental composition of the sample. The development of the LIBS technique has mirrored that of the laser, beginning with its inception during the early 1960s. While first reported as a potential spectroscopic technique by Brech at the Xth Colloquium Spectroscopicum Internationale,¹ initially the LIBS plasma found greatest value as a micro-sampling source for an electrode-generated spark. Regardless, the first LIBS instrument was introduced in 1967, followed by the development of several commercial LIBS instruments by Jarrell-Ash Corporation and VEB Carl Zeiss.² Commercial success was elusive as the technique was largely overshadowed by the development of high-performance elemental analysis techniques such as inductively-coupled plasma spectroscopy (ICP) and conventional spark spectroscopy, which were superior to LIBS in both precision and accuracy. As a result, interest in LIBS was relegated to the physics of basic plasma formation and fundamental studies of breakdown in gases.

During the 1980s, as the laser and other spectroscopic components decreased in both size and cost, and the drive for more portable and versatile instruments increased, LIBS experienced a rebirth. The potential of LIBS as a more convenient atomic emission technique became apparent to both industrial and academic laboratories. Especially in the past decade, research in every

area of LIBS has seen remarkable progress, including plasma characterization, instrumentation, and applicability. Indeed, it is the broad range of the latter that is fueling the increased interest in LIBS, which has been successfully applied to an extraordinary variety of samples, from priceless works of art to sewage; from environmental aerosols to forensic analysis. The revival of LIBS is reflected by the numbers of published journal articles on the subject, which began to increase in the late 1980's and continues to do so each year thereafter, as illustrated in Figure 1-1.³

Today the potential of LIBS as a qualitative and potentially quantitative elemental analysis technique is well documented in virtually every scientific field. The unique advantages of LIBS that have contributed to widespread interest include remote sensing capabilities, in-situ analysis, little-to-no sample preparation, micro-destructive nature, applicability to all media, simultaneous multi-element detection capability and relatively simple instrumentation. While LIBS may currently be limited by its poor precision (typically 5-10%), higher detection limits (relative to conventional techniques), and difficulty in preparing matrix-matched standards, the preponderance of applications reported in the literature may indicate that the advantages overcome the limitations.

Characteristics of LIBS

The principles of laser ablation and plasma formation on a solid target have been extensively covered in previous literature.⁴⁻¹¹ As such, only a brief description of the mechanisms that contribute to atomic emission during the LIBS technique will be covered. LIBS is an atomic emission spectroscopic (AES) technique that shares similar fundamental principles to ICP-OES, microwave induced plasma (MIP-OES), direct current plasma (DCP-OES), flame-OES, arc-OES and spark-OES. All atomic emission techniques exhibit the following basic steps:

- atomization/vaporization of the sample to produce free atomic species consisting of atoms and ions,
- excitation of these atoms,
- detection of the radiation emitted by these atomic species,
- calibration of the intensity to concentration or mass relationship,
- determination of concentration, masses, or other information.⁴

In LIBS, the first step, atomization and vaporization of the sample, as well as the second step, atomic excitation are both achieved by focusing a short-pulsed laser of adequate power density onto the surface of a sample. Laser pulses of 5-10 ns are most commonly employed. Increasing research is being performed on LIBS achieved with picosecond or femtosecond lasers.¹¹⁻¹⁵ Once the laser pulse strikes the target, single- or multi-photon absorption, dielectric breakdown and other, often undefined mechanisms contribute to the surface temperature instantly increasing beyond the vaporization temperature of the material. The subsequent dissipation of energy through vaporization is slow relative to the rate of energy deposition from the laser pulse. This results in vaporization of the surface layer and causes the underlying material to reach critical temperature and pressure, finally causing the surface to explode. Particles, free electrons and highly ionized atoms are released into the surrounding atmosphere and begin to expand at a velocity much faster than the speed of sound, forming a shockwave in the process. If the laser pulse is of long enough duration, as is the case for nanosecond lasers, the expanding plume and the material within will continue to absorb energy from the laser and intense plasma up to a few millimeters in height is visually observed. After several microseconds, collisions with ambient gas species cause the plasma plume expansion to slow down while the shockwave detaches from the plasma front and continues propagating at a rate of approximately 10^5 m/s. As the plasma begins to decay through radiative, quenching, and electron-ion recombination processes, high-density neutral species and clusters of dimers or trimers are formed via condensation and three-body collisions and with the thermal and

concentration diffusion of species into the ambient gas. This usually occurs within hundreds of microseconds after the plasma has been ignited.² The temperature of the plasma and the electron number densities are time dependant and range from 10^4 to 10^5 K and on the order of 10^{15} to 10^{19} cm^{-3} , respectively (Figure 1-2).¹⁶

The temporal properties of the LIBS plasma are reflected in the emission radiation. During the first 1 μs of the plasma, emission is dominated by broad background continuum emission that is caused by bremsstrahlung and recombination radiation resulting from the interaction between free electrons and ions as the plasma cools. While the atoms and ions in the plasma do emit their characteristic radiation during this interval, weaker lines can not be differentiated from the continuum. However, after approximately 1 μs , the continuum begins to subside while the atomic and ionic species in the plasma continue to emit. Consequently, collection of the plasma emission at time intervals after the decay of the background continuum results in superior signal-to-background (S/B) and narrower peaks (Figure 1-3).

Instrumentation

One of the greatest appeals of the LIBS technique is the simplicity of the instrumentation involved in the analysis. The most basic LIBS analysis requires a pulsed laser, focusing and collection optics, a spectral selection device and a detector. The nature of these components can vary greatly depending on the purpose of the analysis (Figure 1-4).

Laser

The choice of laser for LIBS is often dependant on the purpose of the analysis. Several considerations must be made regarding the laser parameters, including: (1) size and portability potential, (2) maximum pulse energy and repetition rate (3) power source and cooling components, (4) beam quality and stability and, (5) safety. Pulsed CO_2 lasers (with a wavelength of 10.6 μm) and excimer lasers (typical wavelengths of 193, 248, and 308 nm) have all been

successfully applied to LIBS.¹⁷ However, these types of lasers are limited by size, the need for specialized optics and safety concerns, and are therefore used almost exclusively in laboratory applications with no eye towards portability and in-field analysis. The primary advantages of LIBS dictate that the optimum laser should be smaller, robust and accessible to researchers in all scientific fields. The most common type of laser that fits these requirements is the solid-state, flash-lamp pumped, Q-switched Nd:YAG laser with a fundamental wavelength of 1064 nm and a pulse width range of 6-15 ns. The Nd:YAG laser is a compact, reliable laser that is produced in a variety of sizes, from a bench-top model for laboratory use to a hand-held instrument that has been successfully incorporated into a portable LIBS system.¹⁸ Output peak pulse energies can vary from a few μJ to 1 J and can be delivered at repetition rates exceeding 50 Hz. Nd:YAG lasers can also be easily frequency doubled, tripled and quadrupled to produce wavelengths of 532, 355 and 266 nm, further increasing the versatility of the laser.

Spectral Resolution

One of the most important components of the LIBS instrumental set-up is the spectral dispersing system. There are many different types of spectrometers available, ranging from inexpensive hand-help models with small spectral bandwidths and low resolution, to larger, more expensive echelle spectrographs which span 190 to 800nm and exhibit superior resolution. The type of spectrometer used is dictated by the nature of the analysis, however some basic considerations include: (1) adequate spectral resolution, (2) size and maintenance requirements, and (3) the spectral range. While higher resolution spectrometers offer obvious advantages, including fewer spectral interferences, they are overall more expensive, exhibit smaller spectral ranges and are less robust and portable. Size and maintenance requirements are obvious considerations when assessing the portability of the LIBS system, and in some cases it may be more beneficial to sacrifice some resolution in favor of a smaller, less expensive system which

can be incorporated into a robust, portable system. The spectral range of the spectrometer is another important factor, especially when multi-element analysis is to be performed. In general, the larger the spectral window, the more information can be retrieved from the sample.

Detectors

The type of detector that is used for LIBS is generally dependent upon the spectrometer. Photodiodes (PD) and photomultiplier tubes (PMT) are highly sensitive devices that produce an amplified electrical signal proportional to incident photons. While these types of detectors offer valuable advantages, such as sub-nanosecond resolution (useful for temporal-based plasma studies), each device can only monitor one wavelength at a time, precluding broad spectral bandwidths. A more common type of detector is one that involves placing many photosensitive elements in an array at the exit slit of the spectrometer. Such an assembly will respond to a much wider spectral range and therefore is more convenient for multi-element analysis. Examples include photodiode arrays (PDA), charge-injection devices (CID) and charge-coupled devices (CCD). One of the major limitations of these devices is that they must accumulate incident radiation for a period of time before the readout is processed, and when it is processed, each pixel is read sequentially, further increasing the response time. Such time-integration precludes detailed temporal studies of the plasma emission. In order to achieve time-resolved LIBS, a micro-channel plate (MCP) must be coupled to the detection system. The MCP regulates when the incident radiation is allowed to reach the detection device, and in doing so it also amplifies the light by converting it to electrons which are then reconverted back to light before detection. Combining an MCP with a time-integrating detector such as a CCD is referred to as an *intensified* charged-coupled device or (ICCD).¹⁹

Advantages of LIBS

No discussion about the characteristics of LIBS would be complete without a closer look at the advantages that have fueled increased interest in the technique. In terms of figures of merit such as precision and limits of detection (LOD), LIBS is mostly surpassed by more traditional techniques such as ICP-MS or ICP-OES. However, the unique advantages that LIBS offers are significant enough to render it a serious consideration in many analytical applications.

Sample Preparation

One of the most attractive features of LIBS is that the analysis can be performed without any sample preparation, in virtually any location. Unlike more conventional techniques such as ICP-OES, the sample does not need to be digested or converted to a solution. As such, the analysis time is drastically decreased and there is less potential for contamination. This is especially appealing for industrial applications of LIBS, which may require continuous sample analysis of raw materials. It also allows for the analysis of samples that cannot easily be digested for ICP analysis, such as extremely hard materials like ceramics and steels. The lack of sample preparation required for LIBS is also applicable to samples of all media. Indeed, one of the greatest benefits of the technique is that it can be performed on solids, liquids, gases and aerosols with minimal instrumental variation.

It is important to note that while LIBS can be performed on virtually any sample without preparation, in some cases this may not provide the best analytical results. For example, the element of interest may not be homogeneous throughout the raw sample. If the ultimate goal is to quantify this element then the best results (and increased precision) will be achieved once the sample has been homogenized, which may require more extensive preparation. In most cases, qualitative analysis can be performed on virtually any sample without any preparation.

However, quantitative analysis may require some minor preparation, dictated by the type of sample and the required degree of precision and accuracy.

Micro-destructive Nature

While LIBS can not truly be considered a non-destructive technique since some amount of sample is always permanently removed from the surface, it can be considered micro-destructive due to the microscopic craters that are achievable under the correct laser conditions. While this may not be so important for applications where there is an abundance of sample, it is imperative in applications where the sample is scarce or precious, or has aesthetic quality and can not appear damaged. Because of this advantage, LIBS has been extended to applications involving the pigment analysis or authentication of priceless works of art²⁰⁻²² and ancient artifacts.²³

Portable and Stand-off LIBS

Arguably one of the greatest advantages of LIBS, and possibly the reason why limitations such as poor precision and sensitivity are tolerated, is the ability to take the instrument out into the field with minimal instrumental modification. There is increased momentum in the world today to achieve analytical information about a variety of samples in a shorter time frame. In some cases, the time it takes to retrieve a sample, transport it back to the laboratory and analyze it may be too long in terms of preventing the threat the sample poses. In other cases, it may be necessary to analyze hundreds or thousands of samples to get accurate results, a monumental task if each sample is to be individually collected and sent back to the laboratory. The underlying factor is that it is simply more convenient to take the instrument to the sample rather than transport the sample to the instrument.

The relatively simple and versatile instrumentation that LIBS employs makes it an ideal portable system for field-work. Small, solid-state lasers are often used in portable LIBS systems with the laser head either mounted in a small probe or laser pulses delivered to the sample via

fiber-optics. Emission is collected using the same fiber-optic and delivered to a miniature spectrometer; data are collected and processed on a laptop computer. One common configuration of these components is to house the spectrometer, laser and battery power supplies in a back-pack and the fiber-optics delivery and collection system in a long probe, a system that is referred to as 'man-portable' LIBS.

LIBS can also be used for stand-off analysis, often referred to as remote sensing, whereby no component of the system is remotely close to the sample. This is especially important when interrogating samples that may be hazardous or are inaccessible (though they must be optically accessible). In order to achieve stand-off LIBS the laser pulse must be focused onto the desired sample surface using a long focal length optical system. Plasma emission is usually collected using the same optical system. Recent research has demonstrated successful detection and identification of organic materials from a distance of 30 m.²⁴

Rapid Analysis

The speed with which a LIBS analysis can be performed is attributed to both the lack of sample preparation that the technique requires and the very short lifetime of the plasma. Assuming a rapidly responding spectrometer and adequate spectral processing software, results can be obtained from a one shot analysis in less than one second. In practice however, especially in quantitative work, it is best to take data from many shots in order to increase precision. Still, depending on the laser repetition rate this can still be accomplished in a fraction of the time necessary to achieve the same results from more conventional analytical techniques.

Challenges to LIBS

As previously mentioned, regardless of the multiple benefits of LIBS, there are several limitations which may arise during specific applications. Often the effects of these limitations

can be reduced to acceptable levels. In other cases, the standards of analytical performance are lowered in favor of the versatility and applicability of the technique to a specific analysis.

Precision

It is generally accepted that the precision of LIBS is one of its greatest disadvantages. Common relative standard deviations (RSD) reported fall between 5-10%, though values can be significantly higher depending on the sample. There are many different factors that contribute to such poor precision, the most important of which is more a property of the sample than the technique itself. The lack of sample preparation, which makes LIBS so attractive, also means that sample remains in its raw state, which most often is completely non-uniform. This, combined with the very small mass of sample that is interrogated, ensures that the sampled mass may not be representative of the bulk sample, and subsequent laser shots on different areas may produce very different spectra. While increasing the number of laser shots may increase the precision, this is still limited by the inherent inhomogeneity of the sample. There are many other factors that will significantly affect the precision, including: choice of analytical emission line, emission signal temporal development, sample translation velocity, detector gate delay, background correction methods, perturbations of the plasma, changing lens-to-sample distance (LTSD), changing fiber-to-sample distance (FTSD), and laser-pulse shot-to-shot instability.²⁵ In many cases computing the ratio of the element of interest to another fixed-concentration element in the sample will alleviate the effect these parameters have on the precision.

Matrix Effects

Matrix effects are one of the greatest challenges to the LIBS analysis and represent a significant obstacle to quantitative analysis. The term 'matrix effect' refers to the physical properties and chemical composition of the sample that affect the element signal such that changes in concentration of one or more of the elements forming the matrix alter an element's

emission signal even though the element concentration remains constant. For example, the signal intensity for carbon in silica is very different from that of carbon in alumina, despite having the same carbon concentration. This is an example of a chemical matrix effect and is especially problematic for samples that appear the same (such as soils) but may exhibit small unknown variations in composition, such as iron or aluminum content. This makes it very difficult to produce a universal calibration curve that will encompass a broad range of soils. Some success in correcting matrix effects has been found by normalizing signal intensities to excitation temperatures and electron densities using the Saha-Boltzmann equilibrium relationships.²⁶

Physical matrix effects are also of concern in a LIBS analysis. Examples of physical matrix effects include differences in specific heat, latent heat of vaporization, thermal conductivity, and absorption between matrices. Each of these factors can affect the mass of sample ablated and therefore influence quantitative results. Compensation for these physical matrix effects can be achieved by producing a ratio between the element of interest and an internal standard, if it can be assumed that the relative ablated masses of both remain constant. Another method of compensation that has been reported involves acoustic monitoring of the spark sound.²⁷ An additional example of an important physical matrix effect is grain size, or particle size. It has been well documented that the LIBS signal is dependant on the particle size and arrangement (pressed pellet, free powder, etc.) of the sample.

Matrix effects are either the primary focus or at least an integral part of much of the current research concerning LIBS. While there is still much work to be done, great progress has been made in identifying the source of different matrix interferences and conceiving different ways to prevent or correct for them.

Applications of LIBS for Soil Analysis

A great deal of research has concentrated on applying LIBS to environmental analysis, with emphasis on detecting hazardous contaminants in a variety of media. LIBS has been applied to liquids (such as waste water, river and ocean samples),²⁸⁻³¹ ice,³³ aerosols (such as factory effluents),³³⁻³⁶ plants,³⁷⁻³⁹ bacteria,⁴⁰ paint,⁴¹⁻⁴² and slags (the residue formed by the smelting of metallic ores).⁴³ Much research has also been focused on LIBS of soils and sediments, especially for the detection of metals and quantification of toxic metals. This section will provide a review of some of the more pertinent research concerning LIBS of soils.

Early work with LIBS of soils focused primarily on determining toxic metals and studies evaluating the numerous matrix effects that soils present. Eppler *et al.*⁴⁴ were able to determine Ba and Pb in spiked soil samples with detection limits of 42 and 57 ppm respectively, well below the Los Alamos screening levels of 5400 and 400 ppm. The soil samples were significantly ground and homogenized before being pressed into pellets and therefore can not be considered 'natural' soil sample. Precision was improved to 4% by use of a cylindrical lens to focus the laser beam and produce larger ablation areas which decreased the effects of sample homogeneity. The effect of analyte speciation on the emission signal was also studied, and while it was determined that the origin of the analyte (for example, nitrate or oxide) affected the signal, this could not be correlated with any physical property of the originating compound. However, the absorptivity of the bulk matrix was also found to affect the emission signal and this was well correlated with increasing plasma electron density which caused significant changes in the concentrations of ionized species.

Barbini *et al.*⁴⁵ found that correcting integrated line intensities of Fe in soil by the plasma temperature substantially improved correlation between LIBS Fe concentration and ICP Fe concentration. Such a correction was achieved by constructing a Saha-Boltzmann plot to obtain

the plasma temperature, and applying this factor to the raw LIBS signal. The poor correlation of the uncorrected LIBS with ICP measurements is assumed to be a function of the matrix effects, which cause significant changes in the plasma temperature and thus the emission signal. The efficacy of using such a technique alone to correct for matrix effects is limited by the assumption of local thermal equilibrium (LTE).

Another matrix effect of great significance to LIBS analysis of natural soils is water content, which was studied by Bublitz *et al.*⁴⁶ They proposed the use of LIBS to monitor Ba ions that are added to soils as tracers in percolation studies. The influence of water content on the intensity of LIBS spectra was investigated using soil samples with 2.5% BaCl₂ added. It was found that with increasing water content to about 6% the relative intensity of the 455.4 nm Ba line increased rapidly, and decreased thereafter exponentially as water content increased. The reason for the initial increase in intensity with increased water content was explained by three different processes. First, the shockwave on the wet sample creates less dust, reducing scattering and absorption of the laser radiation and increasing laser energy that is coupled into the sample. Second, the Ba ions form complexes with aquatic colloids such as fulvic acid and clay minerals, which causes a decrease in breakdown threshold and increased emission.³⁰ Finally, the cohesion introduced by the water content may lead to a larger surface concentration in contrast to dry soil. However, for soil samples with water content greater than 6%, the emission intensity decreases due to plasma cooling by the water as a result of increasing collisions that dissipate the energy from the plasma plume. In addition to this, the exciting laser radiation is absorbed by the water decreasing the efficiency of plasma ignition.

Capitelli *et al.*⁴⁷ compared LIBS to ICP for the detection of heavy metals in a variety of standard reference soils which had been homogenized, dried and pressed into pellets. The

detection limits achieved with LIBS from relatively linear calibration curves were between 30-50 ppm for elements such as Cr, Cu, Ni, Pb, and Zn. These values fall well below the European Union (EU) limits in both sewage sludge and soils established by the European Commission in 1986. In comparison to ICP results, the RSDs for the LIBS measurements were all significantly higher, with the exception of Cr. In the extreme case of Ni the RSD for LIBS was 14.18% compared to a value of 0.79% for ICP. It was hypothesized variations in plasma temperature as well as other matrix effects contributed to this poorer precision relative to ICP results.

One method to circumvent troublesome matrix effects and decrease detection limits in soil is to couple LIBS with laser-induced fluorescence (LIF), first reported by Gornushkin *et al.*⁴⁸ Hilbk-Kortenbruck *et al.* extended this technique to atmospheric conditions for the determination of As, Cr, Cu, Ni, Pb, Zn, Cd and Tl in pressed soil pellets. The latter two elements were determined by LIF, which was accomplished by directing a laser pulse tuned to the wavelength of interest into the LIBS plasma plume to excite fluorescence. Because this laser must be tuned to a specific wavelength, LIF can only be used for the detection of one element, typically one that requires detection limits significantly below what LIBS can achieve.⁴⁹

Some of the more practical aspects of LIBS analysis of soils were reviewed by Wisburn *et al.*⁵⁰ A variety of different soils were dried and pressed into pellets for analysis with a Q-switched Nd:YAG laser. Emission collection was achieved with a fiber optic. One of their most significant findings was the production of a persistent aerosol above the sample surface at high laser repetition rates focused on the same sample spot. This aerosol was characterized as ablated residual material from prior laser pulses that had not relaxed back to the sample surface and was available in the plasma spot location for the next pulse. At lower aerosol concentrations, this will provide increased emission signal, however at higher concentrations, it will actually absorb

more of the incoming laser light, thus reducing the portion of the laser pulse that reaches the solid sample, effectively decreasing the signal. It was found that the optimal repetition rate varied as a function of the sample mean particle size and for a soil sample was 1 Hz.

The crater formed during laser interrogation of the sample spot with multiple pulses was also studied. It was found that there was a slight increase in the emission signal from the second laser pulse that could not be attributed to persistent aerosol due to the much lower repetition rate. Instead it was theorized that the sampling site was enriched with larger particles after the shockwave from the first laser pulse swept away the smaller particles. After the second laser pulse, a sharp decrease in signal was observed which was explained as a crater effect: the deeper the crater became the greater the plasma-to-fiber distance and enhanced shielding of the plasma by the crater walls from the fiber.

Another very important aspect of LIBS soil analysis that was investigated by Wisburn was the effect of soil grain size. The importance of this parameter on any analysis is rather dependent on the analyte of interest and how it is distributed in the sample, for instance if it is a surface contaminant or if it is bound within the particles. To investigate this, soil samples were separated into four different grain sizes by sieving (0.38-1 mm range). Each was contaminated with Cd, which adheres to the surface of the particles. Good linear correlation between signal intensity and Cd concentration for each grain size was found, as well as a decrease in slope as the particle size decreased. While these results are significant in that they show a great dependence of the LIBS signal on the particle size, two important factors must be considered for practical soil analysis. First, most raw soil samples are composed of a broad distribution of particle sizes that exceeds the range studied in this research. In addition to this, these results were based on the assumption of only surface contamination. For many different analytes of interest this is not the

case; rather they may be found tightly bound within the particle, a property that is not often known before the analysis.⁵⁰

The issue of soil grain size was also raised by Theriault *et al.*,⁵¹ who performed LIBS of soil with a cone penetrometer system which probes deep into the soil. They found that the detection limits of Pb, Cd, and Cr increased as the particle size was decreased to less than 106 μm . This variation was explained by considering the soil surface area over which the contaminant was spread. Because a fine-grained material has a larger total surface area per unit mass than a coarse-grained material, the total surface area over which equal contaminant concentrations by mass are dispersed is larger for the fine-grained material and smaller for the coarse grain material, resulting in a thicker surface layer of contamination on coarse-grain material. If the laser spot size is fixed and ablates the contamination on the surface of the grains, there is an overall larger volume of contaminant in the plasma for coarse-grained material, resulting in lower detection limits.

One of the most interesting applications of LIBS on soils has been for the purpose of space exploration. It has been proposed that stand-off LIBS can be used for the exploration of planetary surfaces that are not accessible for analysis by other techniques such as X-ray fluorescence and alpha-proton X-ray spectrometry (APXS), which both require close proximity to the sample, and in the case of APXS, exhibit very slow data acquisition. Because of the similarity between the geological properties of the Martian surface and some Earth soil samples, preliminary research regarding the feasibility of incorporating a LIBS system into a space mission have been conducted using soil samples. Knight *et al.*⁵² studied the effect of decreasing pressure on both the plasma formed on the soil and the emission intensities. It was determined that down to pressures of 1 torr there is an increase in plasma dimensions and emission signal.

At lower pressures, the plasma readily expands into the lower pressure regions increasing in volume relative to those formed in atmospheric pressures. The signal enhancement at lower pressures is the result of increased mass ablation due to decreased shielding of the sample surface from the laser pulse by the more diffuse plasma. It was also determined that pressures of less than 10 torr were required to detect O(II) in the soil due to the increased electron density which causes the ionic oxygen atom to convert to the neutral oxygen atom. Arp *et al.*⁵³ reported on LIBS of ice/soil mixtures which were synthetically produced to mimic the polar surfaces of Mars. They determined detection limits for elements in these mixtures (at a pressure of 7 torr), which were typically 10% soil, were not significantly changed from those obtained by analyzing dry soil.

The determination of carbon in soil is arguably one of the most pressing issues concerning soil analysis due to the current attention to global warming. However, very few papers have been published regarding the potential of LIBS to achieve quantitative data on carbon in soil. Ebinger *et al.* first reported on the analysis of carbon in dried soil samples from farms in Colorado and fields surrounding Los Alamos, New Mexico. Each sample was sieved to <2mm and placed in a quartz tube. A 50-mJ, 10 ns, Nd:YAG laser was focused into the quartz tube and the resulting emission collected via fiber optics and delivered to a 0.5-m spectrograph with an intensified photodiode array detector. Shot-to-shot variations were normalized by taking the ratio of the 247.8 nm C line to a Si line. Verification of the C content was achieved by dry combustion. The results showed good correlation between LIBS signal and the carbon concentration, with an R^2 value of 0.966. In turn, the resulting calibration curve predicted C concentration in other soil samples with an accuracy of 3-14%. The detection limit was reported as 300 ppm.^{54,55} This research certainly demonstrated the feasibility of LIBS as a method for

carbon determination; however, it did not take into account many other variables, including varying soil grain size, applicability of the calibration curve to a broad range of different soil samples, differing Si content, and Fe interference with the C247.8nm line.

Subsequent research by the same group investigated the use of the C193 nm line, which is not susceptible to interference from Fe as is the C247.8 nm line . In addition to this, standardization of the C signal was achieved by taking the ratio of said line to the sum of the Al199 nm and Si212 nm lines, $C/(Al+Si)$. The soils chosen were noted to have similar physical and chemical properties. The resulting C signal was well correlated with the C concentration determined by dry combustion ($R^2=0.95$) and exhibited great reproducibility over a 30 day period. It was acknowledged that the Al and Si content of different soil samples will vary as a function of the soil's mineralogy and texture, which would significantly limit the use of both Si and Al as internal standards. However, it was assumed the those properties were constant for soils as similar as the ones employed in this study.⁵⁶

Martin *et al.*⁵⁷ extended on the results of this previous research by determining carbon and nitrogen in a variety of different soils. A Q-switched Nd:YAG laser was used at 266 nm with typical pulse energies of 23 mJ/pulse. Emission collection was via a fiber optic bundle and detection was achieved with an ICCD. Because this study was only concerned with the soil organic matter (SOM), inorganic soil carbon was first removed by acid washing. Soil was then dried, ground and pressed into pellets. The C247.8 nm emission was averaged from 10 laser shots and the resulting calibration curves showed good correlation up to 4.3% (the highest concentration of carbon). The RSD's for the soil samples were higher for the low C concentration soils due to the increased interference of the Fe peak. It was found that the

standard deviation could be reduced if multiple samples of each soil were measured and more laser shots were averaged.

More recent research concerning carbon in soil analysis was reported at the fifth Annual Conference on Carbon Capture & Sequestration in 2006. Harris *et al.*⁵⁸ analyzed over 200 soil samples from several Midwest states representing a wide variety of textures and sand-silt-clay combinations. These soil samples were analyzed by dry combustion for carbon content and pressed into pellets for LIBS analysis. The results indicated very different calibration slopes for sand, loam or clay soils which correlated well with synthetic soils produced to mimic these compositions. In agreement with previous research, it was determined that the smaller grain-size soils (clay) exhibited a smaller slope than that of large-grain size soils (sand). The conclusion was that the LIBS signal was very sensitive to soil texture and therefore, each field would have a different response or sensitivity and require ‘in-field’ calibration.

Scope of Research

While the analysis of soil samples has received a great deal of attention over the last few years, research concerning the determination of carbon in soil has been lacking, limited to a few proof-of-principle demonstrations by research groups at Los Alamos and Oak Ridge National Laboratories.⁵⁴⁻⁵⁷ Since the sequestration of carbon in soil may offer a means of mitigating the effects of global warming (to be described in Chapter 2), it is becoming increasingly urgent to develop a practical device that can accurately measure terrestrial carbon inventories in order to understand the status of the global carbon cycle. LIBS has been proposed as an in-field carbon monitor due to the robust, compact and low-power properties of its instrumentation.⁵⁹ Before a field-based LIBS instrument can be designed there must be laboratory-based demonstration of the capability to determine carbon in soil. The purpose of our research was to investigate the potential of LIBS for carbon in soil analysis with an emphasis on a minimal sample preparation

and the potential for *in-situ* analysis. The instrumentation used for the majority of the research was compact, light-weight and similar to the components that would be incorporated into a portable device.

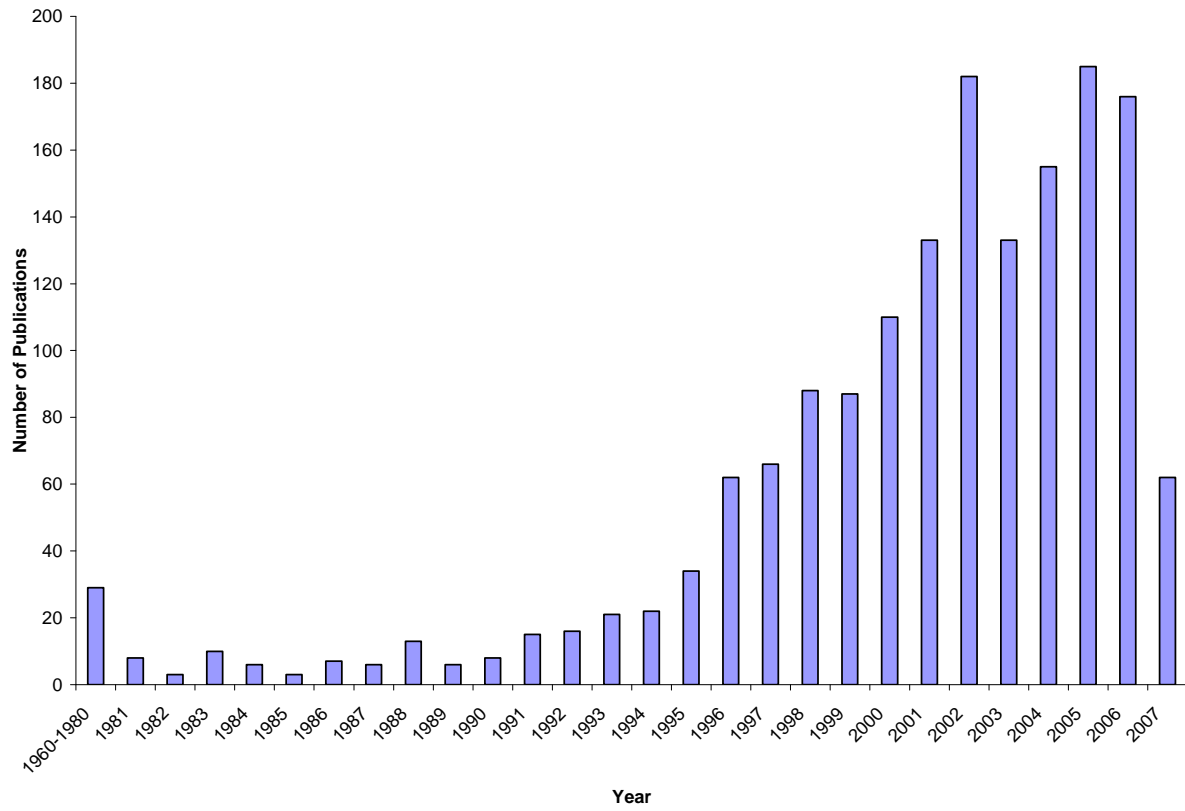


Figure 1-1. Number of LIBS publications per year since 1960.

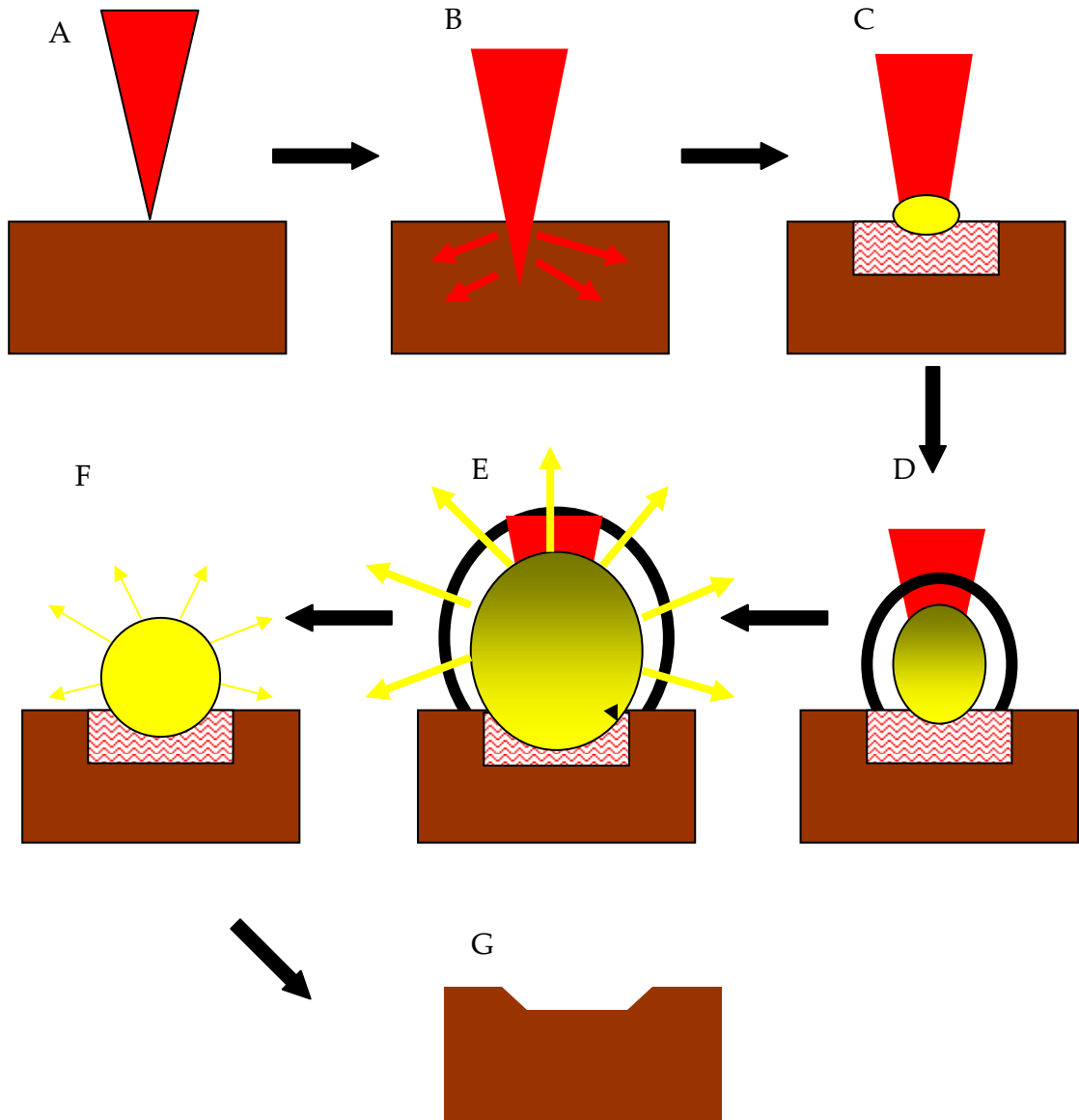


Figure 1-2. Significant events during plasma formation. A) The laser pulse strikes the sample surface. B) Energy is dissipated through the sample. C) Vaporization of the underlying material causes the sample surface to explode. D) Plasma expands while still absorbing energy from the residual laser pulse and a shockwave is formed. E) Radiation is emitted. F) Plasma cools and slows. G) A crater remains after the ablation event.

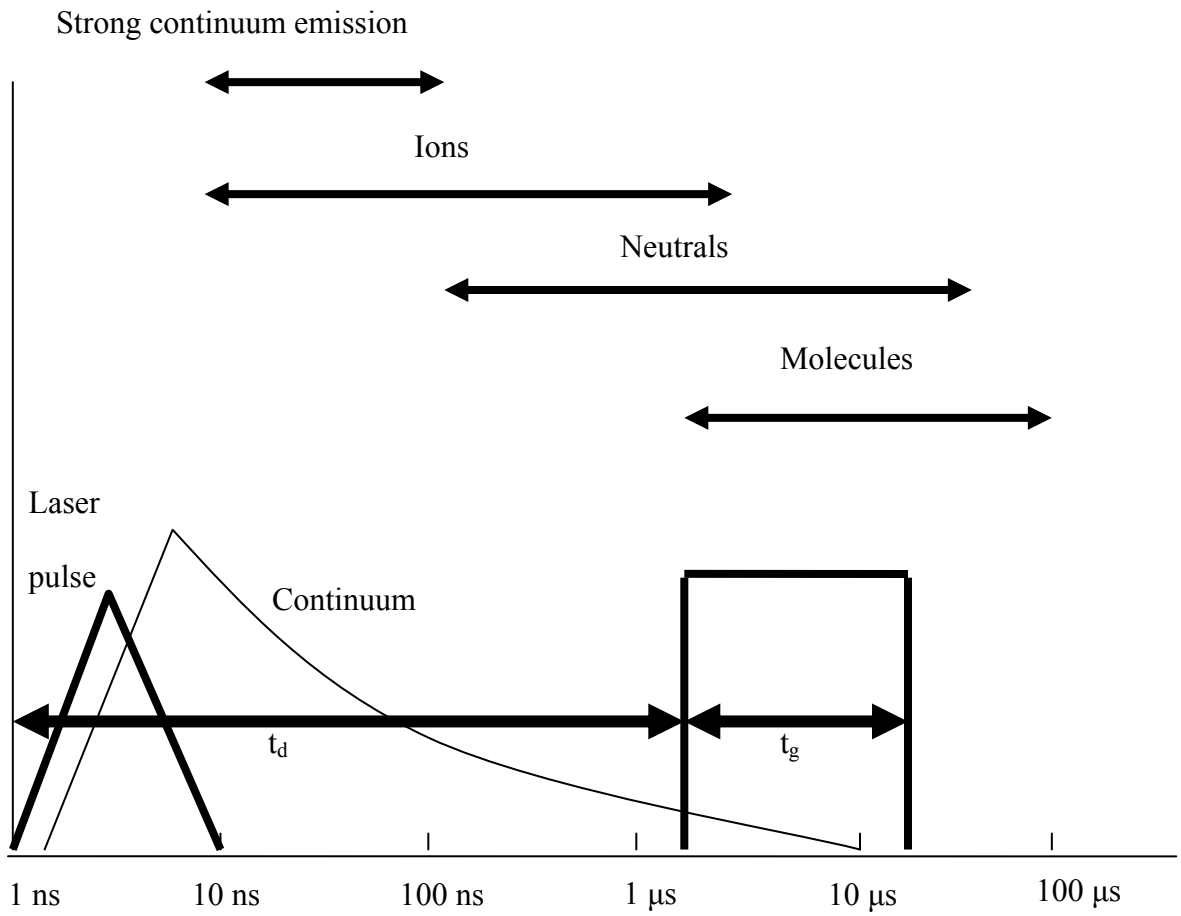


Figure 1-3. Temporal evolution of the LIBS plasma. T_d is the detector delay time and t_g is the gate pulse width, also referred to as the integration time. Constructed with data from ref. 4.

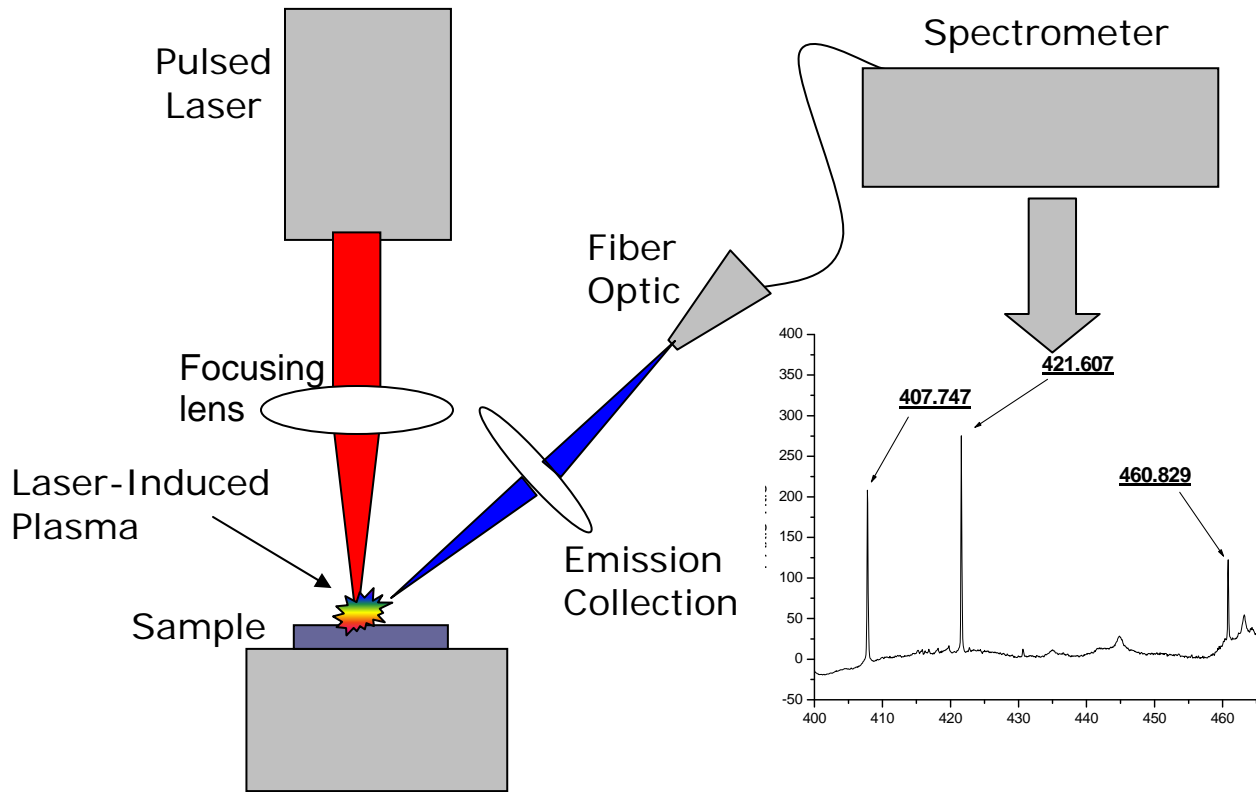


Figure 1-4. Typical schematic of a LIBS set-up

CHAPTER 2 CARBON IN SOIL

The importance of accurately measuring carbon content in soils has become readily apparent with the increased awareness of the causes of global warming. In December 1997, the Kyoto Protocol was established to set target CO₂ emission reductions for ratifying countries. For the United States, the Protocol calls for the reduction in atmospheric carbon emissions by 7% from the 1990 level by the year 2012.⁶⁰ In order to meet these challenging targets, and mitigate the harmful effects that global warming presents, an approach must be formulated that not only reduces current CO₂ emissions but also captures CO₂ from the atmosphere and stores it in long term sinks. A full understanding of the carbon cycle and the rate of carbon fluxes, as well as accurate inventories of carbon in the terrestrial ecosphere, are needed to optimize potential emission reduction techniques. This chapter will introduce the sequestration of carbon in soil as well as current methods that are employed to determine soil carbon levels for the purpose of developing an accurate terrestrial carbon inventory. Finally, the challenges of soil sampling, preparation and analysis will be briefly discussed.

Sequestration of Carbon in Soil

Carbon is the fundamental building block of life and as such exists in appreciable quantities in every ecosphere: the atmosphere, hydrosphere (oceans and seas), biosphere (living matter) and the geosphere (the earth). The global amount of carbon is fixed, however the carbon is readily exchanged between each of these ‘spheres’ during a process that is referred to as the carbon cycle.⁶¹ Figure 2-1 shows the amount of carbon, in gigatons (Gt), that is actively cycling through each sphere. Figure 2-2 illustrates mechanisms that contribute to the carbon cycle as well as approximate carbon fluxes in Gt/year.

Data from CO₂ trapped in ice cores and long term CO₂ monitoring has indicated that the current CO₂ levels are the highest they have been in 650,000 years, at 390 ppm in 2007.⁶² Such elevated levels can be attributed to increased land clearing (destruction of vast rain forests, depleting woodlands) and burning of fossil fuels (oil, coal, and natural gas), which contributes over 5 Gt of CO₂ into the atmosphere each year. Indeed, the atmospheric concentration of CO₂ was 270 ppm prior to the industrial revolution of the 18th century, after which it exponentially increased to the current value of 390 ppm. After the complete expenditure of all fossil fuels in approximately 300-400 years, the atmospheric concentrations of CO₂ are predicted to be 1200ppm.⁶³

Increased CO₂ levels in the atmosphere contribute to a phenomenon referred to as global warming. Carbon dioxide, along with other gases such as water vapor, methane (CH₄), and nitrogen oxide (N₂O), are referred to as ‘greenhouse gases’ because they trap heat from the sun in the earth’s atmosphere, which results in increased global temperatures, a process referred to as global warming.⁶⁴ The ramifications of global warming are ominous, and include decreased vegetation production and accelerated polar ice-cap melting.

There is little argument that atmospheric CO₂ levels need to be reduced; however there is much debate on how to achieve this goal. The obvious recourse is to reduce fossil fuel consumption however current economics depend on fossil fuels and the stunted development of alternate energy sources is reflective of this.⁶³ An alternative to stemming the CO₂ source is to enhance natural carbon sinks (where carbon is stored for long periods of time). As illustrated in Figure 2-1, the largest carbon sink by far is the ocean; however the ability to manipulate such a vast sink is limited and may take hundreds of years to produce appreciable changes. The next largest carbon sink is terrestrial soil, the carbon content of which is double that of carbon in

vegetation, such as plants, trees, crops and grasses. Due to poor land management and agricultural practices during the first half of the 20th century, over half of the maximum soil organic carbon (SOC) has been lost. However this has resulted in a greater capacity of many soils to sequester carbon.

The majority of carbon is introduced into soil as decaying biomass. Plants and other vegetative material withdraw CO₂ from the atmosphere during photosynthesis and convert it to sugars, starch and cellulose. Upon death, soil microorganisms cause decomposition and respire CO₂ in the process. However, an organic residue remains after decay and is referred to as humus. In the absence of oxidation, this organic matter will remain in the soil for hundreds, possibly thousands of years.⁶⁵ Carbon sequestration in soil can be significantly increased by up to 0.1% per year by converting marginal arable land to forest and grassland, planting high yield crops, and not tilling crop lands, especially in warm, moist climates. Even such a seemingly small increase in carbon sequestration can have a huge impact on the global (atmospheric) carbon balance. Current estimates indicate that successful sequestration of carbon in soil can potentially offset 30,000-60,000 million metric tons of carbon that is released by fossil fuel combustion over the next 50 years.⁶⁶

A direct result of the Kyoto Protocol is the establishment of a so-called 'carbon stock market'. In brief, it allows countries that have large carbon sinks, such as forests or vegetation to deduct certain amounts from their CO₂ emission targets, thus making it easier for them to achieve the desired net emission level. Countries that have already met their emission targets, and have additional CO₂ sinks may wish to sell the benefit that these sinks provide (an offset of the target emission levels) to countries that are not on target to meet required emission reductions. Such a "cap-and-trade" system has also been proposed for the national level, where

individuals are responsible for reducing emissions and/or creating carbon sinks and trading carbon credits to meet these targets.⁶⁷ Potential carbon stocks have been valued at approximately \$8 billion in the agricultural industry alone.^{68,69}

While terrestrial soil is the second largest carbon sink, it is currently not recognized as a sink that can be traded as an off-set of carbon emissions. The reason for this is simple: reliable measurements of soil carbon stocks on a national scale are scarce, and high-precision estimates of annual carbon inputs to the soil are even scarcer.⁷⁰ Izaurrealde *et al.* concluded that although there is a “compelling scientific basis for believing that a substantial Canadian C sequestering activity is occurring, the science and supporting measurement protocols have not been developed to the point that this can be adequately quantified at the farm or regional scale and accepted for marketing purposes.”⁷¹ The Soil Science Society of America maintains that in order for carbon sequestration in soil to effectively reduce atmospheric CO₂ more research is needed to better quantify carbon sequestration and improved monitoring and verification protocols must be established.⁶⁶ As such, while sequestering carbon in soil is one of the most promising short-term methods to mitigate increasing atmospheric CO₂, it is severely limited by the lack of analytical techniques to provide quantitatively defensible carbon levels in soil.

Current Methods for the Determination of Carbon in Soil

Typical analytical methods for the determination of carbon in soils and sediments rely on converting carbonaceous material to CO₂ followed by direct or indirect measurement.⁷² The two most common methods for carbon analysis are dry combustion and wet oxidation coupled with a variety of different methods to measure evolved CO₂.

Dry combustion involves combusting the soil sample in a stream of CO₂-free O₂ gas at temperatures above 900°C. These resulting combustion gases are passed through a series of traps that are designed to remove particulates and other interferences. If a medium temperature

furnace is used, the gases may then be passed through a catalyst furnace to ensure complete oxidation. The dry combustion technique can be used to measure organic carbon (C_{org}), inorganic carbon (C_{inorg}) and total carbon by controlling the combustion temperature; C_{org} combusts between 650-720°C and the remaining C_{inorg} is converted to CO_2 between 950-1100°C. In some cases, C_{org} measurements may be inaccurate if carbonate decomposition or incomplete organic carbon oxidation occurs at the lower temperature. While the actual dry combustion method is relatively standard, the method of CO_2 detection and quantification varies. A summary of these different detection procedures is presented in Table 2-1. Dry combustion carbon recoveries for dry, organic samples exceed 95%.⁷²

In the wet oxidation technique oxidizing agents such as KMnO_4 or $\text{K}_2\text{Cr}_2\text{O}_7$ in acidic solutions are used to oxidize the carbonaceous materials in the sample. The chromic acid method, referred to as the *Schollenberger* method, is the most commonly used wet oxidation technique and uses solid $\text{K}_2\text{Cr}_2\text{O}_7$ in the presence of H_2SO_4 or a mixture of H_2SO_4 and H_3PO_4 . The evolved CO_2 represents the total C_{org} content.^{73,74} Another wet oxidation technique that is widely used is the *Walkley-Black* method, in which a known excess of $\text{K}_2\text{Cr}_2\text{O}_7$ is used as the oxidant and back titration is performed to determine the amount of oxidizing agent consumed, which is proportional to the C_{org} .^{74,75} There are many other variations on the wet oxidation technique, including the type of oxidizing solution, the digestion temperature and duration, and the CO_2 detection methods (the same as for dry combustion, listed in Table 2-1).

It is apparent that there are many differences between the two most common methods of carbon quantification. While it is generally accepted that the dry combustion is more accurate and standardized than the wet oxidation method, it requires more complex instrumentation at a greater cost, and has a longer analysis time.⁷³ A variety of automated dry combustion

instruments are commercially available for the determination of *total* carbon content. Most analyze hydrogen and nitrogen as well as carbon and are termed CHN analyzers.

More recently, the potential of visible, near infrared, mid infrared and diffuse reflectance spectroscopy have been investigated as a means of analyzing soil, specifically for carbon content.⁷⁶⁻⁷⁸

The Challenges of Soil Analysis

The greatest challenge to the analysis of soil, regardless of analytical technique or analyte of interest, is the difficulty in obtaining a truly representative sample of soil. There are several factors that contribute to this difficulty, including sampling errors, soil variability and soil homogeneity. Soil variability refers to different types of soils located within a relatively small sampling region. Many environmental and anthropogenic factors can affect the spatial variability of soil, including localized decomposition events and farming practices. Variability can occur in both the horizontal and vertical directions, and must be compensated for with a careful sampling regime. The simplest way to account for it is to take multiple samples; however the hundreds, or possibly thousands of samples that may be needed to obtain representative data can be cumbersome. Due to the importance of determining carbon pools on a regional scale, much attention has been directed toward the spatial distribution of carbon in a variety of different lands.⁷⁹⁻⁸¹

Soils are also highly heterogeneous even within the same soil type and therefore create a so-called resolution problem. Soils are composed of many different constituents that are unevenly distributed throughout a given sample. Inorganic constituents such as quartz are present in three distinct particle size distributions referred to as sand, silt and clay, each of which exhibits different physical and chemical properties related to the different surface area. Table 2-2 shows the physical size ranges of these particle fractions, as well as the sizes of sub-groups

within the fractions. Soil organic matter is composed of humus and biological organisms. Humus is classified as either non-humic substances (carbohydrates, lipids and other metabolic products of organisms) or humic substances (humic and fulvic acids synthesized by microorganisms). Figure 2-3 illustrates the breakdown of soil organic matter. Each of these organic compounds is heterogeneously distributed throughout the soil, adsorbing to the surface of inorganic particles in different degrees and often binding different particles together as aggregates.⁷⁴ Most analytical methods are considered microanalysis techniques, and as a result sampling will not be representative of the bulk sample. Grinding and sieving is often used to produce a homogeneous sample of uniform particle size; however this often disturbs other properties of the soil and is a time consuming process.⁸²

While soil variability and heterogeneity are the two major challenges in soil analysis, there are several other factors that must also be considered. Soils of higher water content have greater vertical variation due to the downward leaching of water soluble components. Water content also affects the pH and porosity of the soil, which may impact specific analytical methods. The amount of water in the soil is often unknown and must first be determined if the technique has a tolerable limit. If the soil must be dried prior to analysis, the drying method must be carefully considered especially if it induces changes in the soil properties. For instance, oven drying soil may result in the oxidation and subsequent loss of carbon, therefore air drying is recommended for soil carbon analysis. Soil density is also a challenging factor, especially when it is necessary to report the concentration of an analyte per unit volume of soil. Soil density is a function of both the particle density and the bulk density. The determination of bulk density is especially important when assessing carbon pool sizes and carbon fluxes, which are usually reported as kg/

m² to a depth of 50cm.⁷⁰ It is apparent that in order for quantitative results to be meaningful, both bulk soil density and particle density must be assessed at the time of analysis.

Clearly, for accurate and precise soil analysis a carefully considered analytical scheme must be developed. Consideration must be given to the inherent variables in soil and the effect these will have on the analysis method. LIBS may be a suitable technique for practical soil analysis due to its portable nature (which precludes costly sample transport) and high-throughput (which allows for the orders of magnitudes of samples necessary to gain representative data). However, as also discussed, LIBS itself may suffer from poor precision due to a variety of instrumental and physical variables. As such, any analysis of soils by LIBS requires an experimental plan that reduces the effects of these variables, and balances the required accuracy and precision with the limits of the technique and sample. The research described in the following chapters describes an experimental scheme that optimizes these parameters and assesses the feasibility of using LIBS for *in-situ* carbon determination

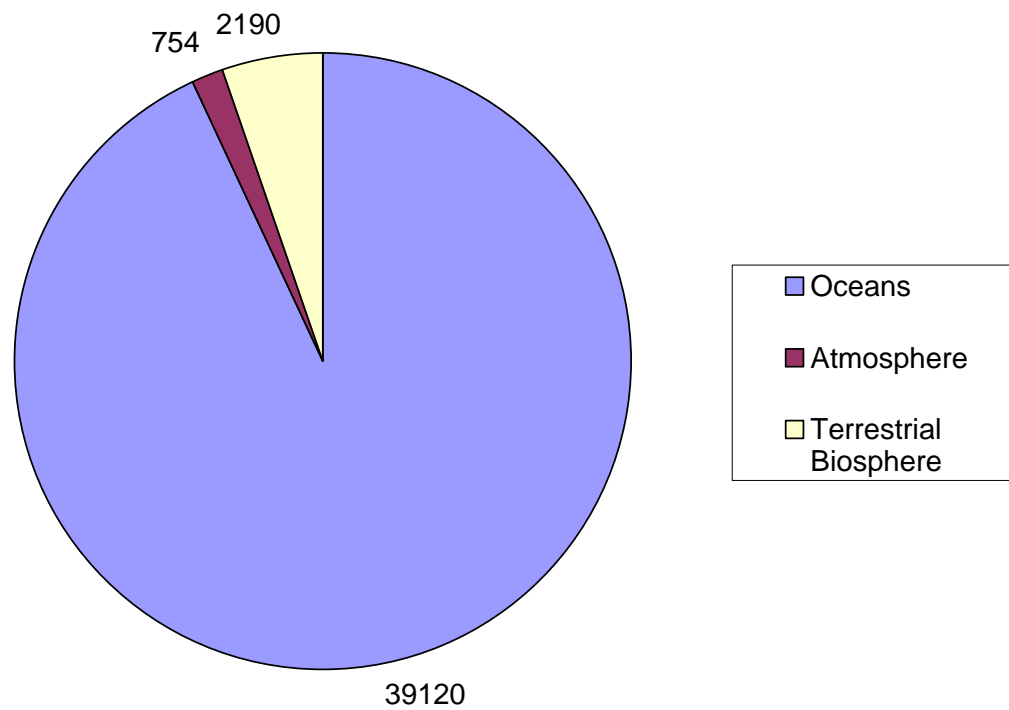


Figure 2-1. Magnitudes of the reservoirs of actively cycling carbon in gigatons (Gt). Produced with data from ref. 61.

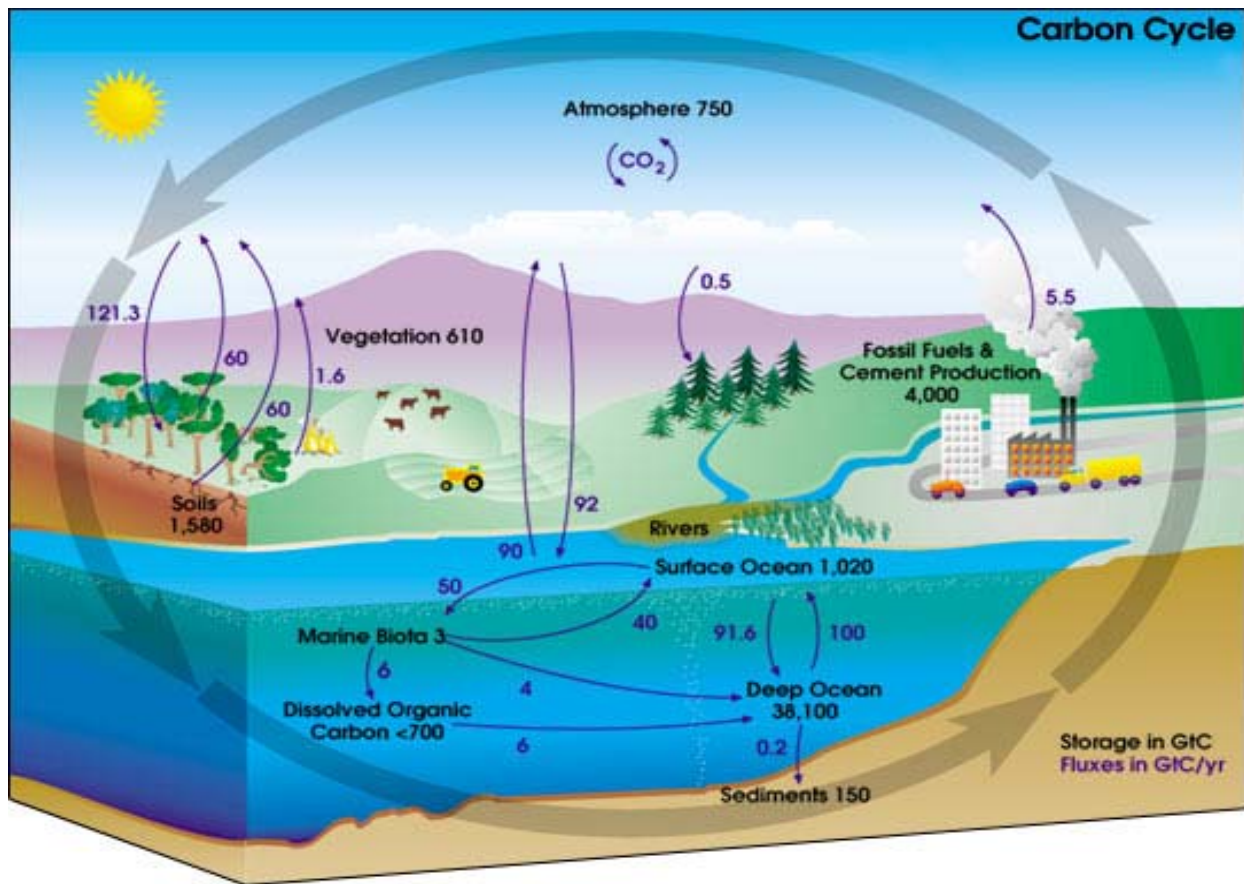


Figure 2-2. Carbon cycle. The flux of carbon between the sources and sinks are represented by the purple arrows. (Reproduced with permission from Teacher's Domain <http://www.teachersdomain.org/resources/tdc02/sci/life/eco/ccycle/index.html>)

Table 2-1. Techniques for measuring CO₂ in combination with dry combustion or wet oxidation.
Information from ref. 72

Type of Analysis	Common means of analysis	Type of measurement
Photometric	Infrared analyzer	Measures differential absorption of infrared energy between CO ₂ and reference gas
Gravimetric	Sorption trap	Measures mass gain in trap after combustion
Volumetric	Gas burette	Measures volume of CO ₂ released after combustion or acid digestion
Conductimetric	Thermal conductivity detector	Measures differential resistance between CO ₂ and reference gas
Titrimetric	Non-aqueous titration	Measures amount of CO ₂ consumed in solution by back-titration with standard solution

Table 2-2. The three major groups of soil size fractions are sand, silt and clay. These can be further subdivided into finer size fractions.

	Diameter (mm, unless otherwise stated)
SAND	
Very coarse sand	2.00-1.00
Coarse sand	1.00-0.50
Medium sand	0.50-0.25
Fine sand	0.25-0.10
Very fine sand	0.10-0.05
SILT	
Coarse silt	0.050-0.020
Medium silt	0.020-0.005
Fine Silt	0.005-0.002
CLAY	
Coarse clay	2.0-0.2 μ m
Medium clay	0.2-0.08 μ m
Fine clay	<0.08 μ m

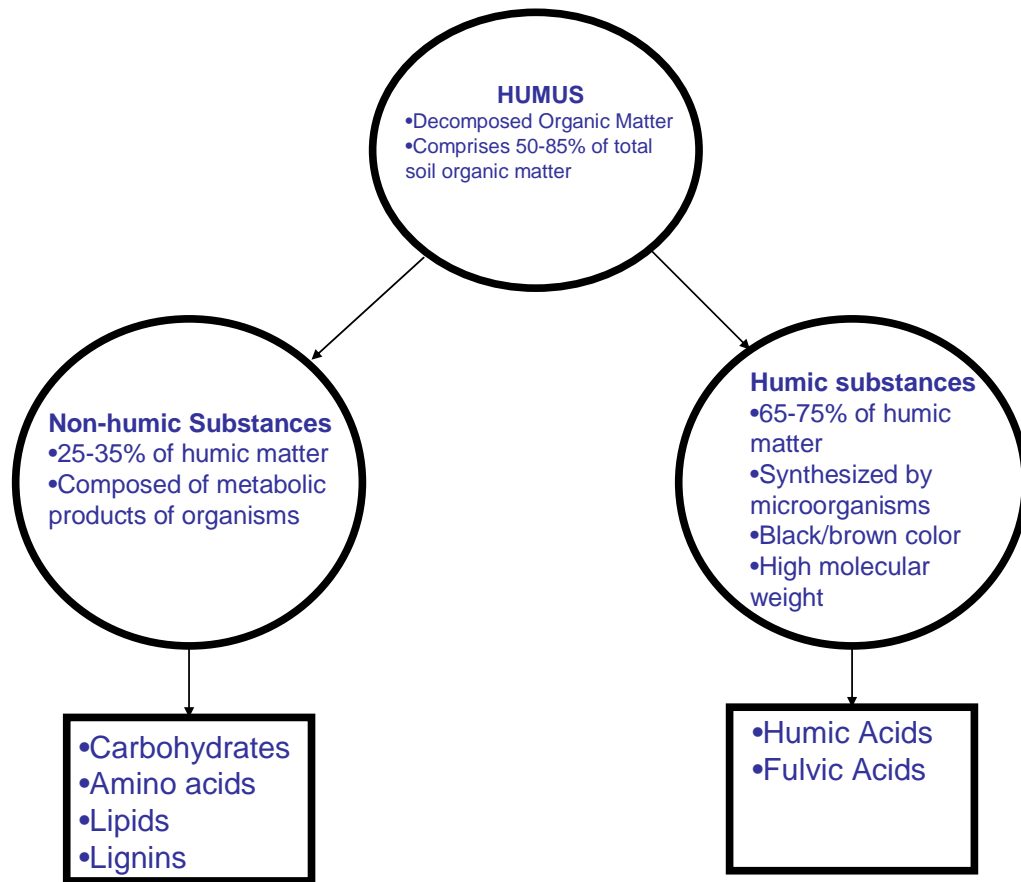


Figure 2-3. Constituents of humus, the major contribution to soil organic carbon.

CHAPTER 3 INSTRUMENTATION AND DATA ANALYSIS

The components of a LIBS system are very simple, as explained in chapter 1. The basic requirements are a pulsed laser, focusing optics, some method of emission collection, a spectrometer coupled with a detector and a computer. Naturally, there are many variations for each of these components, and the choice of which to incorporate into the LIBS system is dependent on the type of analysis and available resources. The instrumental components that were employed in the majority of this research were selected because they were comparable to the type of instruments that may be incorporated into a portable LIBS instrument. That is to say, they are compact and robust, have low power requirements and require little maintenance. Each of these components will be discussed in depth in the following section. The second half of this chapter will describe the optimization of these instrumental components.

Instrumental Components

Laser

The laser used for these studies is manufactured by Big Sky Laser Technologies. It was a flashlamp-pumped Nd:YAG laser operated at the fundamental wavelength of 1064 nm and with a specified maximum pulse energy of 50 mJ. The pulse energy can be changed in increments of 5 mJ. The pulse duration is 6-8 ns and the laser can be operated at repetition rates of up to 20 Hz. Table 3-1 provides a complete summary of the laser specifications. While these specifications state that the laser energy stability is 2%, it was assumed that this was an underestimation of the value and that it had to be measured independently prior to use. The laser consists of two units, the laser head where the pulse is generated, and the integrated cooler and electronics (ICE) system from which the energy and repetition rate are controlled. For this research, the laser head was mounted vertically with the laser pulse directed down onto the

sample stage. This type of laser is classified as a Class 4 laser which means that the output beam, by definition, is a safety and fire hazard. As a result, protective eyewear was worn at all times to prevent accidental exposure to both direct and reflected beams.

Optics

A quartz plano-convex focusing lens with a diameter of 1" and a focal length of 2.5" was used to focus the laser. The lens was housed in a 1" lens tube which was mounted in a steel cage system (Figure 3-1). This allowed for the lens to be easily moved up or down while still remaining on axis with the laser. The lens was located approximately 11" from the laser aperture. The diameter of the ablation area produced on a copper surface, with a pulse energy of 50 mJ was approximately 0.35 mm (Figure 3-2).

Fiber Optics

The fiber optic used to collect the plasma emission was produced by Ocean Optics, Inc. especially for the LIBS2000+ spectrometer unit. The fiber bundle actually consists of seven individual fibers, each of which collects a certain portion of the plasma radiation and transmits it to an individual spectrometer. The fiber bundle has a nylon jacket and PVC sheathing. The fiber cores are pure fused silica and the cladding is doped fused silica. The core diameter of each of the individual fibers is 600 μm . The numerical aperture of the optical fibers and the probe is 0.22, which yields an acceptance angle of 24.8° in air. The probe houses a collimating lens which has a focal length of approximately 1".

Spectrometer

The spectrometer used for this research was the LIBS2000+ and was also manufactured by Ocean Optics (Figure 3-1). As the name implies, it is a commercial spectrometer that is uniquely designed for LIBS applications. It is in fact not one spectrometer but seven individual miniature spectrometers which each cover a specific spectral range (approximately 100 nm). Each of the

fibers in the fiber optic bundle connects with one spectrometer in the LIBS2000+ unit. The resolution at full-width half-maximum (FWHM) is 0.1 nm, though this value varies depending on the spectrometer. Radiation was dispersed by a grating, and detection achieved by a CCD with 2048 pixels for a combined total of 14,336 pixels. The integration time was fixed in spectrometer mode at 2.1 ms. Detection could be delayed up to 135 μ s in 500 ns intervals.

The LIBS2000+ system is very convenient for LIBS applications due to its broad spectral range, portability and ease of use. However, it does suffer from several disadvantages, the most significant of which is the poor sensitivity. This is due in part to the fact that each channel receives only 1/7th of the total radiation collected. In some cases it may not be necessary to acquire the whole spectrum, but rather a specific spectral range which may correspond to one of the seven spectrometer channels. If this is the case, a single fiber can be coupled to the channel of interest. As a result, instead of receiving 1/7th of the collected radiation, that channel will receive all of it, which will improve the sensitivity. Another disadvantage to the seven spectrometer system is the discontinuity between each channel in the total spectrum. Often, very significant differences in background and overall sensitivity can occur between adjacent channels causing the spectrum to exhibit sharp jumps (Figure 3-3). One of the causes of these differences in background and sensitivity between channels is the orientation of the individual apertures in the fiber probe. As illustrated in Figure 3-4, the arrangement is a circle of six apertures and the seventh in the center. Depending on the positioning of the fiber probe, each of these fibers will view a slightly different portion of the plasma. It is often necessary to optimize the emission collection of one or two channels at the expense of other less important channels.

Software

The software that is used to process the spectral data is called OOILIBS, also produced by Ocean Optics, Inc. OOILIBS is a simple, user friendly program that displays the individual

spectra almost instantaneously after each laser shot. The laser can be run in external trigger mode, which means that the software specifies the laser repetition rate and the acquisition delay time. The software can also control the number of laser shots fired, the number of cleaning shots used, any necessary background correction, and average or individual data collection. There is a spectral line database available to identify specific lines; however at the time of this research, it had not been developed enough to provide accurate results and therefore was not used. In addition to this there is the option to monitor specific lines during the analysis, including calculating the mean intensity and area, standard deviation and RSD after each subsequent laser shot. This is especially helpful for rapid analysis (the mean intensity of a chosen line after 100 shots is immediately available after the last shot); however for this research a more advanced data analysis program separate from the OOILIBS software was used.

Optimizing Instrumental Parameters

Laser Energy

Before any measurement can be undertaken, it was necessary to determine the stability of the laser pulse. While the manual specifications indicated that the stability was 2%, there are many factors that may change this, including the age and use of the laser and the chosen energy. Instability in the laser pulse energy will result in variable plasmas and poor precision; therefore it is essential to ensure that the laser exhibits a tolerable energy instability.

To measure this, the focusing lens was removed from the LIBS system and a power meter was positioned on the sample stage. The laser was run in continuous mode at a repetition rate of 1 Hz and an oscilloscope displayed the measured energy. Thirty-two measurements were taken at expected laser energies of 30, 35, 40, 45 and 50 mJ. The mean energy, standard deviation and relative standard deviation (RSD) for all laser shots, the first ten laser shots and the remaining 22 laser shots are reported in Table 3-2. Surprisingly, it was determined that the maximum laser

pulse energy of the laser was actually 57 mJ rather than 50 mJ as stated by the manufacturer. With respect to the energy stability, it was found that when all laser shots were included in calculating the mean, the average RSD (for all energies) was 6.1%. However, when the first ten shots were abandoned, the average RSD decreased to 3.6% (when omitting the 50 mJ measurements, which exhibited an unusually high RSD). The stability for the highest pulse energy of 57 mJ, which was the one that will most likely be used for soil analysis, was 2.3% when the first ten shots were abandoned. Due to the significantly increased instability of the laser during the first ten shots, the data from these shots were discarded in subsequent measurements.

Optimization of the Spectrometer

The only way that delayed acquisition of emission can be performed is to control the timing of the laser pulse relative to the fixed timing of the CCD integration. Figure 3-5 illustrates how the Q-switch can be controlled by the software to fire the laser, and create a plasma at different times relative to the commencement of CCD acquisition. Positive values of the Q-switch delay correspond to plasma formation after the CCD begins acquisition, thus radiation from the entire lifetime of the plasma is integrated, and there is no true delay. If the Q-switch delay is set to zero, acquisition occurs at the same time as plasma formation. Negative Q-switch values correspond to emission acquisition at 500 ns intervals after plasma formation. For instance, if the Q-switch delay time is set to -0.5, radiation from the first 500 ns of the plasma will not be collected. Both positive and negative Q-switch delays have advantages. When emission from the entire plasma is collected with no delay signal intensities are greater and species that have prohibitively high ionization potentials may be detected. However, without a delay, the initial continuum is collected, which increases the background and can obscure sensitive emission lines.

In order to determine the best Q-switch delay time for the C247.8 nm line, 15 measurements were taken on a soil sample and averaged for delays of +4 μ s to -4 μ s. From this data, the minimum detectable concentration of carbon, C_L was determined for each delay time (Equation 3-1).

$$C_L = kC(RSD)_B \left(\frac{1}{S/B} \right) \quad (3-1)$$

S is the intensity of the 247.8 nm signal after the background, B, is subtracted, RSD_B is the relative standard deviation of the background, C is the concentration of carbon and k is a statistical factor equal to 3. For positive Q-switch delay times, S and B remain relatively constant (Figure 3-6). This is expected because there is no delay (emission acquisition begins at different time periods before the plasma is formed) and as such radiation from the entire plasma is collected each time. However, once the Q-switch delay time becomes negative and delays occur at intervals of 500 ns, both S and B decrease and S/B increases. A Q-switch delay time of -1 μ s was found to yield the lowest minimum detectable concentration of C and employed for subsequent studies. It should be noted that this corresponds to a concentration of 1.4% C; however for practical purposes C was still detected at concentrations lower than this.

Optimization of Fiber Probe Position

The placement of the fiber optic probe is a crucial parameter in LIBS analysis. The fiber must be placed in a position that renders it as insensitive as possible to the spatial inhomogeneity and shot-to-shot instability of the plasma. Commonly the fiber is either mounted close to the plasma at a 30-45° angle, so called side-collection, or plasma emission is focused on to the fiber by the same lens that focuses the laser and a dichroic mirror, termed back-side collection. Both orientations provide unique advantages. The back-side viewing is less sensitive to spatial

inhomogeneities of the plasma because emission collection is from the top rather than from a single side, which may not be representative of the whole plasma. In addition to this, back-side collection is also insensitive to the vertical position of the plasma, which may change if the sample height is not constant. One of the drawbacks of back-side emission collection is the use of a dichroic mirror. It is very difficult to find a dichroic mirror that will transmit the laser at 1064 nm while reflecting all UV and visible radiation in the spectrometer spectral range of 200-900 nm. In addition to this, the longer path length that emission must travel to the fiber, coupled with the incomplete reflection at the mirror will result in radiation losses that decrease signal intensity. Side-collection does not suffer from these limitations, and also requires less optical alignment.

To determine the best fiber position, spectra from a graphite pellet were collected using both collection orientations. For the back-side emission collection, a 1" dichroic mirror was mounted in a cube at a 45° angle along the laser axis. The mirror transmitted the 1064 nm laser light and reflected UV and visible light. Emission from the plasma was focused onto the dichroic mirror and reflected to a plano-convex lens that focused the light onto the fiber probe. The emission was slightly defocused to ensure that each channel on the 2 mm probe was illuminated. Side-collection was achieved by mounting the fiber on a movable arm and carefully aligning it until the position that provides maximum signal intensity was reached. No spectrometer delay was used in order to collect the maximum emission possible.

The results of this study proved that the side-collection configuration provided superior sensitivity in all channels of the spectrometer (Figure 3-7). The C247 signal and background obtained by placing the fiber so close to the plasma were almost 12 and 2 times greater respectively than those obtained using back-side collection. Even with the higher background,

the S/B was nearly 7 times greater for the side-collection configuration. Clearly, placing the fiber closer to the plasma provided significantly increased sensitivity and was consequently chosen as the best position of the fiber probe for the remainder of the study.

Optimizing Lens-to-Sample Distance

The lens-to-sample distance (LTSD) is an important parameter that must be held as constant as possible in order to obtain reproducible spectra. This can be a challenge when analyzing samples of different heights, or when a single sample does not have a uniform surface. If the sample is moved farther from the focal point of the laser, the irradiance (W/cm^2) of the sample decreases. In cases where the breakdown threshold of the sample is low, or the laser energy is high, this can be beneficial because the laser beam samples a greater area. However, if the spot size is too great, a breakdown will not occur. Depending on the physical and chemical properties of the sample, there is an optimal LTSD that must be kept constant for a set of samples.

In order to determine the best LTSD a graphite pellet was placed on the sample stage and spectra were collected at 1 mm increments above and below the focal point of the lens (measured as 2.5"). Ten shots at maximum laser energy were recorded and averaged. The results indicated that the greatest C247 signal was found when the focal point was 2 mm above the sample surface (Figure 3-8). Incidentally, this position also yielded the lowest standard deviation in measurements. It is important to note that the measured focal point of the plano-convex lens used in this research was measured using room light and may be slightly different for the 1064 nm laser. Regardless, the results of this experiment provide the optimum LTSD and fiber-to-sample-to distance (FTSD) based on maximum C247 signal intensity. In order to ensure a constant LTSD and FTSD, regardless of different sample heights, a laser positioning system was constructed. With the graphite pellet at the height that provides the best signal, a small helium-

neon laser was directed over the sample surface toward a photodiode connected to a voltmeter. Half of the laser beam was blocked by the sample and the voltmeter measurement for the blocked beam was recorded. When samples of different heights were placed on the sample stage, they were moved either up or down until they blocked the same portion of light as the graphite pellet in its optimal position. While using this positioning system allowed for each sample to be analyzed under the same conditions, little could be done to account for the variations in height within the sample itself, such as the case for particulate soil matter.

Data Analysis

Once the required number of spectra had been collected for a sample, it was necessary to garner the required information by processing the data. As previously mentioned, the OOILIBS software had a mode which allowed the user to collect statistics during the analysis; however the information provided was limited to simple statistics, with no regard to the trends or patterns which may appear within a sample. Instead, the data collected during this research was processed using Microcal Origin™ and a Matlab program written specifically for the analysis of LIBS data. Both the peak area and the background subtracted peak intensity were calculated (Figure 3-9). A comparison between the statistics (standard deviation, standard error) produced from calculating either the intensity or integral revealed that they were both very similar, however in general, computing the integral yielded slightly lower RSD's than the intensity, most likely due to the dependence on more data points than the one pixel used to calculate intensity. The Matlab program also calculated the intensity and integral of the background (B), the noise (N), and RSD_B .

Table 3-1. Specifications for the Big Sky Ultra Nd:YAG pulsed laser.

Repetition Frequency (Hz)	Up to 20
Pulse energy (mJ) ^a	Up to 50
Beam divergence (mrad) ^b	<7
Energy stability (%) ^c	2
Beam diameter (mm) ^d	2.8
Pointing stability (μ rad) ^e	50
Jitter (\pm ns Q-Switch) ^f	<2
Energy drift over 8 hours	<10%

a) Nominal FWHM. b) Angle containing 86.5% energy. c) Variation from mean for 99% of shots
d) Nominal value. e) Full angle, 99% of shots. f) Measured from Q-Switch sync output.

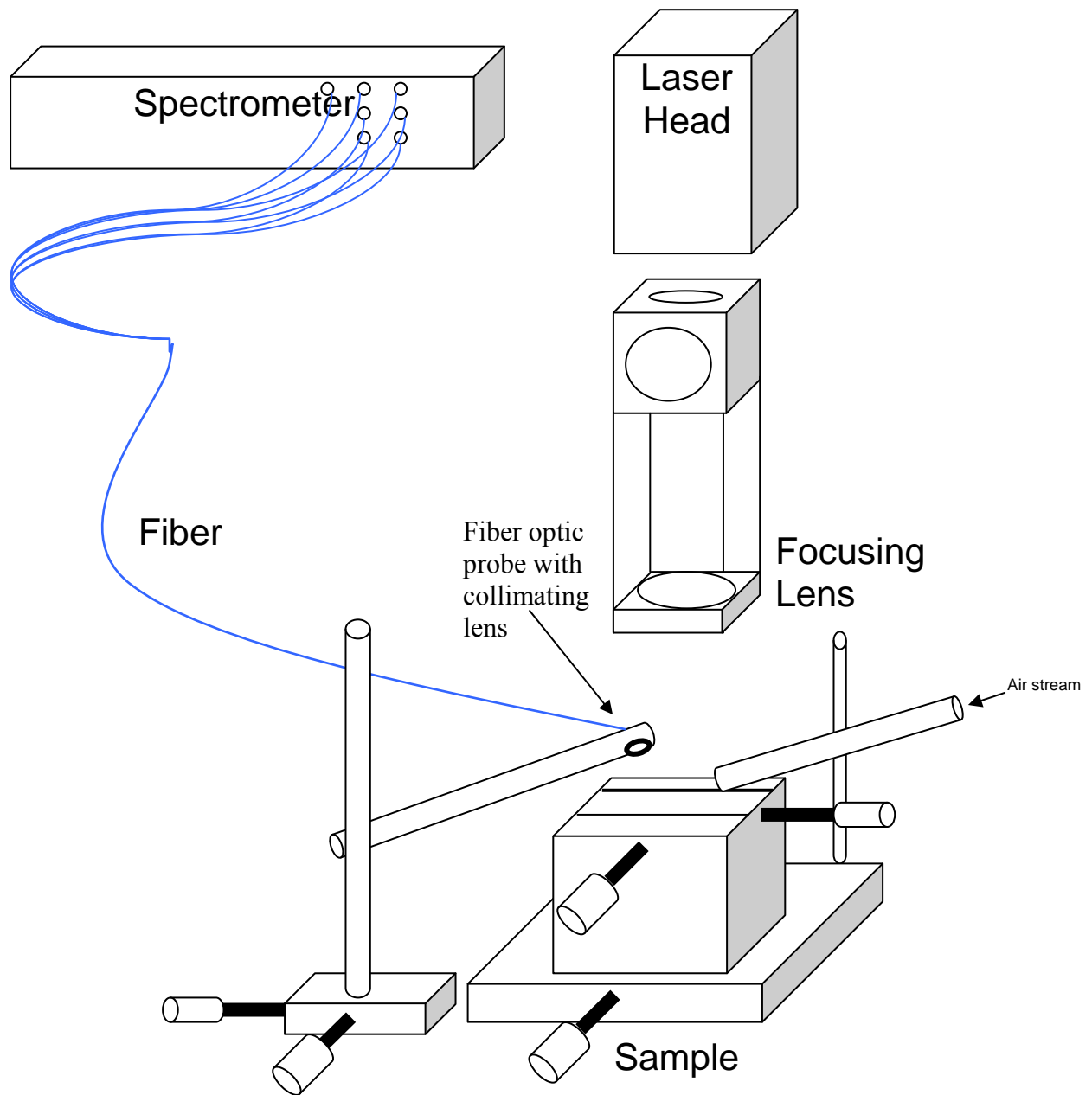


Figure 3-1. Configuration of LIBS instrumentation.

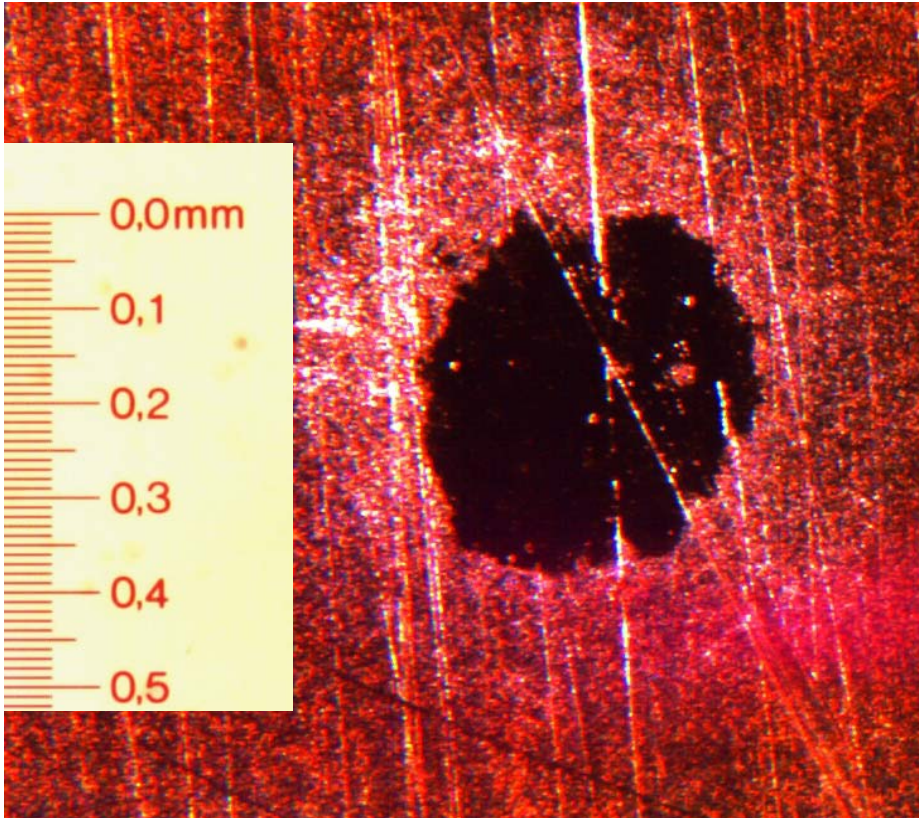


Figure 3-2. Ablation area produced on copper foil by a 50 mJ laser pulse and a 2.5 inch focal length lens. (Note, only the black area is considered the ablation area).

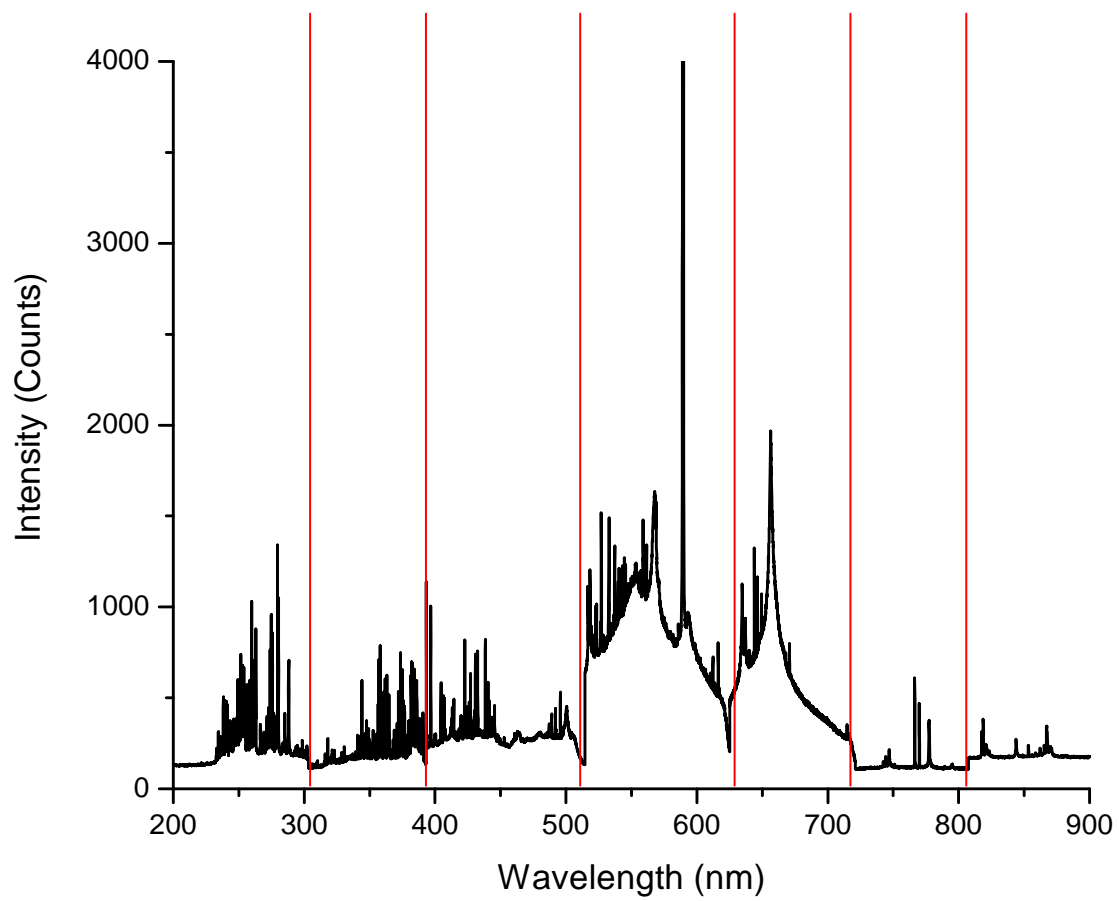


Figure 3-3. A soil spectrum that clearly shows the discontinuities between different spectrometer channels in the LIBS2000+ unit.

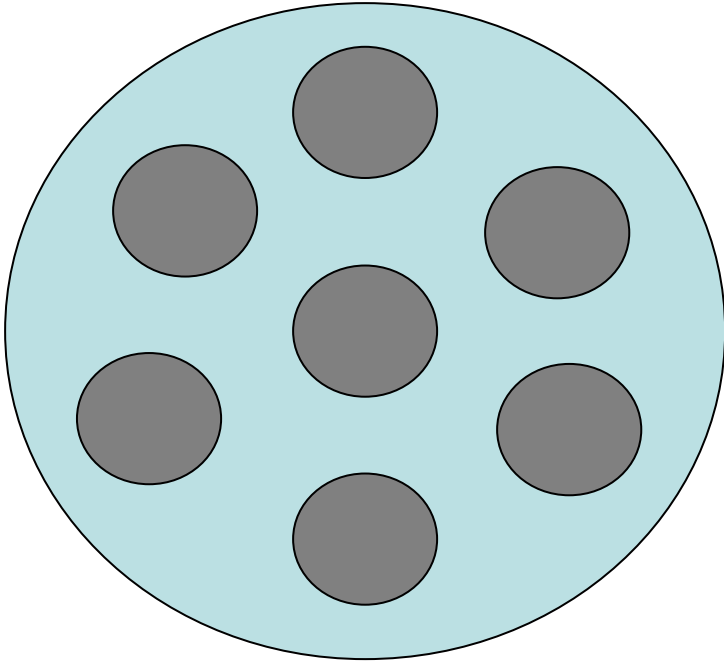


Figure 3-4. Arrangement of the individual fiber apertures in the fiber optic probe

Table 3-2. Mean pulse energies of the Big Sky laser measured with a power meter.

Expected pulse energy (mJ)	Mean pulse energy of 32 laser pulses (mJ)	Mean pulse energy without first ten laser pulses (mJ)	Mean pulse energy of first 10 laser pulse (mJ)
25	29 ± 1.7 (5.9%)	30 ± 2.2 (7.2%)	29 ± 1.4 (4.8%)
30	35 ± 1.9 (5.3%)	36 ± 2.4 (6.7%)	34 ± 1.3 (3.8%)
35	40 ± 1.5 (3.8%)	40 ± 1.7 (4.3%)	40 ± 1.4 (3.6%)
40	46 ± 2.3 (5.1%)	47 ± 2.9 (6.2%)	45 ± 1.7 (3.7%)
45	51 ± 3.7 (7.2%)	54 ± 2.7 (5.0%)	50 ± 3.7 (7.4%)
50	57 ± 1.8 (3.2%)	59 ± 2.2 (2.3%)	57 ± 1.3 (2.3%)

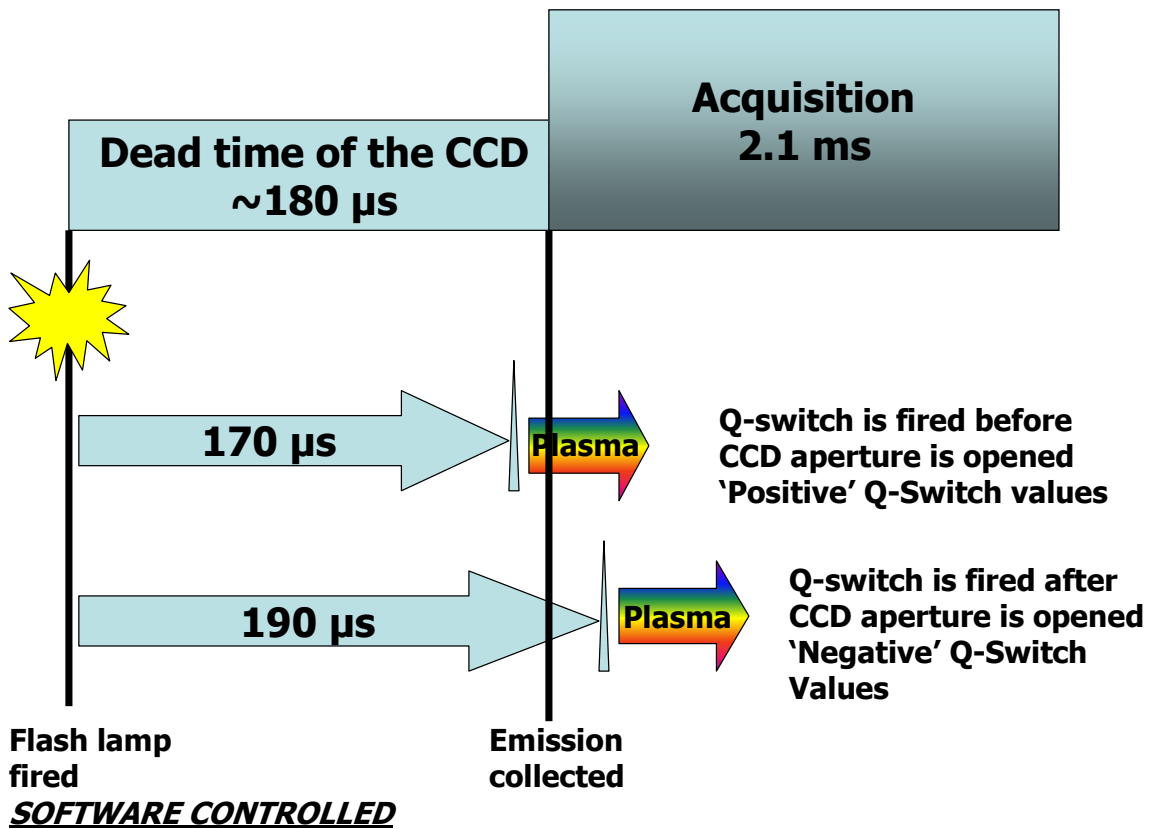


Figure 3-5. Controlling the CCD emission acquisition delay time by manipulating the laser Q-switch.

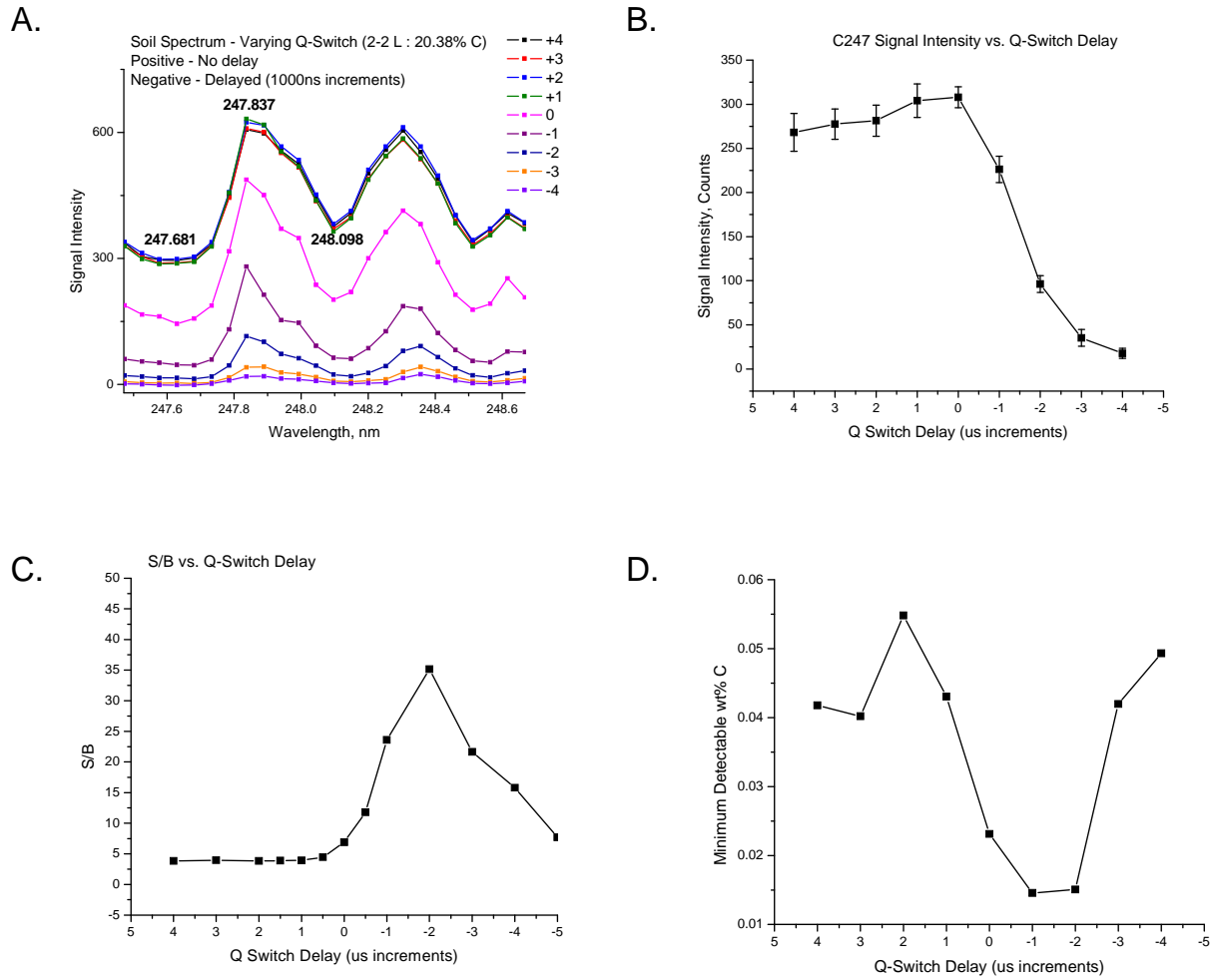


Figure 3-6. Results of changing the Q-switch delay times on soil spectra. A) The C247 line drastically changes with spectrometer delay. B) C247 signal intensity vs. delay. C) C247 S/B vs. delay. D) C_L vs. delay.

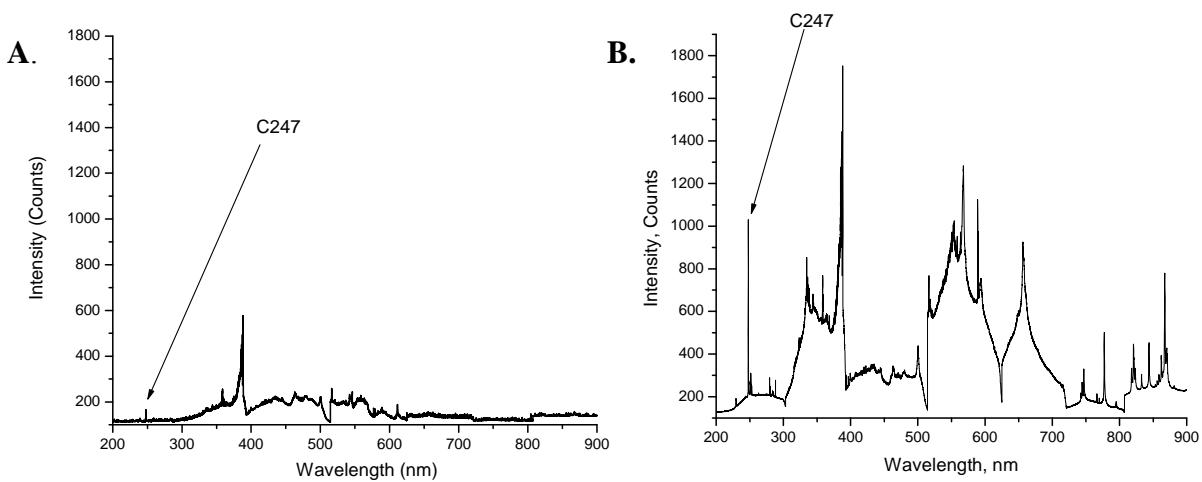


Figure 3-7. Graphite pellet spectra with A) back-side emission collection and B) side emission collection (Note: Only the C247 line is identified because it was used to determine increase in signal intensity)

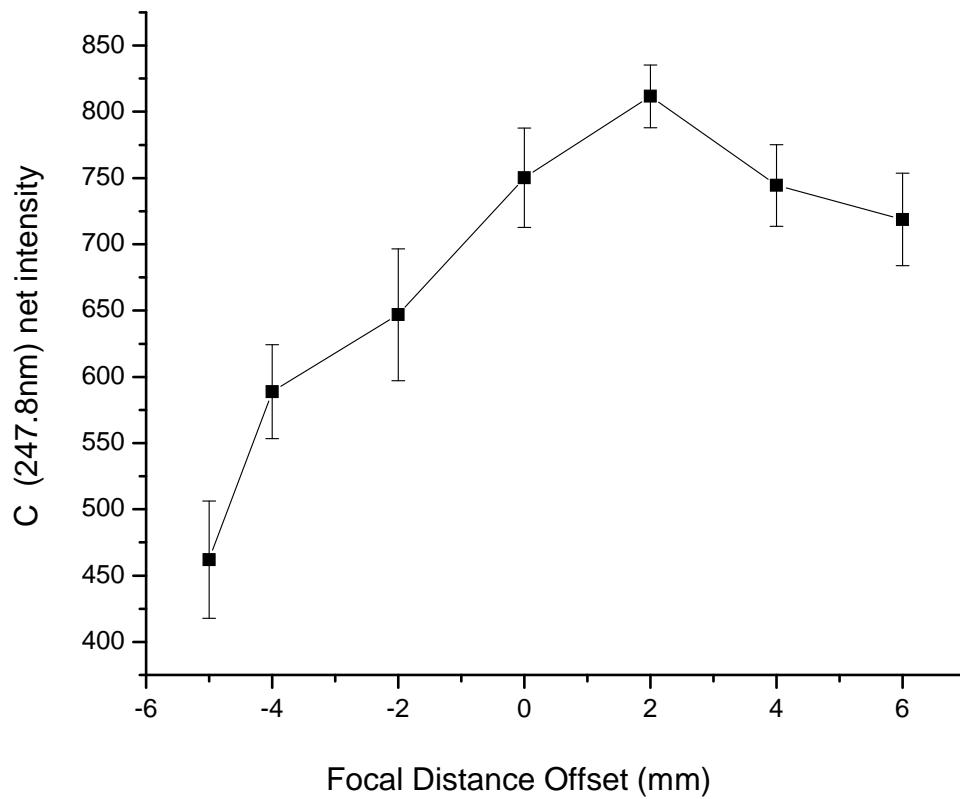


Figure 3-8. C247 signal intensity (the average of 10 shots) as a function of focal point offset (error bars are ± 1 standard deviation).

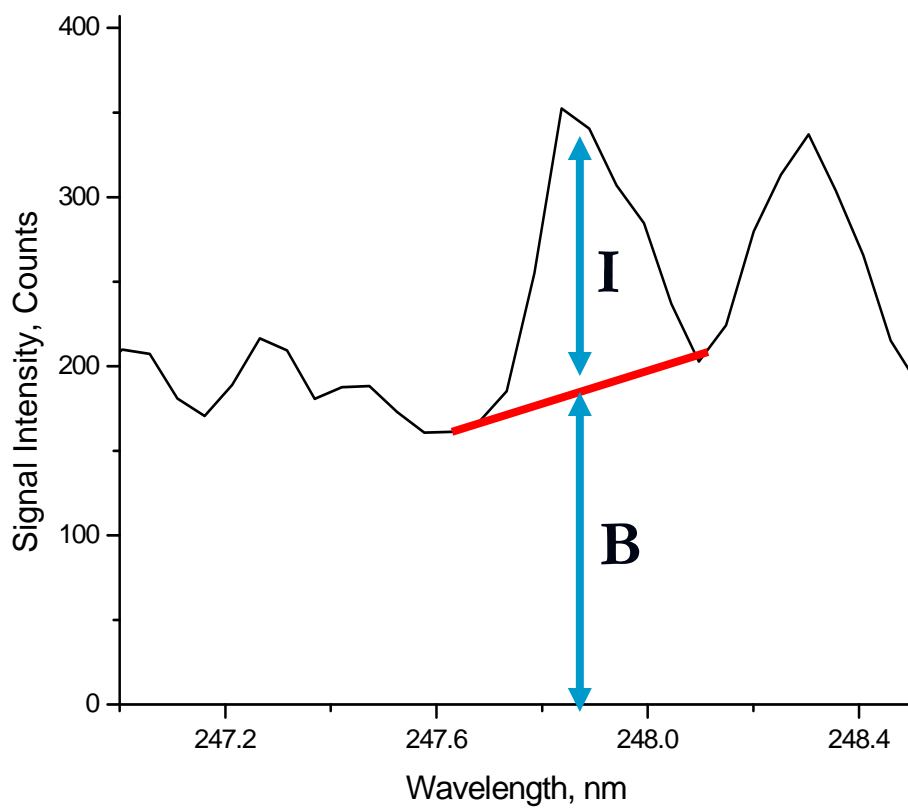


Figure 3-9. Calculation of intensity (I), background (B) and area (above the red line).

CHAPTER 4 SAMPLE PRESENTATION AND SAMPLING CHARACTERISTICS

One of the most important advantages of the LIBS technique is the ability to analyze a variety of materials without the need for extensive sample preparation. Indeed, one of the motivating factors behind this research is the potential to analyze soil samples in their natural, unperturbed state with a portable LIBS system. However, before this can be achieved the technique must be validated in the laboratory, and this presents the question of how to prepare the sample for measurements with as little modification as possible. In addition to this, an optimized sampling regime must be established that accounts for the chemical and physical heterogeneity of soil samples and maximizes the information obtained during the analysis.

Sample Presentation

Pressed Pellets vs. Mounting Tape

The majority of research that has been conducted on soils has involved grinding soil samples in a ball mill and using a pellet press to produce tight, compact pellets.^{44,47-50,54-58} There are many advantages to using pressed pellets for LIBS; most significantly, the sample surface is completely flat and there is uniform mass ablation. However, pressing pellets is time consuming, can introduce contamination and often requires the use of binders, many of which contain carbon and are therefore precluded in carbon analysis. In addition to this, the pressure used during the pellet production will have a direct effect on the mass ablated and the LIBS signal. As such, it must be ensured that the exact same pressure is applied for each sample, no easy feat with a manual pellet press. Finally, and possibly the most compelling disadvantage, pressing soils into pellets completely destroys the integrity of the soil sample such that subsequent LIBS analysis will in no way simulate the analysis of the same soil in its natural state. Simply, if laboratory analysis is conducted on pressed pellets, then in order for the results

to be valid for in-field analysis, samples must also be pressed into pellets. Obviously, this additional sample preparation defeats the high throughput capability desired for the portable instrument.

An alternate method of sample presentation is to mount the sample on a microscope slide using double-sided foam mounting tape. This is achieved by attaching the desired area of tape onto a standard microscope slide and removing the backing to expose the adhesive. The tape is then firmly pressed onto a thin layer of the sample and the excess, unstuck sample is gently tapped away. The tape is then fully covered with a monolayer of practically undisturbed soil particles. The so-called mounting-tape sample preparation method is very quick, cheap, introduces few contaminants, and minimizes sample modification. Due to these very attractive qualities, it was the method of choice for sample preparation during this research.

In order to study the effects of the using the mounting tape sample preparation, LIBS analysis was performed on a pressed soil pellet and the same soil mounted on a microscope slide (Figure 4-1). The soil pellet was prepared by applying in excess of 16,000 psi for 30 seconds. One drop of water was added to the pellet before pressing to make the sample more cohesive. In general, a binder would be used for this task; however common binders such as cellulose and wax contain carbon and would therefore interfere with the LIBS carbon signal. The resulting pellet was 13 mm in diameter with a height of approximately 4 mm. Both samples were analyzed using the same laser and spectrometer parameters (pulse energies of 57 mJ, a delay time of 1 μ s and repetition rate of 1 Hz). For the slide sample, two laser shots were used for each of 50 sample spots and data from each shot were collected (termed first-shot and second-shot). The purpose for this double-shot analysis will be discussed later in the chapter. The resulting 50 spectra were collected, and the average integrated C247 peak was determined for both the first

and second shot measurements. For the pellet sample, measurements from 5 separate sample spots were collected. Each spot was subjected to 5 cleaning shots (to remove contaminants imparted by the pellet press) and 10 subsequent measurement shots. The C247 signal was averaged for each of the five spots, and then the average C247 integral was determined for the whole sample.

The soil sample chosen for this comparison contained 9.15% carbon. All soil carbon concentrations in our research were measured by dry combustion at the Department of Chemistry's CHN laboratory using an Elemental Analyzer from Carlo Erba Instruments operated at a temperature of 1020°C and using a sample mass of approximately 2 mg. The average C247 peak area produced from 50 second shots on the microscope slide was 35.4 ± 4.6 , an RSD of 11.7%. The average for 5 spots of 10 shots on the pellet was 18.1 ± 2.9 , an RSD of 16.3%. One possible reason for significant decrease in C247 signal for the pellet was that much less mass was ablated than for the microscope slide mounted sample. As the pellet was produced under great pressures, the sample was highly compacted and the laser energy penetrates less into sample, ablating less mass. Moreover, inspection of the C247 signal as a function of shot number on the pellet indicated that crater effects were contributing to the poor precision. As the number of laser shots increased on a spot, the crater became deeper which resulted in a greater LTSD and FTSD as well as shielding of the plasma by the crater walls. This is evident by the decrease in C247 signal as the shot number increased (Figure 4-2).

Based on these results, the use of microscope slides to mount the soil samples was judged superior to pressed pellets for LIBS measurements due to increased mass ablation and measurement precision. In addition to this, mounting the soils on microscope slides maintained

the original physical properties of the soil, and as such allowed for further studies of the effects of grain size on LIBS signal.

Analysis of Bare Mounting Tape

The tape that was used to mount the sample to the microscope slide was produced by Scotch 3M and consisted of a foam center coated on both sides with an adhesive. The foam backing and the adhesive coating are composed of acrylic and vinyl polymers which contain high concentrations of carbon. For this reason, the tape was extensively analyzed to determine the extent of carbon interference. First, nine separate measurements on different spots of the bare tape were collected. The C247 line was not detected in any of them (Figure 4-3a). Following this, 12 shots were collected on the same spot of the tape. Each of the resulting spectra were compared, and it was determined that carbon was not detected after the first shot; however, it was detected after subsequent shots (Figure 4-3b). A plot of the shot number directed on the same spot and the resulting C247 intensity showed that the maximum amount of carbon (approximately 55 counts under these specific instrumental conditions) was detected for the second laser shot, after which time the signal decreased, until a plateau was reached after 6 shots (figure 4-3c). To investigate the reproducibility of this phenomenon, 10 pairs of shots were taken on the tape. In each instance, the first shot yielded no carbon peak and the second shot produced a carbon peak of with a net intensity of approximately 60 counts (Figure 4-3d).

Images taken of the ablation spots after a number of different laser shots illustrated that the first laser shot did not produce a discernible crater and the surface of the tape merely exhibited signs of localized melting. It is possible that the breakdown threshold of the acrylic adhesive is not reached under these sampling parameters; however the first shot modified the surface of the tape, allowing for the second shot to produce plasma and for carbon detection to occur.

Regardless of the mechanism, this occurrence suited the purposes of this research well. During

the soil measurements using the mounting tape substrate, no more than two consecutive measurements were taken on the same spot. If the soil acted as the first barrier and the acrylic adhesive of the tape acted as the second barrier, it would have required at least three shots on the same spot to produce carbon interference from the tape.

Grain size

All natural soils are classified according to % sand, % silt, % clay and as such exhibit a wide range of particle sizes both between and within a soil sample. Previous research by Wisburn *et al* revealed that the slope of the calibration curve decreases with decreasing grain size for analytes that are primarily present as surface contaminants.⁵⁰ In order to study the effect of matrix grain size on the C247 signal, five different particle size fractions of quartz (SiO₂, Alfa Aesar) were spiked with graphite (pure carbon) and measured. Quartz was chosen as the matrix due to its physical and chemical similarities to the main components of soil. Separation of the quartz sample into different size fractions was achieved at the University of Florida's Soil Science Department by sieving and water separation. The resulting fractions had particle sizes in the following ranges: >500 μm, 250-500 μm, >30 μm, 18-30 μm, <18 μm and 0.5-1 μm. However there was not enough of the last sample for LIBS measurements. Samples of each size fraction were then spiked with 0-19 % graphite by weight. The method of sample homogenization was critical in maintaining the uniform particle size of the sample. The usual method involved adding small, methacrylate balls to the sample and blending in a ball mill for a specific period of time. The methacrylate balls produced a homogeneous matrix by breaking up and mixing the particles; however, this significantly decreased the grain sizes. In addition to this, microscopic inspections of the samples after blending with plastic mixing balls indicated that the quartz particles were not uniformly covered with the graphite. This uneven coating is possibly due to the mixing balls continuously knocking the graphite off the particle. In order to

maintain the same grain sizes and ensure uniform coating, the samples were milled for 15 minutes without mixing balls. Microscope images were taken of each sample after it had been affixed to a microscope slide using a Nikon Labophot microscope with a 4X magnification (Figure 4-5). It is clear that graphite was much more homogeneously distributed in the quartz samples of smaller grain size than the larger ones. In addition to this, as the concentration of graphite in large grain size quartz matrix increased, the number of quartz particles decreased and the graphite coated larger areas of the tape surface. This resulted in some of the laser shots sampling 100% graphite and significantly affected the precision of the sampling.

The average integrated C247 peak of 25 separate measurements on each sample was determined and a plot of signal vs. carbon concentration was constructed for each of the particle fractions (Figure 4-6). The statistics for each size fraction (Table 4-1) illustrate how the precision of the measurements significantly increased as the particle size of the matrix decreased. This trend was expected considering the higher degree of heterogeneity associated with the larger grain sizes. The homogeneity of the smaller grain sizes resulted in sampling that was more consistent and representative of the bulk sample. Table 4-1 also illustrates how the slopes of C247 signal vs. carbon concentration decreased with the particle size. This was in agreement with the results of Wisburn *et al.*⁵⁰ The decreasing slope was due to the decreased mass of carbon that was sampled per shot as the particle size of the quartz matrix decreased. As illustrated in the microscope images of the samples (Figure 4-5), the larger quartz particles were completely coated in graphite which concentrated more graphite into the ablation area of the laser beam. However, as the particles became smaller and closer in size to the graphite particles almost no coating occurred, and the graphite and quartz were more independently distributed resulting in fewer concentrated areas of carbon and a more homogenous mixture.

One troubling detail evident in Figure 4-6 is the large C247 signal that was produced with the blank quartz samples, especially for the three smaller particle size fractions. The initial assumption was that the bulk quartz sample contained some carbon contamination. To measure this, each of the five size fractions was analyzed by dry combustion. The results indicated that trace amounts of carbon were present, with the concentration increasing as the particle size decreased (Table 4-1). Indeed, the 0.5-1 μm quartz fraction, which was not used for the LIBS analysis due to limited sample, had a carbon concentration of 0.118%, 10 times greater than the carbon concentration of the 500 μm fraction. In spite of this, such a contamination is still very small, less than 0.1% for the quartz samples used in this study, and could not account for such a large carbon signal.

To further study this, the smallest grain size fraction was pressed into a pellet and measured by LIBS. Several cleaning shots were used to remove surface contaminants introduced by the pellet press, and a total of 20 measurements were taken. Interestingly, the carbon peak was not detected. Based on these results, it can be concluded that the quartz sample was not contributing to the large carbon signal in the blank particle size fractions. The only available source of carbon was the mounting tape, yet previous studies had exhaustively shown that no carbon was detected on the tape after the first shot, and only a small peak was detected for subsequent shots, the magnitude of which did not account for the large carbon signal. In spite of this, LIBS measurements were taken on bare tape and then immediately on fresh quartz covered tape to monitor the difference in carbon measurements. As expected, no carbon was detected on the fresh tape, however on the quartz covered tape a large carbon peak appeared.

The mechanism behind this amplified carbon detection on the tape is unknown; however, it seems that small particles adhere to the viscous adhesive resulting in a physical or chemical

change to the LIBS plasma causing the carbon ablation from the tape to increase. To evaluate this supposition, extensive studies of the plasma diagnostics as a function of particle-tape composition would be required. Such an investigation would be the content of a full PhD study. However, it should be noted that the magnitudes of the carbon signal for each of the three blank quartz size fractions were very similar, indicating that this may be a fairly constant interference that could be accounted for by merely subtracting the blank signal from the spiked sample signals. Another assumption that could be made is that this tape-carbon enhancement effect seems limited to samples of very fine powders, unlike the rather coarse soil samples used in this research.

The results of this quartz particle size study illustrated the great dependence of LIBS signal on matrix particle size and analyte distribution. It is clear that LIBS measurements performed on soils that have a high % sand composition can not be directly compared with soils that have a high % clay composition. It is also clear that soils with high % sand compositions will likely yield intolerable precision which will preclude accurate quantitative results. However, there were many variables that were not considered in this study which limited the direct application of these results to natural soils. For instance, the form of carbon in this study, graphite, in no way simulated the actual sources of carbon in soil, mostly organic acids, biological materials and inorganic carbonates. This difference will undoubtedly significantly affect the plasma properties and the resulting carbon signal. In addition to this, the distribution of graphite in quartz is not truly representative of how carbon is distributed in natural soils, where it may either be trapped inside particles, heterogeneously coating them or as free organic matter. One final consideration is the actual matrix itself, which is certainly more complex than simple quartz and may contain many elements that may chemically or physically interfere with carbon. Natural soil matrices

also exhibit a wide particle size distribution unlike the almost uniform quartz particle size fractions which were used in this experiment.

Sampling Characteristics

Number of Laser Shots

The number of measurements on a soil sample was a very important parameter that was directly related to the precision of the analysis. As previously discussed, soils are inherently heterogeneous and any given soil sample will be composed of a variety of particles exhibiting an array of different physical and chemical compositions. To illustrate this fact more clearly, Figure 4-7 shows microscope images of three soil samples which exhibit different organic content and particle sizes. The yellow circles superimposed on the images represent the approximate area that would be ablated by the focused laser. This was determined by the diameter of the crater produced on copper foils under the same conditions and was about 0.35 mm². It is plain to see that each laser shot will be sampling very different sized particles of visibly different composition (for reference, the dark particles are likely organic matter whereas the translucent particles are likely silica). This heterogeneity can partially be compensated for during LIBS measurements by increasing the mass analyzed (defocusing the laser to increase the ablation area) and averaging out the differences by taking a many more measurements. However, defocusing the laser risks decreasing the energy density of the laser and not forming a breakdown. Instead, increasing the number of laser shots, and therefore the total mass analyzed was preferred.

To investigate how the number of laser shots (on separate sample spots) affected the precision, LIBS measurements on two dried soil samples were collected. One of the soils had low organic content and high % sand and the other had high organic content and was less coarse. The samples were fixed to a microscope slide and subjected to 50 laser shots; the sample was

manually moved between each shot to ensure fresh sampling. The RSD of the background subtracted C247 intensity was noted after each subsequent shot (Figure 4-8). It was found that for both soils, regardless of their physical or chemical differences, the RSD was relatively constant after 20 shots on different spots. To further investigate the effect of the number of laser shots on the RSD, three microscope slides were prepared of the same soil and each slide was subjected to as many separate laser shots as sample availability would allow, approximately 290 shots per slide and 856 shots total. The average C247 signal was then calculated for each individual slide, and for all 856 shots (Table 4-2). Surprisingly, increasing the shot number up to 290, and even to 856, did not improve on the RSD achieved after only 20 shots. In addition to this, the differences in both average C247 peak area and the associated RSD between the slides were very small, indicating that the intra-sample precision for the technique, when using greater than 20 shots, is high. However, the inter-sample RSD of 19% was rather high and will certainly affect the accuracy of the results. However, these experiments revealed that the greatest contribution to this poor precision is not the LIBS technique, but rather the soil heterogeneity itself, something that can only be improved by excessive grinding and milling. Therefore, if little sample preparation is desired, the inherent heterogeneity of the soil will contribute to the poor precision.

Repetitive Laser Shots

Wisburn *et al.* also reported on the occurrence of a persistent aerosol that was formed over the sample surface after the first shot on the soil and contributed to enhanced signal intensity after the second shot in the same spot. However, it was reported that this phenomenon was only achieved at repetition rates in excess of 1 Hz and all results were produced on soil pellets.⁵⁰ However, measurements obtained from the same spot on tape-mounted soil revealed that even at repetition rates of 1 Hz, greater signal intensity was achieved for the second shot on the same

spot. This was surprising since to the naked eye, it looked as though there was no soil left to sample after the first shot, least of all the second shot. Initially it was thought that the carbon signal increased because the second shot was measuring only the carbon from the mounting tape, and indeed, based on the adhesive-particle carbon enhancement reported previously, this may be a contributing factor. However, this significant increase in signal occurred across the entire spectrum and not just for carbon. A plot of signal intensity vs. shot number for carbon and calcium (which was certainly not present in the tape) revealed the same trend (Figure 4-9 a,b). The carbon signal was prevalent until around the 175th shot on the same spot and the calcium signal was prevalent until the 80th shot. One explanation was that airborne particles that had been liberated from the sample by the force of the plasma shockwave were either entering into the plasma or interacting with the laser beam along its axis and forming mini-plasmas. When watching the sampling in the dark, it was easy to ascertain these small plasma events occurring up to an inch above the sample surface. The emission from these small independent plasmas was likely contributing to the long lifetime of the calcium and carbon signals.

To reduce this effect, which decreased the amount of laser energy available for the next sampling spot, a stream of air was directed over the target surface to sweep any loose particles from the sampling areas. This drastically decreased the number of laser shots that still produced carbon or calcium emission, however, even with the air stream carbon and calcium could be detected until approximately the 20th shot (Figure 4-9 c,d). The greatest difference was that without the air, the emission intensity for both elements was very random, increasing or decreasing with no discernable pattern. Yet with the air stream, the emission intensity reached a single maximum, usually after the first or second shot, and exponentially decreased to zero after 10- 20 shots (it takes longer for the carbon signal to disappear due to the carbon being measured

in the mounting tape). To ensure that this increase in signal intensity after the second sampling shot was reproducible, a suite of 38 soil samples were analyzed with 100 laser shots on the same spot. For each soil, the maximum carbon signal was achieved after varying numbers of laser shots (between 3-6 shots) but never after the first shot. The same pattern was seen for iron, though the shot number for the maximum iron signal did not correspond to that of carbon (this was achieved between shots 2 and 4).

Microscope images of the tape-mounted soil after one laser shot show that there was no discernable crater and the soil sample had not been ablated through to the tape surface (Figure 4-10). The tape had a very distinctive surface composed of small bubbles and was easy to recognize. The soil sample remaining after the first shot was a very fine powder with no individual particles visible at 4X magnification. The cause of this signal enhancement after the second shot was not fully understood, however it was hypothesized that the first laser shot prepares the sample surface to provide for maximum ablation efficiency during the second shot. That is to say, the energy from the laser pulse interacts with more sample in the second shot than it does in the first shot. The particles of the original soil samples were often larger than the diameter of the focused laser beam and as such it is plausible that the plasma was formed on the surface of one particle, shielding any sample adhered to the surface of the tape from ablation and possibly wasting energy from the laser pulse if only a portion of the pulse was used on the particle during ablation (Figure 4-11). However, the combination of the initial laser pulse, the resulting plasma shockwave and the continuous air stream sweeps the area of any large particles, leaving a thin, uniform monolayer of soil powder. As such, when the second laser pulse interacts with the sample, the entire laser pulse interacts with sample without any large particles obstructing part of it. Regardless of the mechanism for the second shot signal enhancement, it

was clear that sensitivity could be increased across the spectrum by utilizing repetitive shot sampling; one initial preparatory shot and a second shot on the same spot from which data is collected.

Conclusion

As a result of the preceding observations, a sampling regime optimized for possible soil analysis was evaluated. The advantages of mounting the soil samples on a microscope with adhesive tape, namely simplicity and maintaining particle size integrity far outweighed pressing the samples into pellets. Furthermore, it was determined that for at least one soil sample, the precision of C247 LIBS analysis on the slide exceeded that of the same soil in pellet form. While this may not be the case for all soils, it was deemed an acceptable trade-off considering the ease with which slides could be prepared in-field. While evidence indicates that there may be some physical or chemical process occurring between the small sample particles and the tape adhesive that resulted in enhanced carbon signal from the tape, this was assumed to be a constant contribution for each laser shot. A study of matrix grain size on LIBS signal revealed that there was a significant effect on the C247 signal intensity and RSD. Ideally, when measuring different soils they should be all be ground and homogenized to approximately the same size in order to minimize grain size effects between samples and to increase precision. However, since this would not be a feasible option for in-field analysis, care should be taken that only soils containing similar particle size distributions are compared.

With respect to the sampling population, it was established that a minimum of 20 laser shots should be taken on a soil sample in order to account for the heterogeneity of soils. Taking many more than 20 laser shots did not seem to improve the RSD. Finally, it was determined that using a preparatory laser shot on the soil surface before the sampling shot significantly increased the signal intensity of the entire spectrum. It should be noted however that for 38 soil samples,

the C247 signal intensity from the first and second shots were proportional, with an average increase of 1.7 observed for the second shot. However, due to the weak nature of the C247 line, the increase in sensitivity was exploited and second shot measurements were employed for the majority of this research.

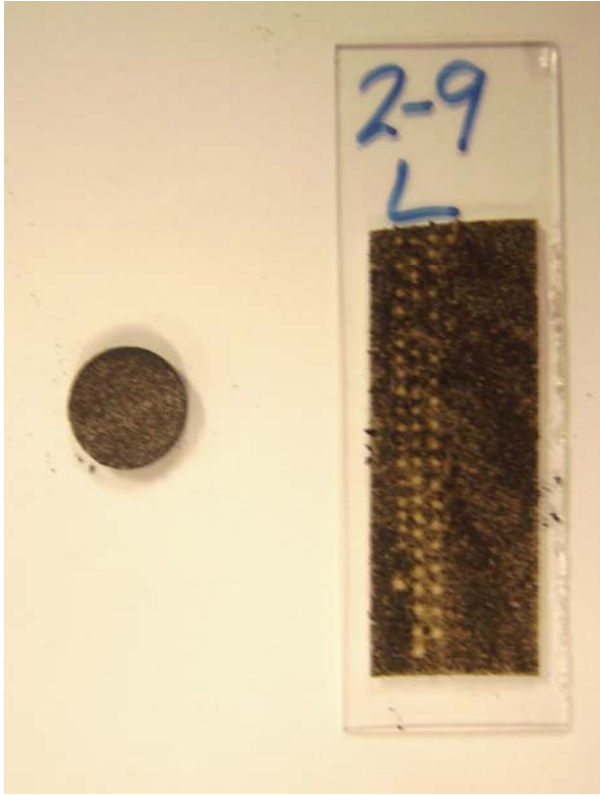


Figure 4-1. An image of a pressed pellet and soil mounted on a microscope slide.

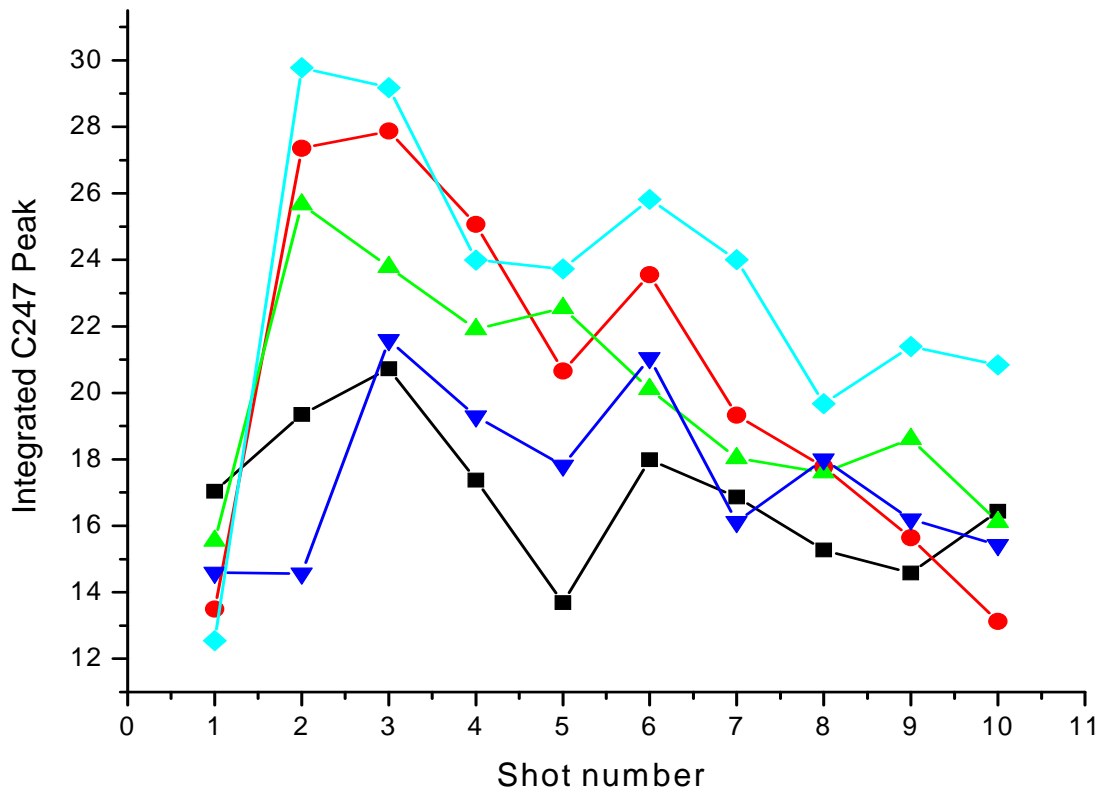


Figure 4-2. C247 signal as a function of shot number on the same pellet spot for five different locations.

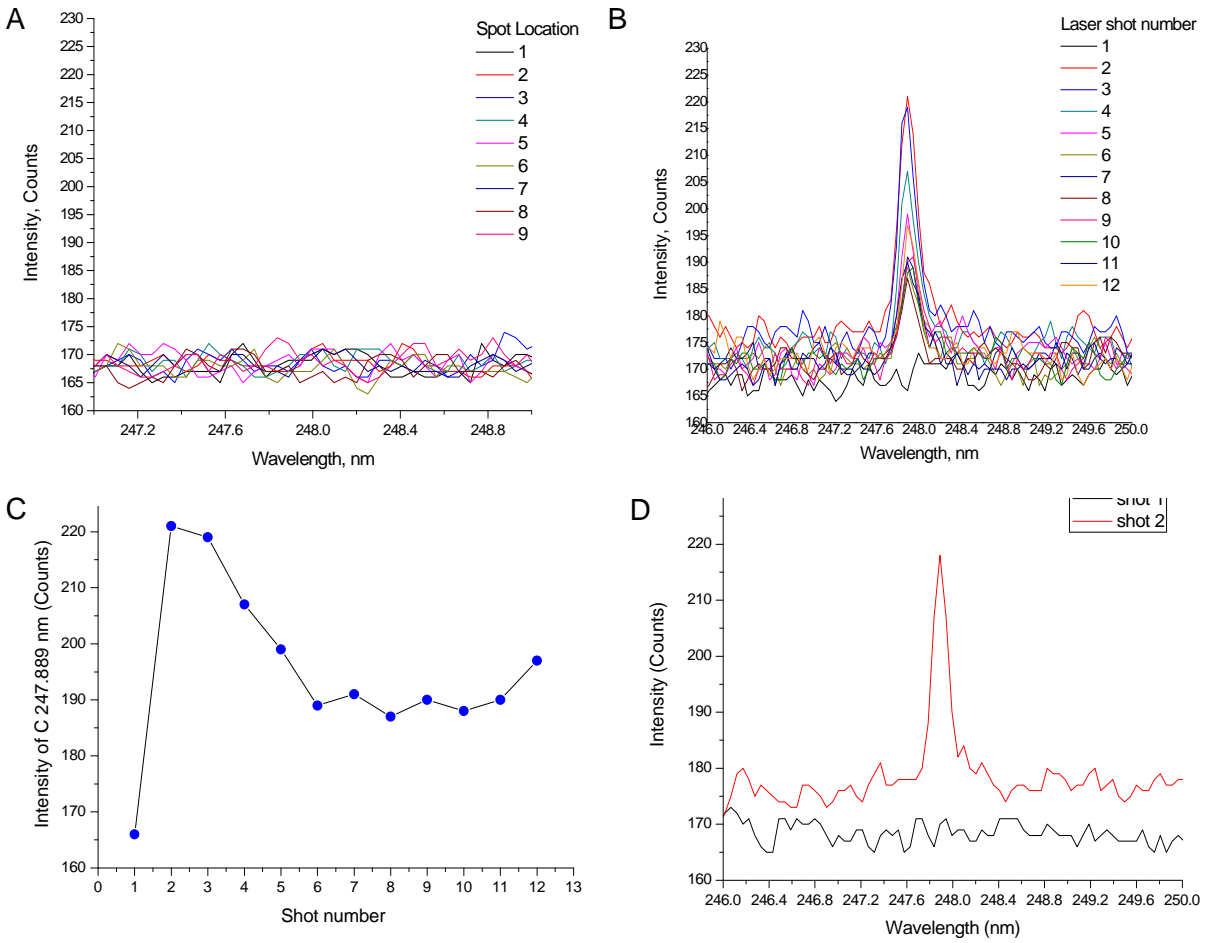


Figure 4-3. Analysis of bare mounting tape. A.) Spectra from 9 different locations of the tape surface. B.) Spectra from 12 consecutive shots on the same tape spot. C.) The C247 signal intensity as a function of shot number on the same spot. D.) Spectra from the first and second shot on tape.

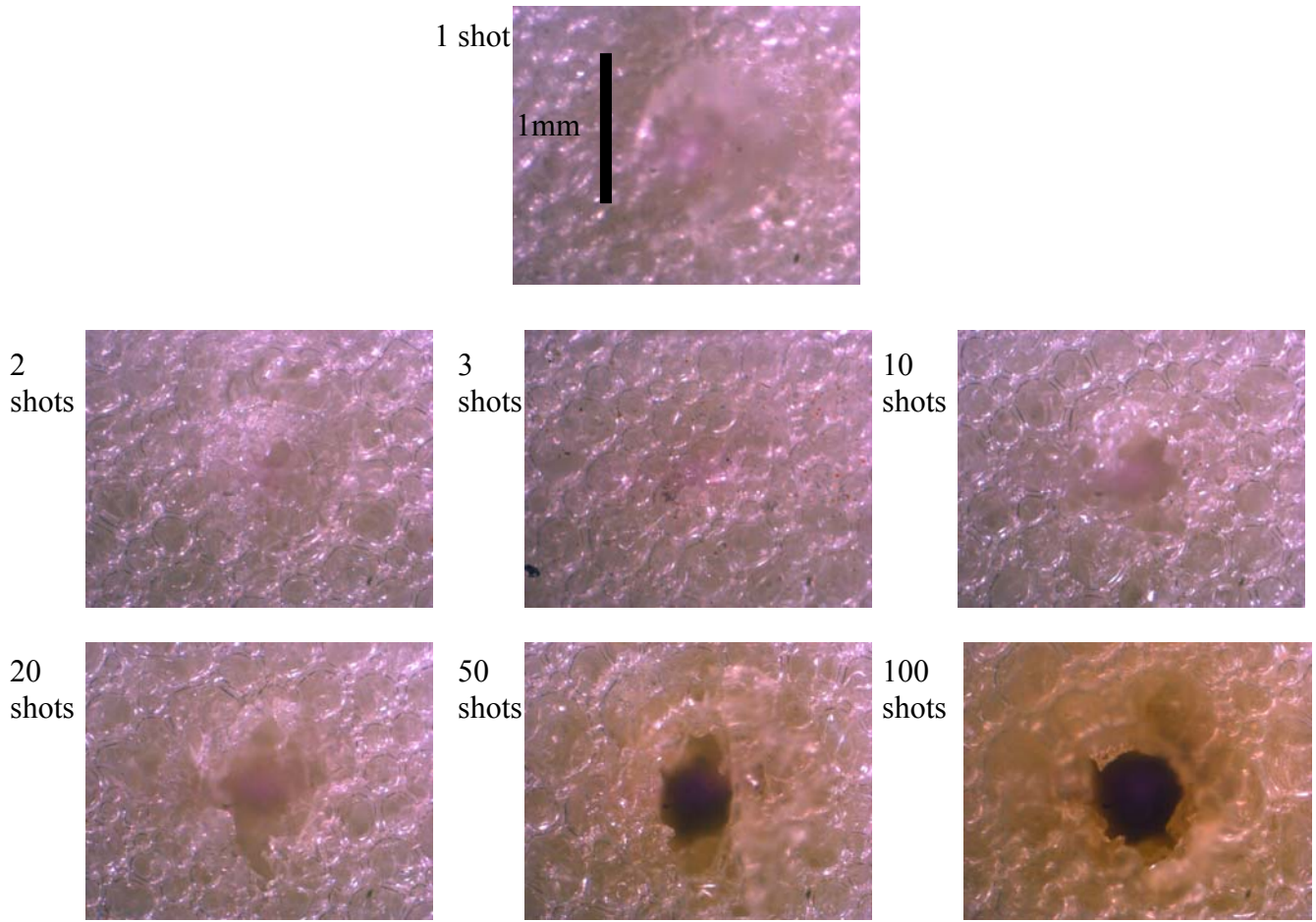


Figure 4-4. Microscope images (4X magnification) of the craters produced on mounting tape after the indicated shot number.

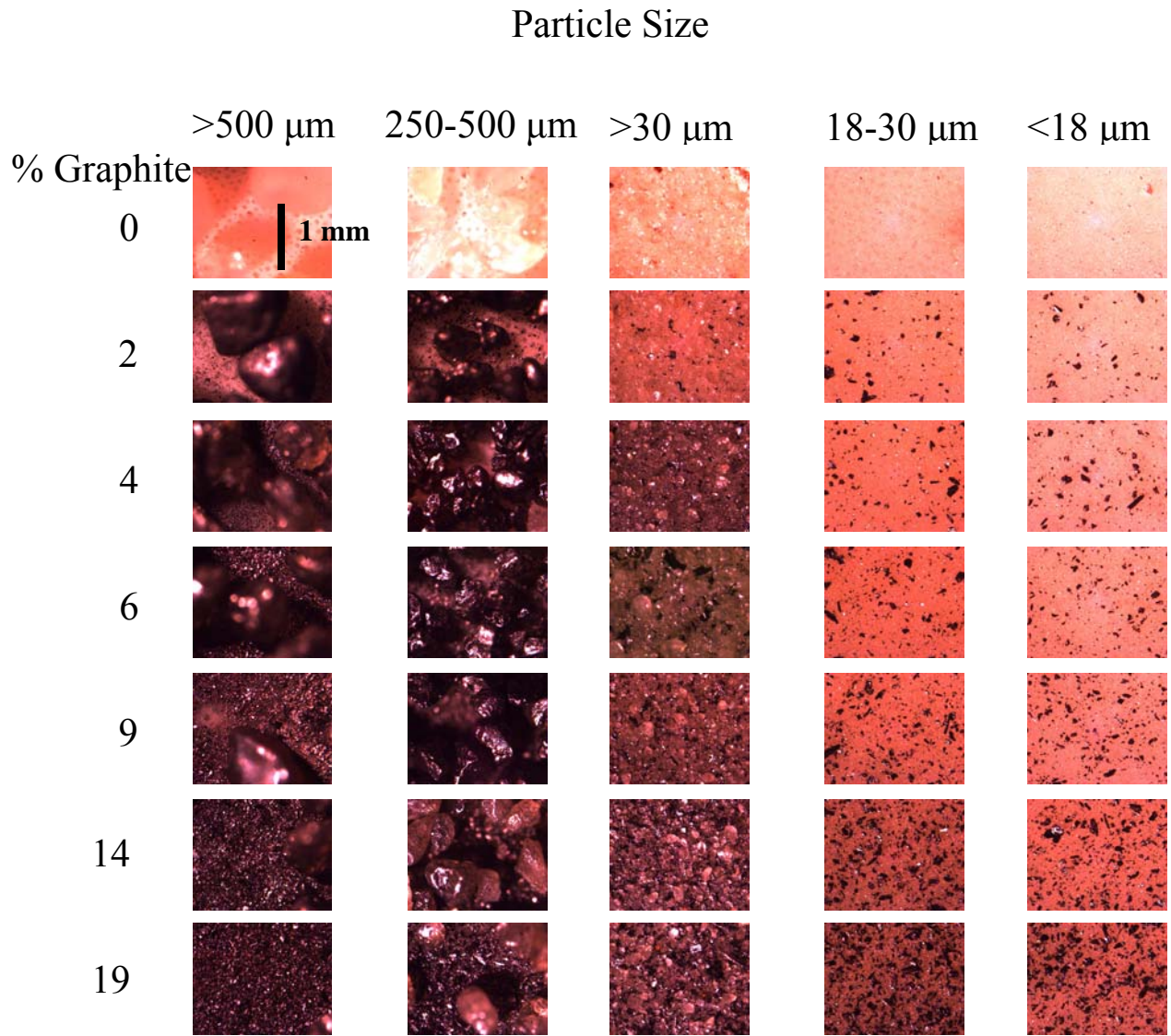


Figure 4-5. Images of different quartz fractions spiked with graphite (4X magnification).

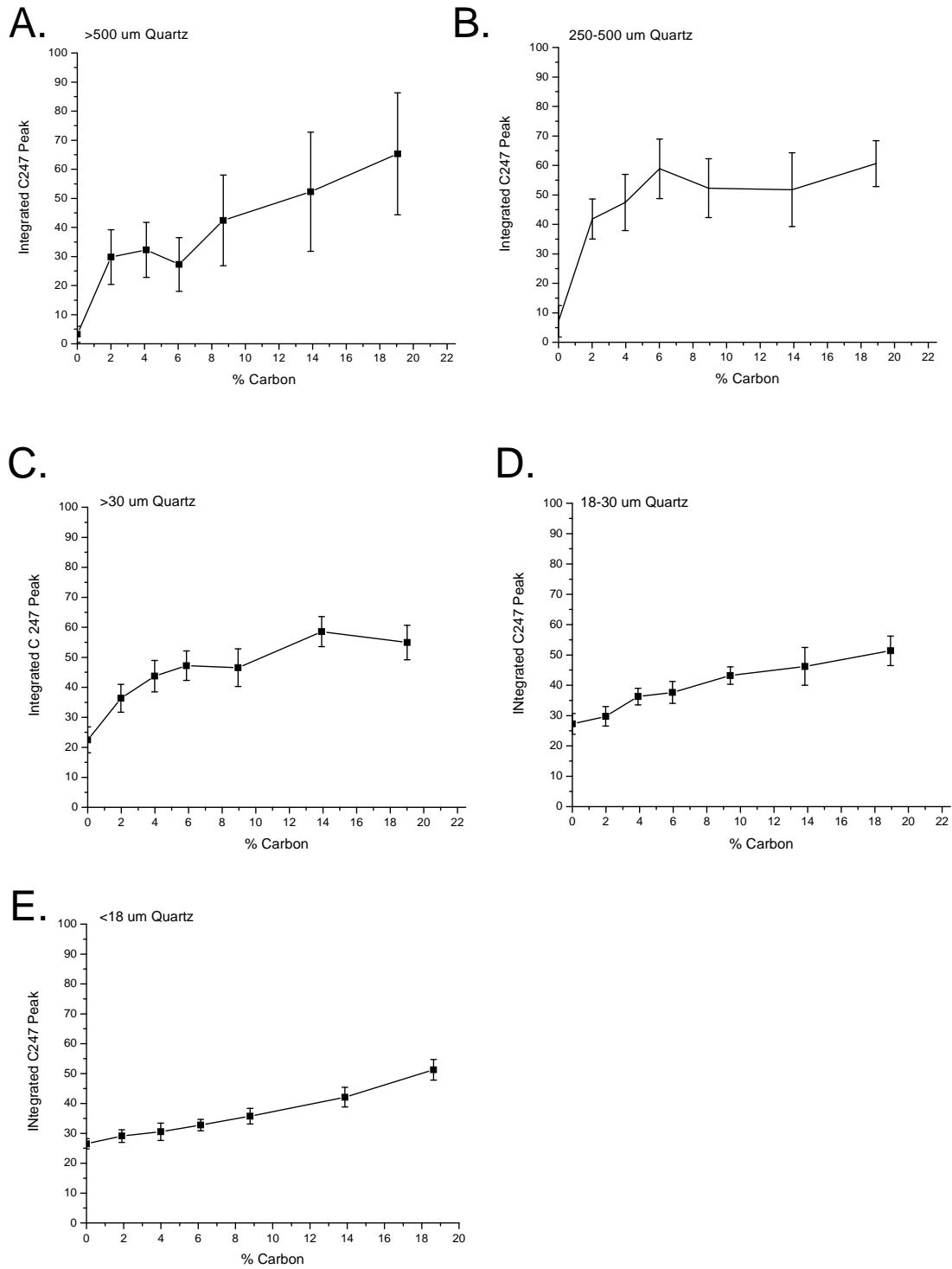


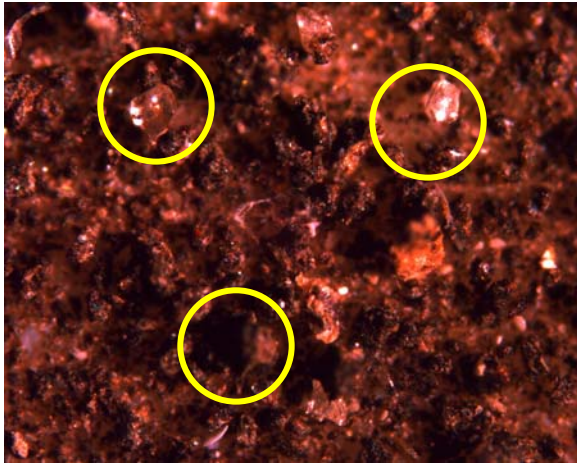
Figure 4-6. C247 peak as a function of carbon concentration (wt %) for different particle sizes of quartz matrix (error bars are ± 1 standard deviation).

Table 4-1. Statistics for the analysis of quartz size fractions spiked with graphite

Quartz particle size	Average RSD for all carbon concentrations (%)	Correlation coefficient (R)	Slope (C247 area/% C)	Carbon concentration (wt %) ^a
>500 μm	40 \pm 20	0.9143	2.74	0.01
250-500 μm	26 \pm 21	0.7554	1.83	0.001
>30 μm	12 \pm 21	0.8691	1.52	0.016
18-30 μm	10 \pm 2	0.9657	1.25	0.020
<18 μm	7.2 \pm 1.2	0.9898	1.30	0.034
0.5-1 μm ^a				0.118

a) Determined by dry combustion. b) Not used in study due to limited sample

4X Magnification



10X Magnification

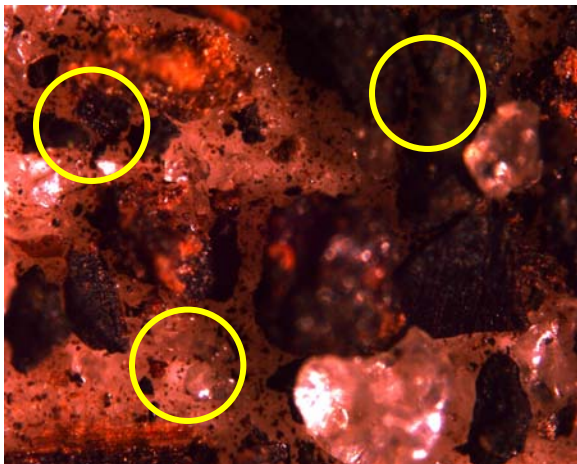
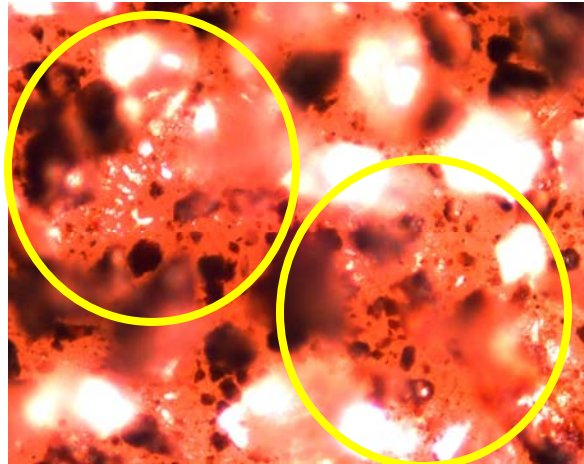
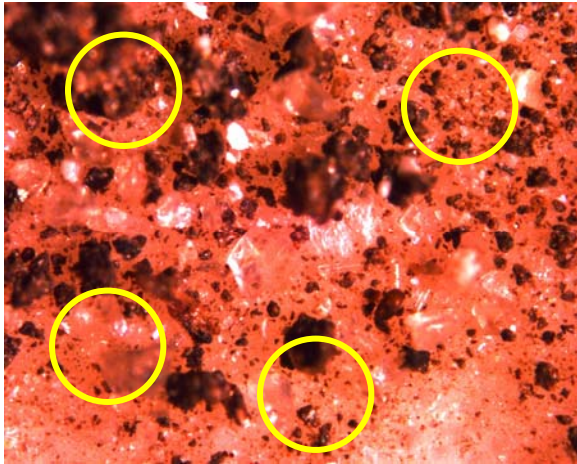
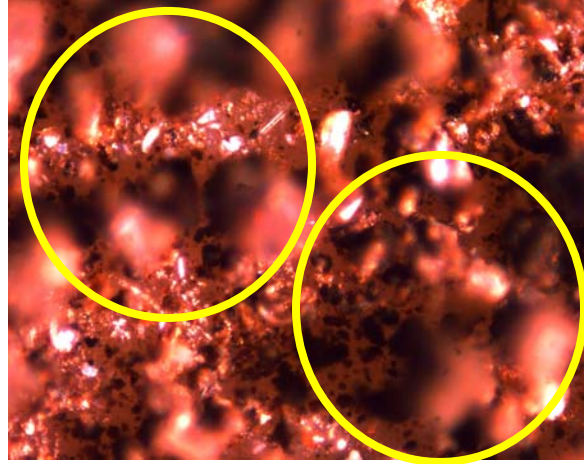


Figure 4-7. Microscope images of three soils to illustrate heterogeneity. The yellow circles represent the ablation area of the focused laser beam, approximately 0.35 mm². (Note: the 10X magnification are not the same areas as the 4X magnification areas)

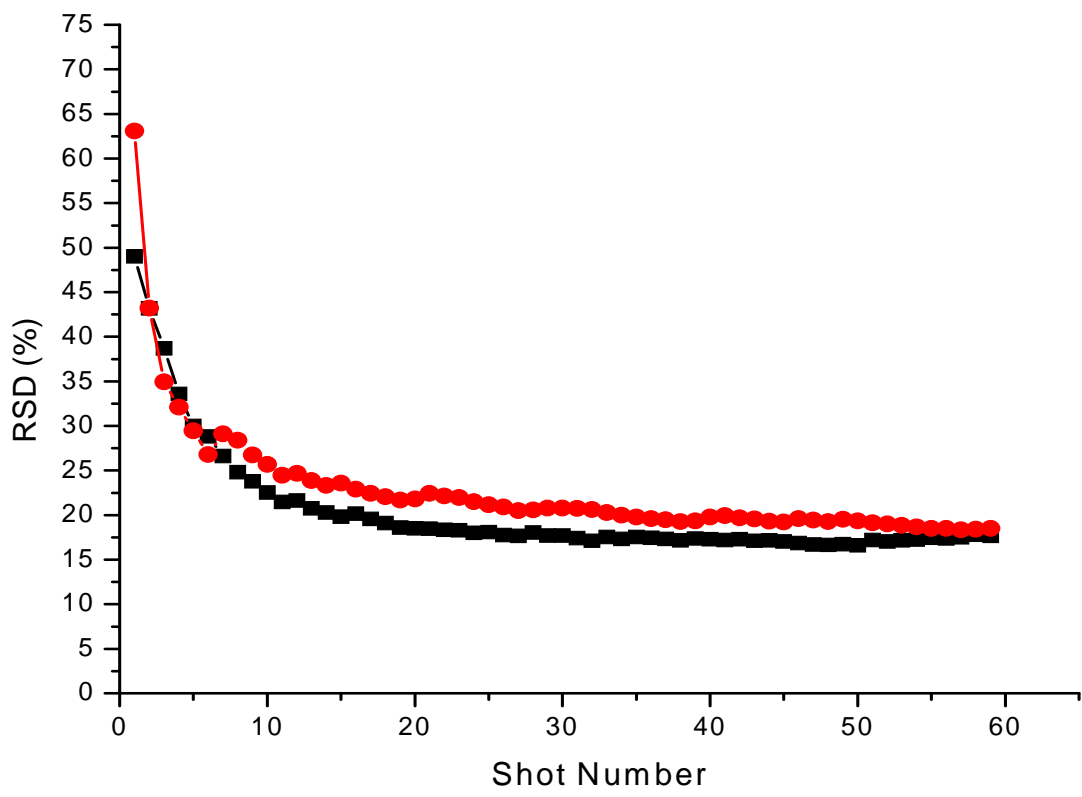


Figure 4-8. The RSD of the C247 signal intensity as a function of the number of shots on separate spots.

Table 4-2. The C247 statistics for intra-sample and inter-sample measurements.

Slide	Number of spots sampled	C247 Area	RSD (%)
A	272	28 ± 5	19
B	293	28 ± 6	19
C	291	27 ± 5	18
Average of the shots taken on all slides	856	28 ± 5	19

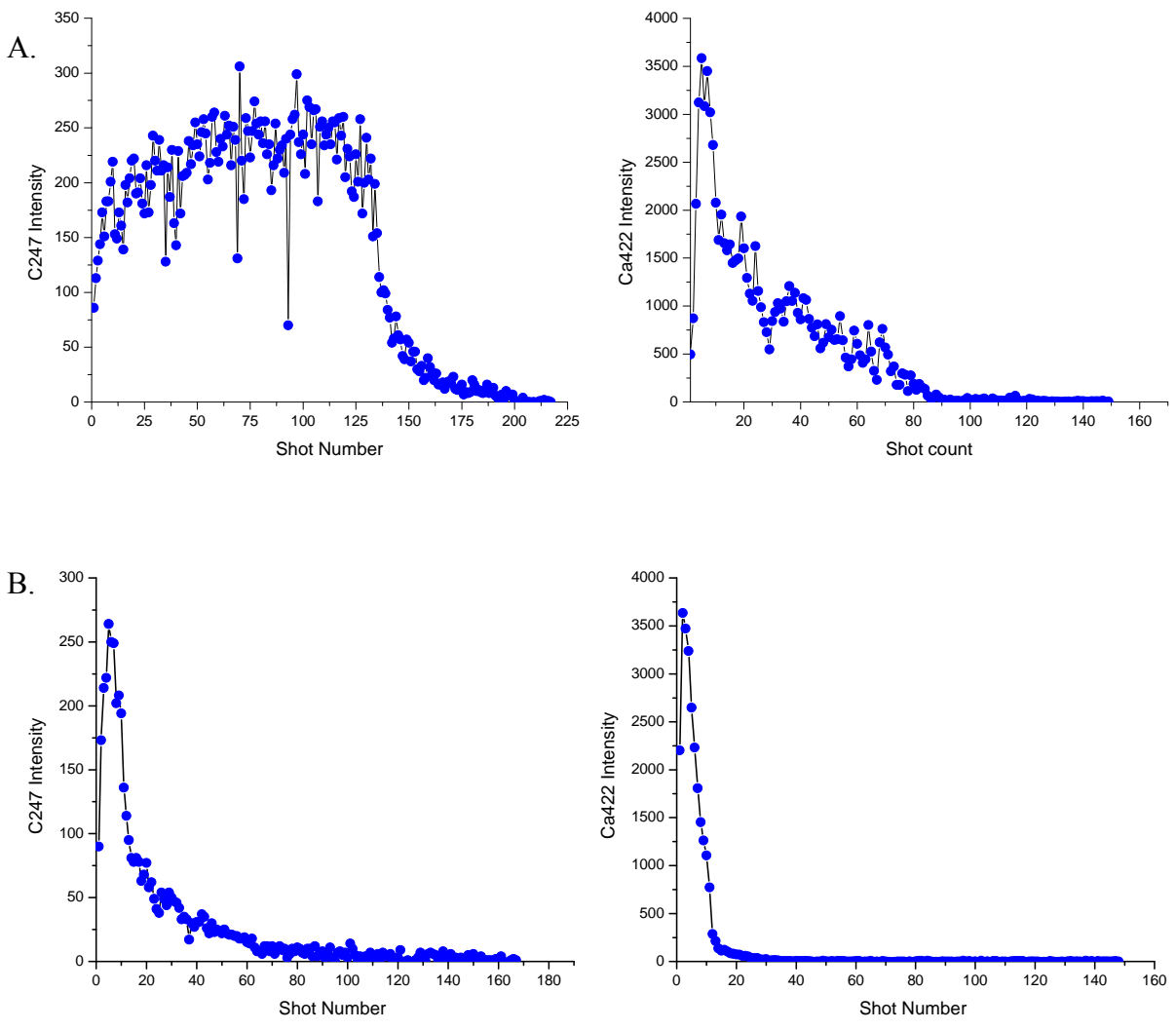


Figure 4-9. The C247 and Ca422 signal intensities as a function of shot number on the same spot A). without air stream B). with air stream.

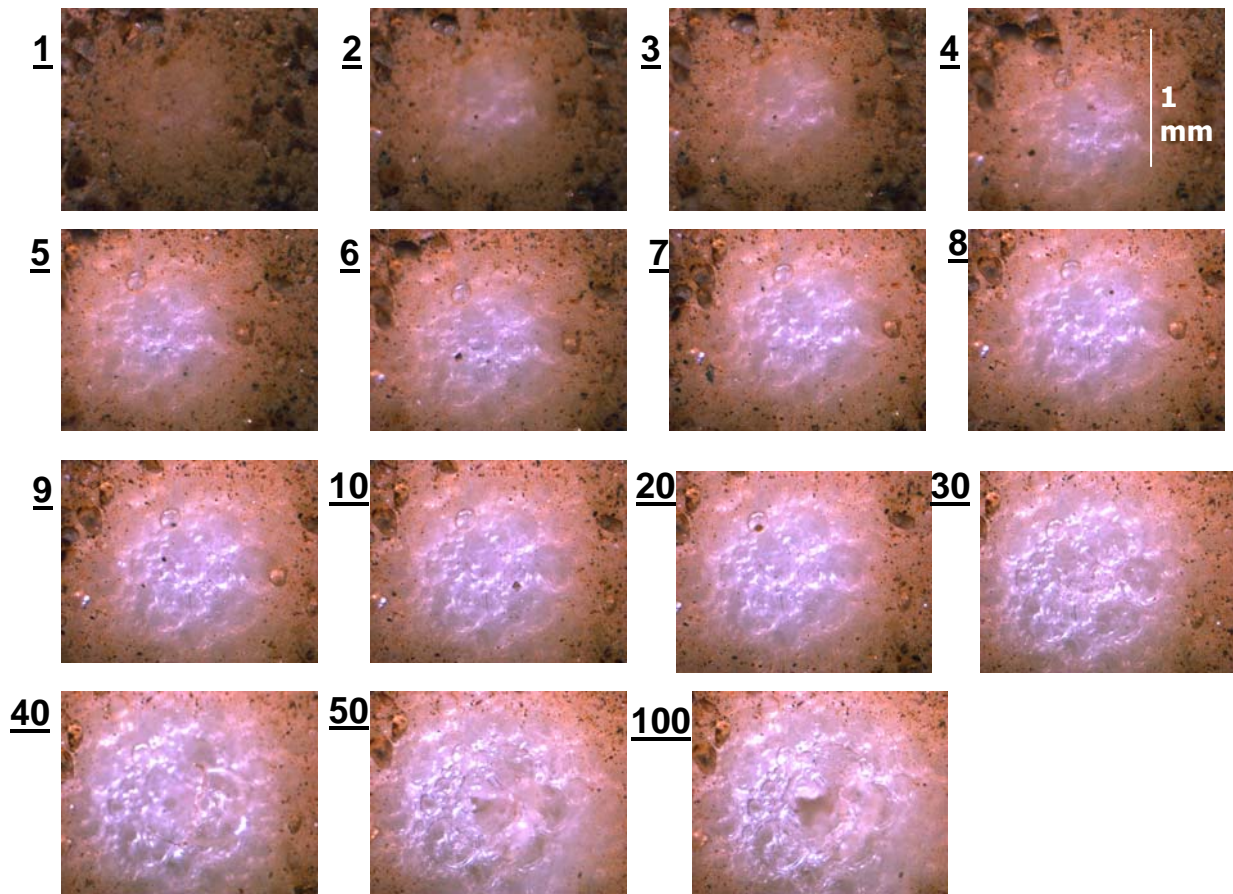


Figure 4-10. Microscope images of soil after the indicated number of laser shots (4X magnification).

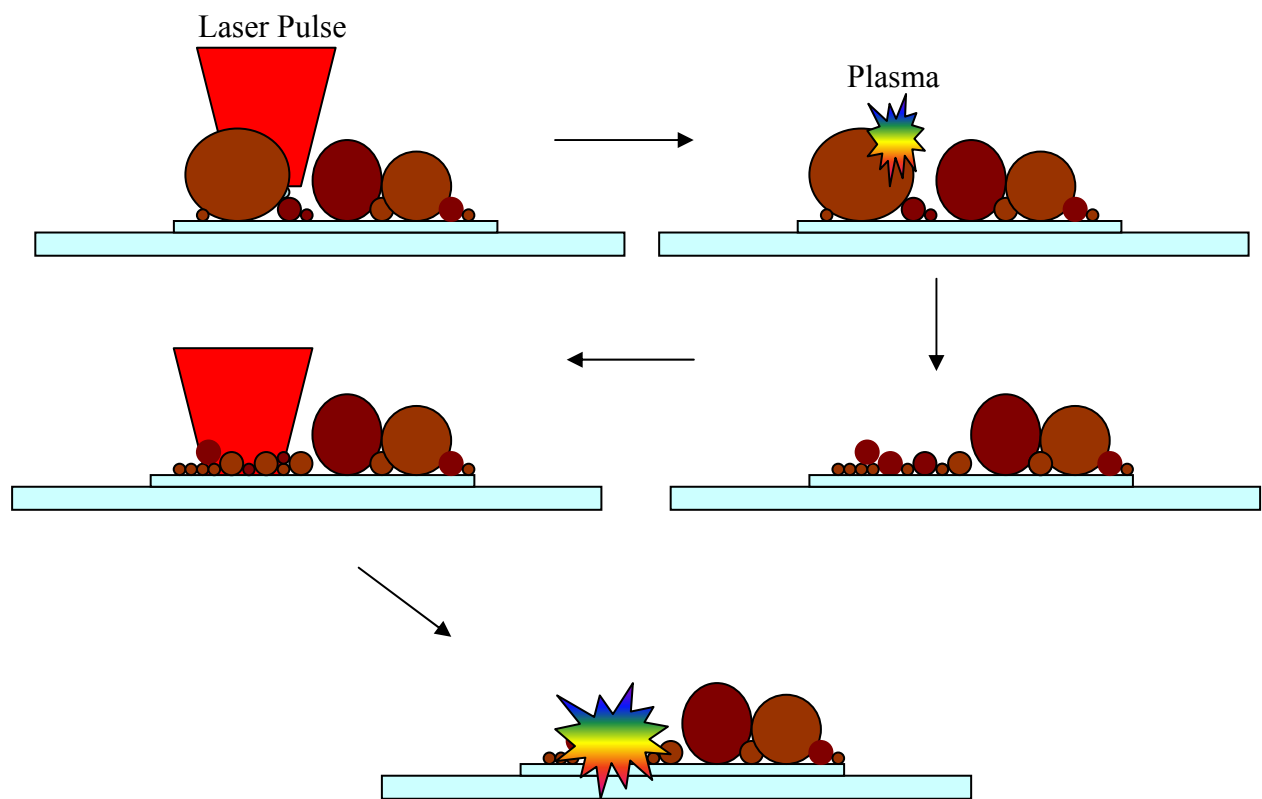


Figure 4-11. Proposed mechanism for the second shot signal enhancement on soil.

CHAPTER 5

THE SPECTROSCOPY OF CARBON AND CALIBRATION CURVES WITH SIMULATED SOILS

The emission properties of carbon have been well studied, especially for the detection and potential quantification of molecular fragments such as C₂ and CN.⁸⁴⁻⁹⁰ Much of the previous work concerning atomic carbon emission has been achieved by monitoring the 247.8 nm line. This chapter will discuss the characteristics of this line and why it was chosen for this research, as well as alternate aspects of the carbon spectrum which were considered for quantitative analysis. The second half of this chapter describes the results of calibration curves that were produced from graphite spiked silica and aluminum silicate powders and subsequent validation with natural soil samples.

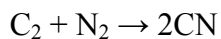
The Spectroscopy of Carbon

Choice of Analytical Line

To determine the best emission line of carbon for quantitative purposes using the Ocean Optics LIBS2000+ spectrometer, emission from the ablation of a graphite pellet was studied. Initially, spectra were taken with no acquisition delay. This was because the ionization energies of the carbon atoms are relatively high, and are therefore expected to be more prominent early in the plasma lifetime, where the temperatures are high enough to sustain emission. When no delay was used, the graphite spectrum showed four emission lines in the UV region: three ions that produce emission lines at 229.6 nm, 251.1 nm and 283.8 nm and have ionization energies of 53.5 eV, 27.5 eV and 27.5 eV respectively and one stronger atomic line that emits at 247.8 nm and has an ionization potential of 7.7 eV (Figure 5-1). When an acquisition delay of 1 μs was applied, the three ionic lines were not detected and the emission intensity of the atomic line decreased. To further study the temporal properties of the C247 emission, spectra were taken on

a graphite pellet using an Acton Spectra-Pro-500i spectrometer with an ICCD detector which allowed for the integration time to be changed. Spectra from the graphite pellet were collected for 200 ns at increasing delay times. The maximum C247 emission was achieved approximately 200 ns after plasma formation, and steadily decreased thereafter as the plasma cooled (Figure 5-2). However, these data did not reflect the high continuum emission that was also occurring at such early intervals in the plasma life time, and even though the C247 emission had substantially decreased by 1 μ s, earlier research, discussed in Chapter 3, revealed that the S/B was at a maximum.

It was initially proposed that the CN bands might be used for quantitative analysis of carbon in soil. However, previous research has indicated that the CN molecule in the LIBS plasma is principally formed through the reaction of a carbon dimer and atmospheric nitrogen:



Evidence indicates that the majority of the C_2 available for this reaction is from the photodissociation of compounds in the sample that contain carbon double bonds or delocalized carbon bonds rather than the recombination of carbon atoms in the plasma.⁹⁰⁻⁹² Because of this, the use of the CN band for quantitative analysis seems relegated to unsaturated organic compounds and not for carbon in soil, which originates from a variety of organic and inorganic sources. Besides, inspection of the CN bands in a spectrum of soil showed that due to the high background in the 300-400 nm spectrometer channel and the multitude of interfering species, the CN band head at 388 nm was unresolved and barely detected, and the two lower wavelength bands at 387 and 386 were not resolved at all (Figure 5-3).

The carbon atomic emission line at 247.8 nm was the most distinct line in the graphite spectrum and was the obvious choice to monitor. Information concerning the energy levels,

relative intensities and exact wavelength for carbon were obtained from the NIST atomic line database.⁹³ In order to assess the accuracy of the LIBS2000+ spectrometer, the actual measured wavelength of 247.837 nm was compared with the true wavelength of 247.856 nm. A difference of 0.019 nm corresponded to less than one pixel and indicated high accuracy in the UV channel. The precision of the spectrometer was also assessed by collecting 100 spectra on a pure, homogenous graphite pellet. The RSD of these measurements was an acceptable 2.4%.

Curves of Growth

To determine the linear concentration limits of calibration linearity, theoretical curves of growth (COG) were constructed using a software program developed in our group. At high concentrations of analyte, a calibration curve is expected to exhibit non-linear behavior, although the actual concentration at which this will occur varies as a function of plasma temperature, electron number density, emission line monitored and matrix composition. The theoretical COG's for the C247 line were calculated assuming a matrix of SiO₂ and plasma temperatures of 8000, 1200 and 16000 K. While the use of such a simplified matrix undoubtedly introduced some error in the results, it would be impossible to account for all components of the soil matrix as well as their relative concentrations. From the calculated theoretical COG's shown in Figure 5-4, it is clear to see that the theoretical integrated C247 peak varies greatly with plasma temperature. For instance, the relative C247 peak areas are 0.0053:0.26:1 for plasma temperatures of 8000 K, 12000 K and 16000 K respectively. Despite the signal disparities for different plasma temperatures, all three COG's indicated a departure from linearity for carbon concentrations in excess of 8 %.

While these COG's provide useful information concerning the theoretical LIBS response, it is important to realize that the inhomogeneity of soil samples precludes the direct use of these calibration curves. As previously discussed, and is evident from Figure 4-7, each plasma that is

formed on a soil surface will vary greatly in chemical composition due to the heterogeneity of the soil composition. In addition to this, the slight differences in LTSD's that the uneven surface topography produces will cause different laser irradiances. Both these factors contribute to highly variable plasma temperatures and electron number densities and because of this, a theoretical calibration curve based on such broad assumptions will not produce accurate results when applied to natural soil samples.

Experimental Calibration Curves

Silica and Aluminum Silicate Artificial Soils

Before any LIBS measurements on soil samples were undertaken, an attempt was made to produce calibration curves for carbon in matrices with chemical compositions similar to the main components of most soils. Due to the complex nature of soils, it would be impossible to produce perfect matrix matched standards; instead, fine silica (SiO_2) and aluminum silicate (Al_2SiO_5) powders were used. Each matrix was spiked with 0-10% graphite powder by weight. The powder mixtures were then homogenized with a ball mill for 15 minutes and mounted on microscope slides as previously described. Approximately 20 spectra were taken on each slide and the average C247 intensity calculated. No preparatory laser shot was used for these analyses because unlike natural soils, these samples were very extremely fine powders and the entire layer was ablated with one shot.

Two things were evident from the calibration curves shown in Figure 5-5. First, both matrices exhibited a definite linear correlation between LIBS carbon signal and the % carbon. Second, the slope for the graphite in silica curve is greater than that of the graphite in aluminum silicate. This is a prime example of how dependent LIBS is on matrix effects; two matrices that are similar in chemical composition, save for the presence of aluminum in one, produced very different LIBS responses. One important thing to note when considering these curves is that

after concentrations of carbon in excess of 6% both curves reach a plateau. When points after 6% were removed from the curve, a linear fit could be applied that produced a correlation coefficient, R , of 0.9880 for silica and 0.9932 for aluminum silicate. It should also be noted that both curves exhibit a non-zero intercept. Samples of silica and aluminum silicate were submitted for dry combustion CHN analysis, which revealed that both contained carbon at concentrations of approximately 0.1 %. However, such a concentration can not explain such a large signal. It was determined that the same particle-adhesive effects were contributing greater carbon from the tape. However, the linearity of these curves up to 6% provide further evidence that this contribution is likely constant for all sampling shots.

When constructing these potential calibration curves, it was realized that their use for natural soil samples would be limited. The effect of the two different matrices on the LIBS signal is significant, and such a matrix effect was expected to be more pronounced for soil samples, which are much more varied in chemical and physical composition. Based on this knowledge, the possibility of constructing a universal LIBS calibration curve for all soil samples is not reasonable. Furthermore, it was considered highly unlikely that a calibration curve produced from graphite spiked silica or aluminum silicate powders would be highly accurate predictors of % carbon in natural soils. However, the level of accuracy required for carbon in soil measurements is still in question, and these results provided a good foundation for studying carbon in a soil-like environment.

LIBS Measurements of Powdered Soil Samples

Before any measurements of natural soils were undertaken, soil standards were obtained from NIST. These four soils, Buffalo River Sediment (SRM 2704), Estuarine (SRM 1646), River Sediment (SRM 1645) and Montana Soil (SRM 2710) were very fine powders and considered completely homogenous. Only two of the soils, Buffalo River and Montana Soil

were certified for carbon; therefore, all soils were submitted for dry combustion CHN analysis. Several soil samples were also collected independently from different arbitrary locations in Marion County, Florida (referred to as locations A, B and C). At each location, samples were taken from depths of 1', 4' and 7' using an auger. Soil samples from around the University of Florida campus were also collected (termed S, SE and NE, referring to the collection location relative to the Chemistry Department) and one sample was provided by Aerodyne Research, Inc from Massachusetts. These samples were all air dried for one week and ground with steel balls in a ball mill for half an hour to produce a fine powder much like the NIST standards. CHN analysis was performed several times for all nine soils and the results are reported in Table 5-1. It can be seen that for all three sampling locations, A, B and C, the soil samples taken from 4' and 7' contained much less carbon than samples taken from 1'. This was expected, since the soil organic matter (SOM) decreases significantly with soil depth. As such, these samples were not included in the LIBS analysis.

Each sample was analyzed with 100 single laser shots, each on a fresh sample location. The average C247 signal intensity was calculated and plotted against the %C determined by CHN analysis (Figure 5-6). From this plot, one which the calibration curves produced from graphite spiked silica and aluminum silicate, are also imposed, two distinct groupings of the soils emerged. The grouping first is composed of the soil samples collected from Marion County, plus the Aerodyne soil. These soils formed a steep slope slightly greater than that of graphite in silica. The second group of soils exhibited a slope slightly less than that of the graphite in aluminum silicate.

The equations of the line for both silica and aluminum silicate calibration curves were used to predict the carbon content in the soil samples based on their average C247 intensity (Table 5-

2). The accuracy of each curve to predict the carbon content varied greatly, with a range of 5.2 - 155 %. If the soil that produced an accuracy of 155 % is omitted, the range was reduced to 5.2 - 64.5 % with averages of 34.9 % for the aluminum silicate curve and 23.3 % for the silica curve. Still, one problem with these results is that they were obtained with advance knowledge of which curve to apply to which soil (based on Figure 5-6). It is still unknown what properties of the soil matrix caused such separate and distinct slopes, though particle size can be dismissed as a cause because all soils were extensively ground to a fine powder. Without firm evidence as to why one soil aligned with the silica curve and another with the aluminum silicate curve, it would be impossible to know which to apply to an unknown soil. Furthermore, the results of this research indicate that even in the absence of particle size effects, it would be impossible to produce a universal carbon calibration curve that is applicable to all soil samples. This includes calibration curves produced from simulated soils or from a range of standard soils.

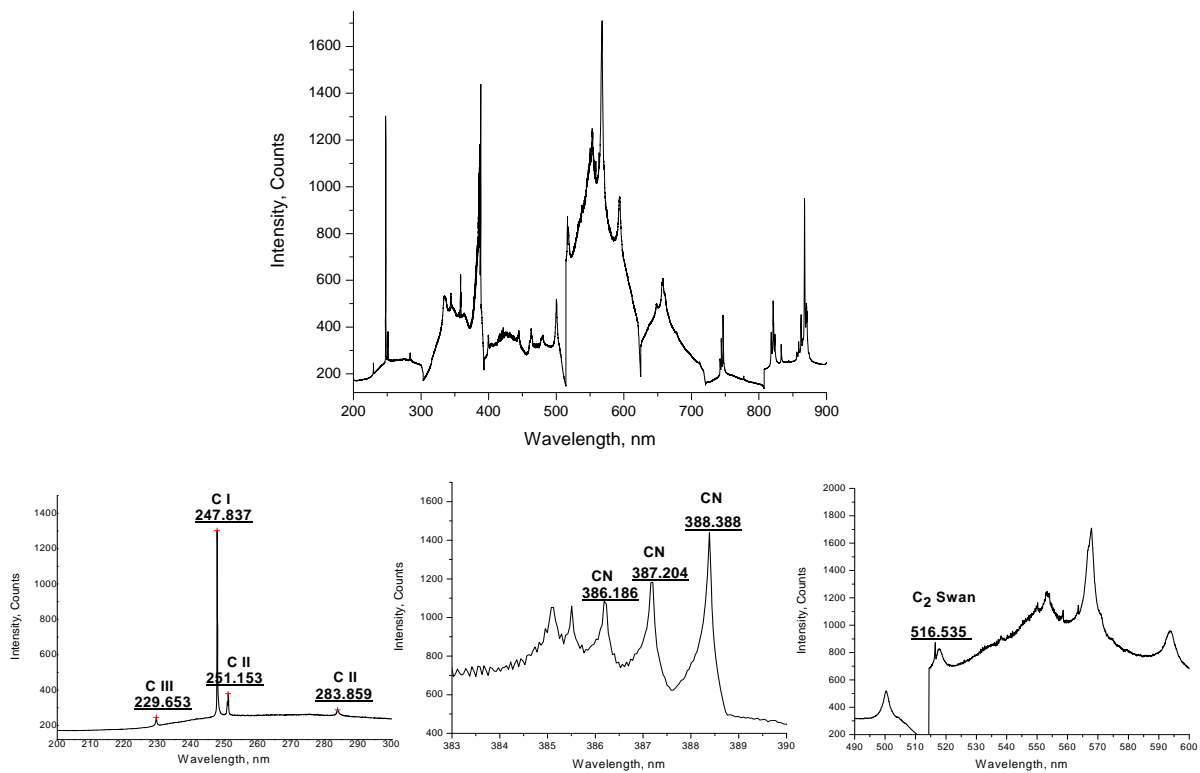


Figure 5-1. Full spectrum of carbon taken on a graphite pellet with prominent lines and bands identified.

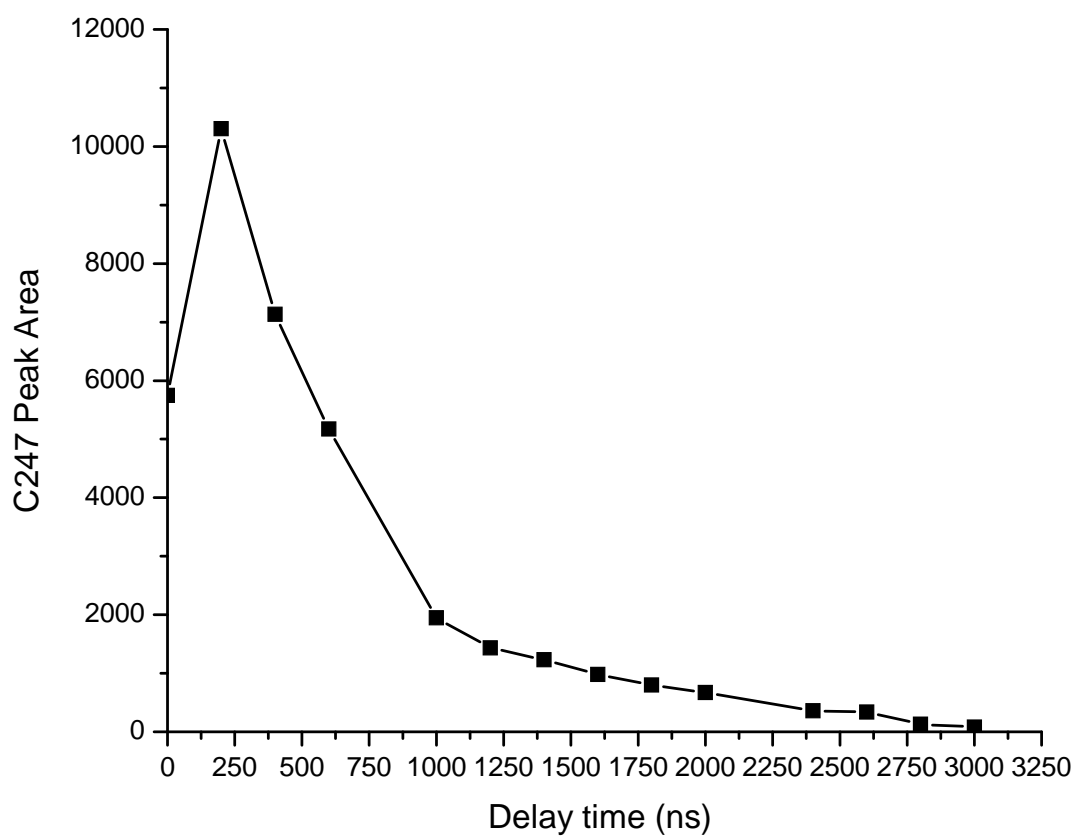


Figure 5-2. C247 peak area as a function of spectrometer delay time. The integration time is fixed at 200 ns.

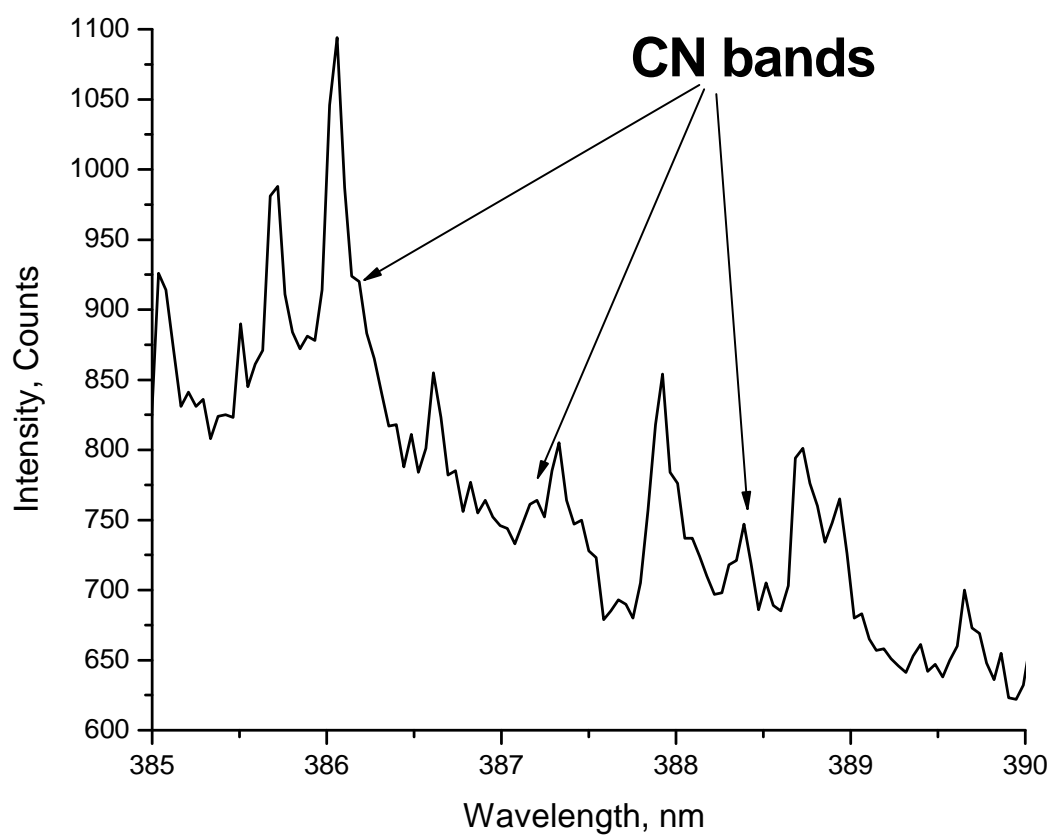


Figure 5-3. The CN molecule, with a band head at 388 nm, is barely detected in a soil sample.

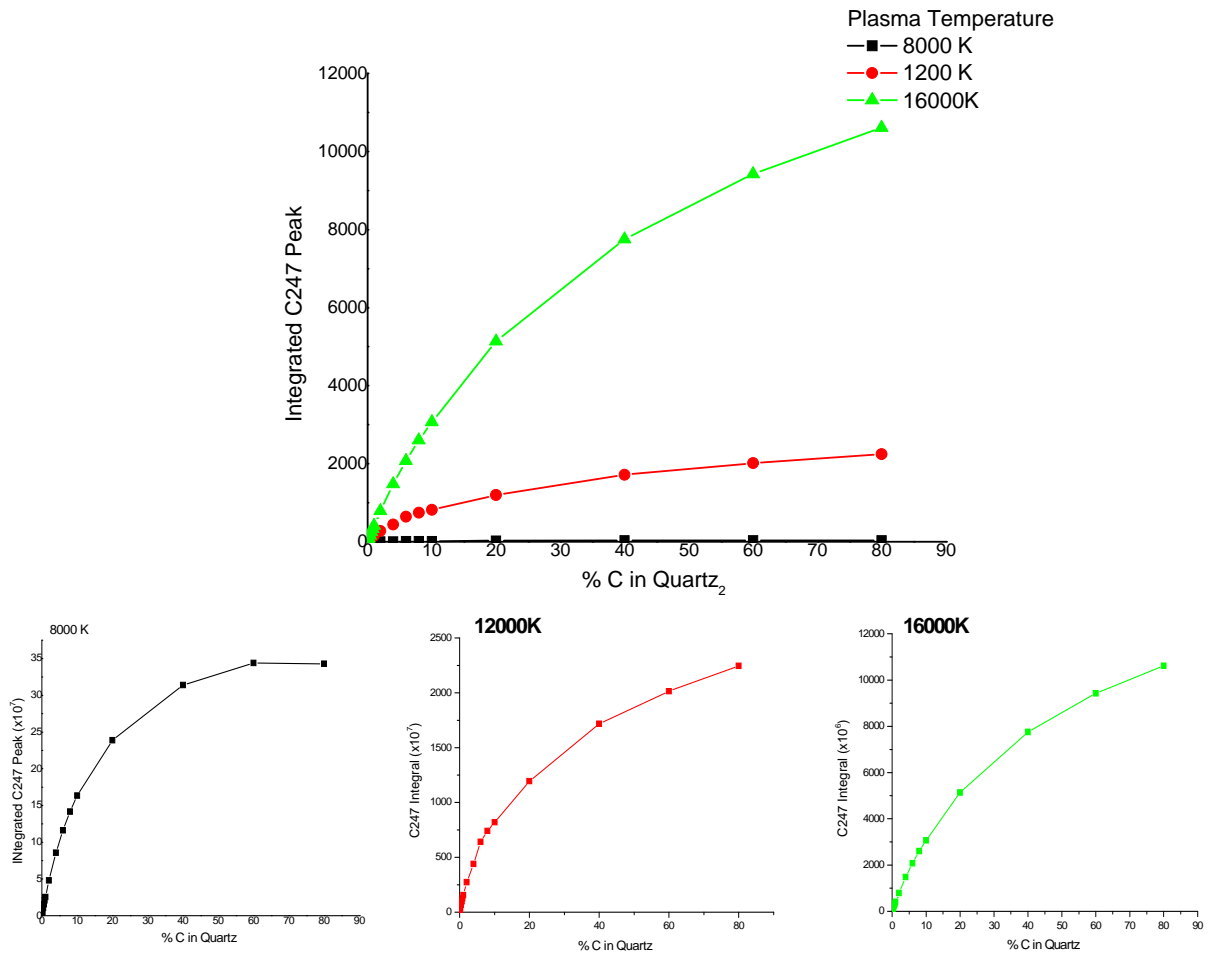


Figure 5-4. Theoretical curves of growth for carbon in a silicon dioxide matrix at three different plasma temperatures.

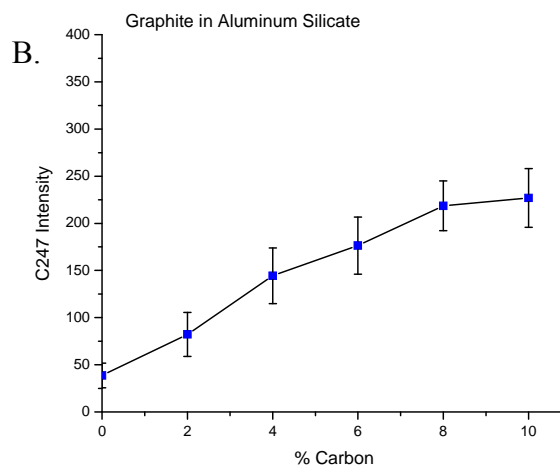
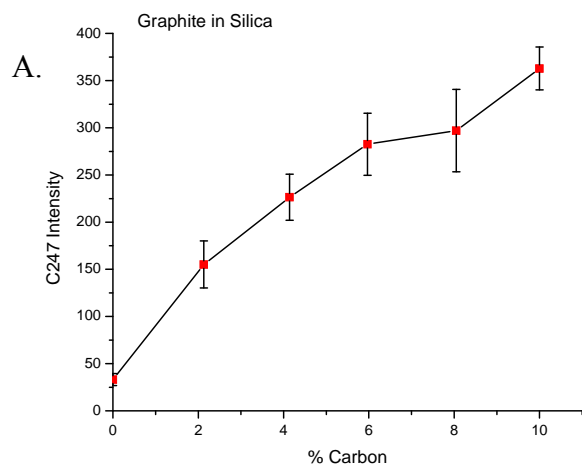


Figure 5-5. Calibration curves produced from graphite in A) silica and B) aluminum silicate (error bars are ± 1 standard deviation).

Table 5-1. Carbon content of soil samples determined by CHN analysis

Sample Name	% C (1 st CHN Analysis)	% C (2 nd CHN Analysis)	Δ %C	Average (% C)
Buffalo	3.271	4.58	1.3	3.9 ± 0.1
River	5.029	5.090	0.06	5.1 ± 0.1
Estuarine	1.624	1.758	0.13	1.7 ± 0.1
Montana	1.730	1.876	0.14	1.8 ± 0.1
A1	1.043	1.157	0.11	1.1 ± 0.1
A4	0.143	0.128	0.01	0.1 ± 0.1
A7	0.093	0.074	0.02	0.1 ± 0.1
B1	0.168	0.186	0.02	0.2 ± 0.1
B4	0.049	0.068	0.02	0.1 ± 0.1
B7	0.056	0.058	0.002	0.1 ± 0.1
C1	1.576	1.524	0.05	1.6 ± 0.1
C4	0.085	0.071	0.01	0.1 ± 0.1
C7	0.034	0.033	0.001	0 ± 0.1
Aerodyne	1.024	1.043	0.02	1.0 ± 0.1
S	7.190	7.06	0.13	7.1 ± 0.1
SE	2.901	2.741	0.16	2.8 ± 0.1
NE	4.091	3.712	0.38	3.9 ± 0.1
			Average = 0.1	

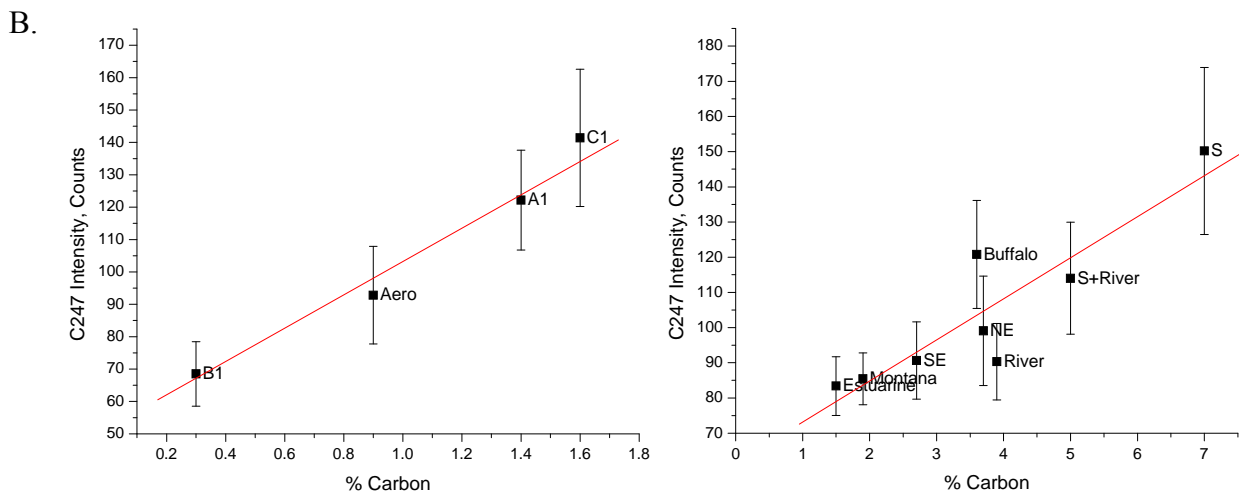
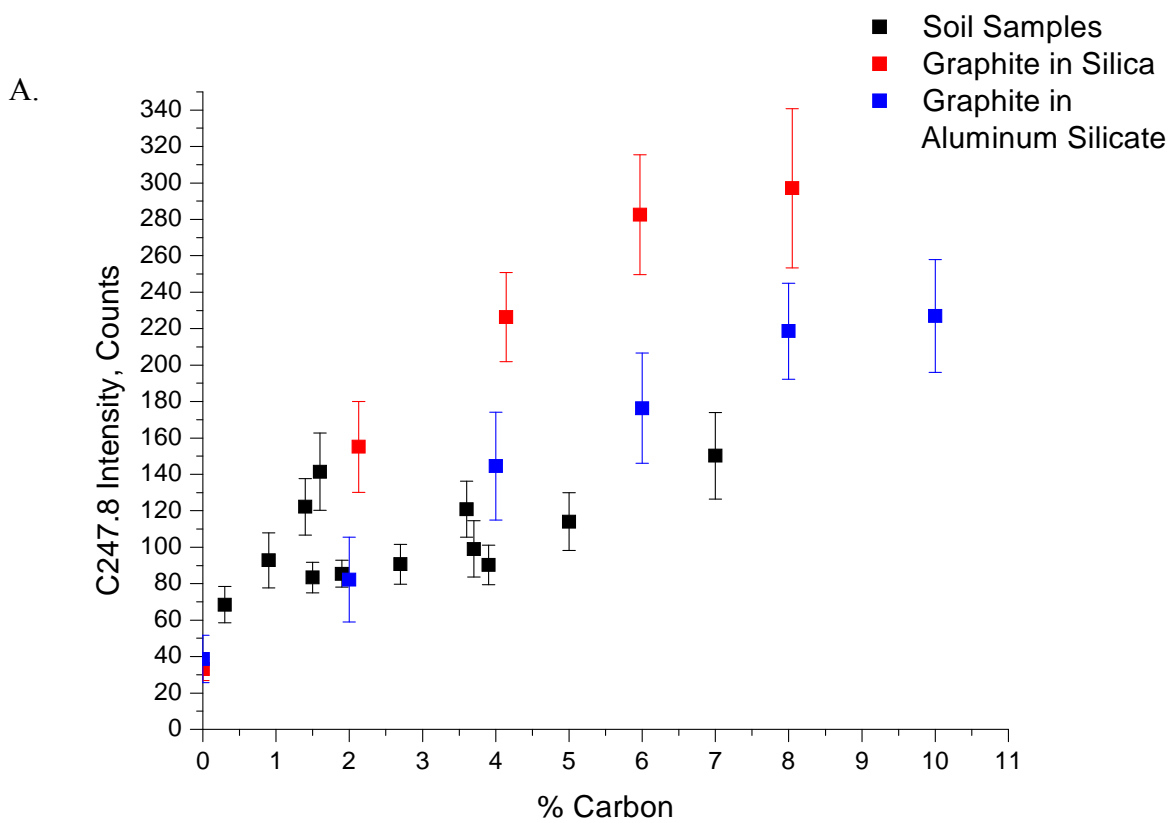


Figure 5-6. Results of LIBS measurements on finely ground soil samples A) With graphite in silica and aluminum silicate calibration curves B) The two separate, distinct slopes formed by the soils (error bars are ± 1 standard deviation).

Table 5-2. Predicted carbon content of soils using the applicable silica of aluminum silicate calibration curve.

Sample Name	True Carbon Content (%)	Predicted Carbon Content (%)	Absolute Difference (%)	Relative Difference (%) ^a
From graphite in SiO ₂ curve				
A1	1.1	1.8	+0.7	+38
B1	0.2	0.5	+0.3	+64
C1	1.6	2.3	+0.7	+31
Aerodyne	1.0	1.1	+0.1	+5
From graphite in Al ₂ SiO ₅ curve				
Estuarine	1.7	1.9	+0.2	+10
Buffalo	3.9	3.4	-0.5	-14
Montana	1.8	1.9	+0.1	+7
NE	3.9	2.5	-1.4	-54
SE	2.8	2.2	-0.6	-30
River	5.5	2.2	-3.3	-155
				Average=34
				Average=45

a.) Calculated from $((\text{Predicted \%C} - \text{True \%C}) / \text{Predicted \%C}) \times 100$

CHAPTER 6 LIBS MEASUREMENTS OF NATURAL SOILS: IS QUANTIFICATION POSSIBLE?

Introduction

The complex nature of soil samples presents numerous difficulties to any analytical technique, but more so to LIBS, which is especially sensitive to sample heterogeneity. In order to assess the potential of LIBS for *in-situ* soil measurements, the previously described sampling regime must be applied to natural soils that have not be extensively modified. To achieve this, 38 soil samples collected from various locations on the Gulf Coast of Florida were obtained from the University of Florida's Soil Science Department. The soils had been previously analyzed for carbon content by dry combustion and represented a carbon concentration range of 0-20%. All samples had been completely dried and mildly ground to break up excessively large particles and to reduce heterogeneity. Figure 6-1 shows microscope images of each soil at a magnification of 3.5X and it is clear that the soils are very different with respect to particle size and chemical composition. The darker soils have higher carbon content due to the black/brown contribution of humus, the major contributor to soil organic matter.

CHN Analysis

The original dry combustion CHN analysis that was conducted by the Soil Science department was performed on the coarse soil samples and as such it was unlikely that the reported carbon concentrations by weight were representative of the bulk sample. Accurately knowing the carbon content of these soils was a critical factor, and while dry combustion is relatively accurate (specified as within 4 % of the true value), it is still a microanalysis technique, and as such is sensitive to sample heterogeneities. To study the accuracy and precision of dry combustion for carbon determination, all 38 soils were submitted for multiple CHN analyses over several months. Table 6.1 presents the average, RSD and range of the reported carbon concentrations for each soil sample. The average RSD for all soil samples is 37%. This poor

precision is undoubtedly a combination of the great sample heterogeneity and the small mass of sample analyzed. As such, it is unlikely that dry combustion can yield a highly accurate measurement of carbon concentration that is representative of the bulk sample. In the absence of an alternate method, such poor accuracy was tolerated and the average carbon concentration was used for correlation with LIBS signal. However, as a consequence, there will be some unknown error associated with the stated carbon concentration of each soil.

LIBS Measurements of Natural Soils

All soil samples were subjected to LIBS using the previously established optimized sampling regime. Because the soils had not been characterized in terms of texture and particle size, the surface density of the soil on tape was determined and assumed to be proportional to the average grain size of the soil. Surface density was determined by weighing the microscope slide and the adhesive tape before and after the application of the soil layer. The difference between these two measurements represented the weight of the applied soil sample, which was then divided by the surface area of the tape (approximately 1.9 cm²). The resulting surface densities ranged from 3.7 to 38 mg/cm². The soils that exhibited the greatest surface densities corresponded to the soils that were composed of the largest particle sizes. Since it had been previously established that the LIBS signal exhibits some dependence on particles size, these surface densities were used to correct the LIBS C247 signal for soil grain size.

LIBS measurements of the soil samples were obtained using the maximum laser energy of approximately 57 mJ at a repetition rate of 1 Hz. This allowed ample time to manually maneuver the slide to fresh sample locations. Forty separate locations were sampled, for a total of 80 laser shots, with two shots used per spot. A gentle air stream was directed over the soil surface to remove liberated particles. Once the data were collected, the average C247 peak area was separately calculated for the 40 first shots and the 40 second shots. Figure 6-2 shows the

correlation plots of LIBS signal vs. % carbon for both the first and second shot data. Previous studies on soils indicated that the C247 signal from the second shot on the same spot is proportional to that of the first shot (by a factor of between 1.6 and 2.0) and as such, besides an increase in signal, the correlation plots were not expected to be significantly different. This is supported by Figure 6-2, which clearly shows a very similar trend between first and second shot measurements. One important advantage of using the two shot sampling method is the increase in precision that it provided relative to first shot measurements. Figure 6-3 is a histogram that compares the range of both first and second shot RSD's associated with the average C247 peak areas for each of the natural soil samples. From this histogram, it can be seen that the majority of second shot soil measurements provide lower RSD's and thus higher precision than the same measurements collected from only the first shot. This higher precision for the second shot measurements is most likely due the homogenizing action of the first preparatory shot.

There are several important features to note about the plots in Figure 6-2. First, there was no evident correlation between LIBS C247 signal and the average % carbon determined from CHN analysis across all different soil samples. This was expected based on previous results that established the dependence of LIBS on properties such as matrix particle size and chemical composition. Due to this, it would not be feasible to expect one correlation plot to produce a single calibration curve applicable to all soils, regardless of texture or chemical composition. Second, the plots showed that there was an upper concentration limit of approximately 6%, after which the C247 signal plateaus. This would indicate that under these measurement conditions LIBS would not be applicable to high carbon soil samples. The third point of interest from these plots was the high carbon signal that the soils containing less than 1% carbon produced. There are two possible explanations for this. Unlike the quartz particle size fractions, which also produced a large signal for trace carbon, these soil samples contain iron, which has a weak

emission line that possibly interferes with the C247 line and may be contributing to the signal. This will be discussed further in the next section. Another potential explanation for such a large 'blank' signal is the same mounting tape contribution seen in measurements taken on the quartz samples. While microscope images indicate that even after two shots on the soil sample the tape is not visible, it is possible that it is not necessary to actually reach the tape in order for it to cause some interference. As was previously discussed, it seems that as the particle size of the sample decreases there is an amplification of the carbon signal observed from the tape relative to the carbon signal produced from the tape alone. This phenomenon was prevalent for the quartz particle size fractions on the order of tens of microns, and was not seen in the larger fractions which resemble most of these soils. If this is the case, then it has to be assumed that this tape contribution is relatively constant and the contribution is the same for each shot.

A number of normalization factors were applied to the LIBS soil measurements in an attempt to minimize the matrix effects and to observe any increase in correlation. Some success has been previously reported using silicon as an internal standard.⁵⁴⁻⁵⁶ However, no improvement was found when the C247 signal was normalized with the Si288 line. This was hardly surprising considering a simple visual inspection of the soils revealed how variable the silicon content was (the large, translucent particles which can be seen in some soil samples in Figure 6-1 are silica particles). In order for any other soil component to be used as an internal standard, it must be shown that it exhibits a relatively constant concentration, or that the concentration is proportional to carbon content. It is likely that any success that has been achieved by normalizing the carbon signal with silicon was performed on soils with very similar chemical compositions (i.e., they were collected from similar locations, had been subjected to the same environmental factors).

Normalizing the C247 signal to surface density proved to be the most promising method. Figure 6-4 shows such normalization transforms the raw measurements and produces a much more linear correlation plot. Based on these results, it would seem that correcting the LIBS signal for the physical rather than the chemical matrix effects is the most promising method to relate C247 signal to carbon content. This is advantageous because the physical properties of any given soil are easier to assess during in-field analysis than the chemical composition. In order to correct the LIBS signal for chemical matrix effects, the chemical composition of the soils would have to be determined prior to LIBS measurements. In some cases, this may be as simple as determining high iron content based on color; however, even subtle differences in chemical compositions will contribute to significant chemical matrix effects and reliable analytical techniques would be necessary to classify soils into groups of similar composition for LIBS measurements.

High-Resolution LIBS Measurements on Soils

One potential problem with the C247 line was the possibility of an interference from the weak iron ionic line at 247.8 nm and atomic line at 247.9 nm. To study the extent of this interference, a pure iron powder was analyzed, as well as a 1:1 mixture of iron and graphite powders (Figure 6-5). The spectrum of iron powder revealed that the iron atomic line is detected at 247.99 nm. A small shoulder on the left of the peak corresponded to the ionic iron line. The spectrum of the graphite/iron mixture revealed that the Fe_{247.98} line was not resolved from the C_{247.83} line. While the extent of this interference was expected to be minimal due to the low iron content of these soil samples, it was still necessary to ensure that the poor correlation between the LIBS carbon signal and the carbon content was not due to the unresolved iron peak contributing to the carbon signal.

To investigate this, LIBS measurements were performed on the same soil samples from the previous study and emission radiation was spectrally resolved using an Acton SpectraPro-500i spectrometer with a 3600 grooves/mm grating which provided a resolution of approximately 0.02 nm. This resolution was high enough to fully resolve the carbon and iron lines (Figure 6-6). Most other experimental conditions were maintained, including a laser pulse energy of approximately 60 mJ, spectrometer delay time of 1 μ s and an integration time of 100 μ s. Samples were mounted vertically and shifted manually after every two sampling shots to ensure a fresh sample location. Emission was collected by a 2" lens and focused onto the 35 μ m slit of the spectrometer. The focusing lens produced 1:1 inverted image of the plasma onto the entrance slit of the spectrometer, and alignment was achieved using a flat graphite pellet. However the soil samples used in these studies were far from flat, and the positioning of the laser induced plasma could be horizontally translated by up to 1 mm depending on the size of the particle where the plasma was formed. As such, this optical configuration was highly sensitive to the coarse textures of soils and emission collection efficiency was not always optimal or reproducible.

The resulting LIBS measurements produced with the high resolution spectrometer are shown in Figure 6-7. It is clear that there is no increase in correlation between the LIBS carbon signal and the carbon content; indeed, the trend is very similar to the results achieved using the lower resolution Ocean Optics spectrometer. Normalizing these results by the surface density of the samples (Figure 6-8) did not significantly improve the correlation as it did for the previous data. The C247 peak produced using the high resolution spectrometer were completely resolved, and therefore wholly due to carbon alone. If the poor correlation observed with the Ocean Optics spectrometer were due to the iron spectral interferences, the fully resolved carbon peak would significantly improve the correlation. This does not occur, and therefore it can be

concluded that the lack of correlation between LIBS signal and carbon observed with the Ocean Optics measurements must be attributed to other matrix factors and is not caused by an iron interference.

One other important aspect to note concerning these results is the poor precision. As previously mentioned, this was likely due to the optical arrangement of the emission collection. For many soils, the RSD was double that achieved using fiber optic emission collection. It is likely that the precision can be increased by further grinding the soils to fine powders or analyzing pressed pellets; the flatter surfaces will minimize the plasma translation with respect to the spectrometer entrance slit. However, such additional samples preparation steps are cumbersome, and fiber optics is likely the best method of emission collection when analyzing natural soils of varying textures.

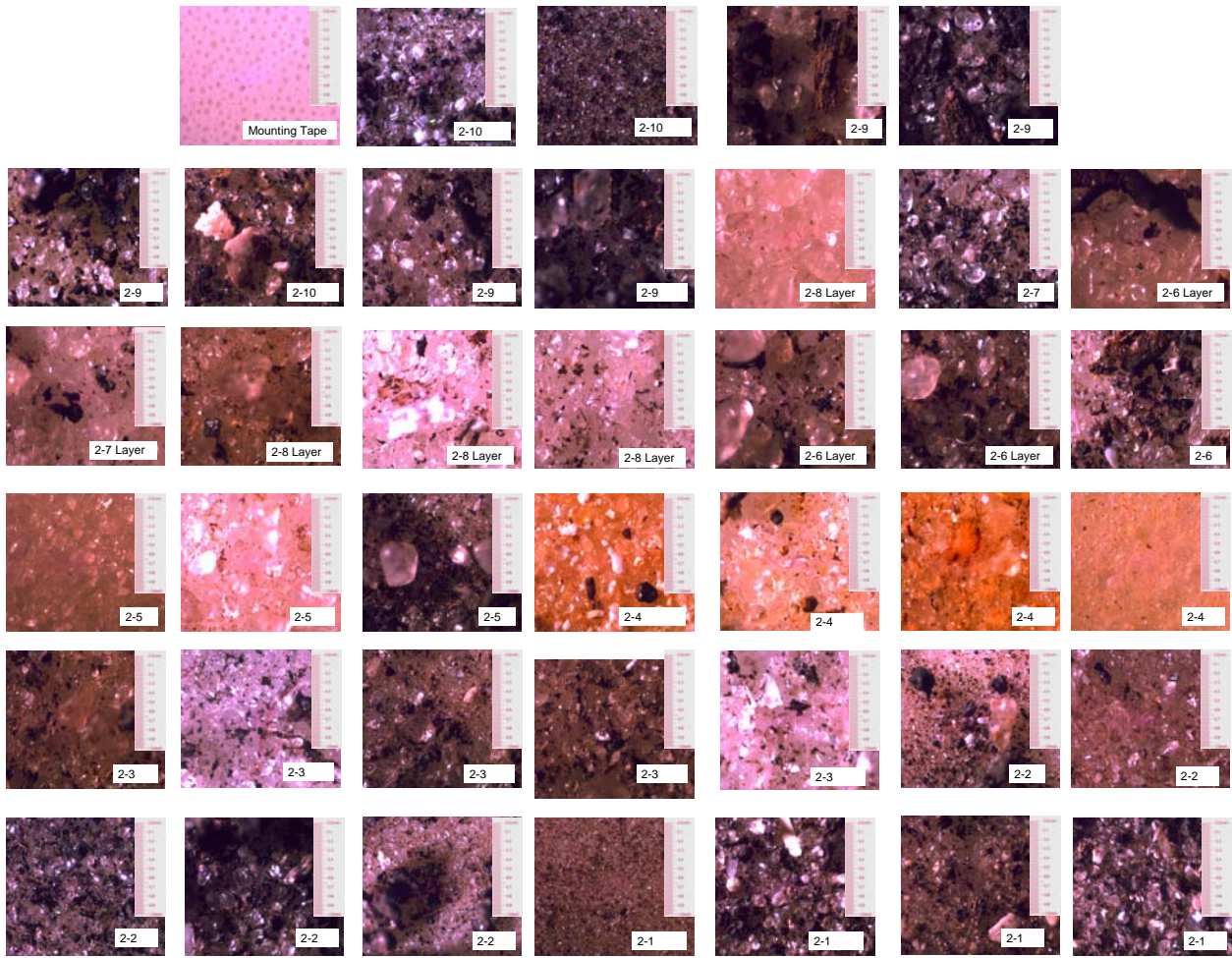


Figure 6-1. Microscope images of natural soil samples (3.5X magnified).

Table 6-1. Results of dry combustion CHN analysis performed on a suite of natural soil samples.

Soil Label	Number of CHN analyses	Average carbon Concentration (%)	RSD of CHN analyses (%)
1	3	7.1	16
2	6	12.1	13
3	3	9.2	13
4	6	6.0	13
5	3	9.2	43
6	6	8.2	10
7	3	0.3	26
8	3	19.4	6
11	6	2.0	18
12	3	1.2	7
13	3	6.9	56
14	3	0.8	30
15	3	2.6	33
16	3	0.4	9
17	3	0.5	54
18	3	5.7	17
19	3	0.4	51
20	5	0.0	66
21	3	9.5	64
22	3	6.8	62
23	6	0.9	26
24	3	0.5	5.0
25	6	5.2	44
26	3	0.7	43
27	3	0.6	20
28	6	15.6	20
29	3	14.1	18
30	3	9.5	16
31	3	0.7	26
32	3	1.7	68
33	3	0.5	14
34	3	11.6	62
35	3	8.0	58
36	3	8.5	49
37	3	11.4	60
38	3	12.5	58

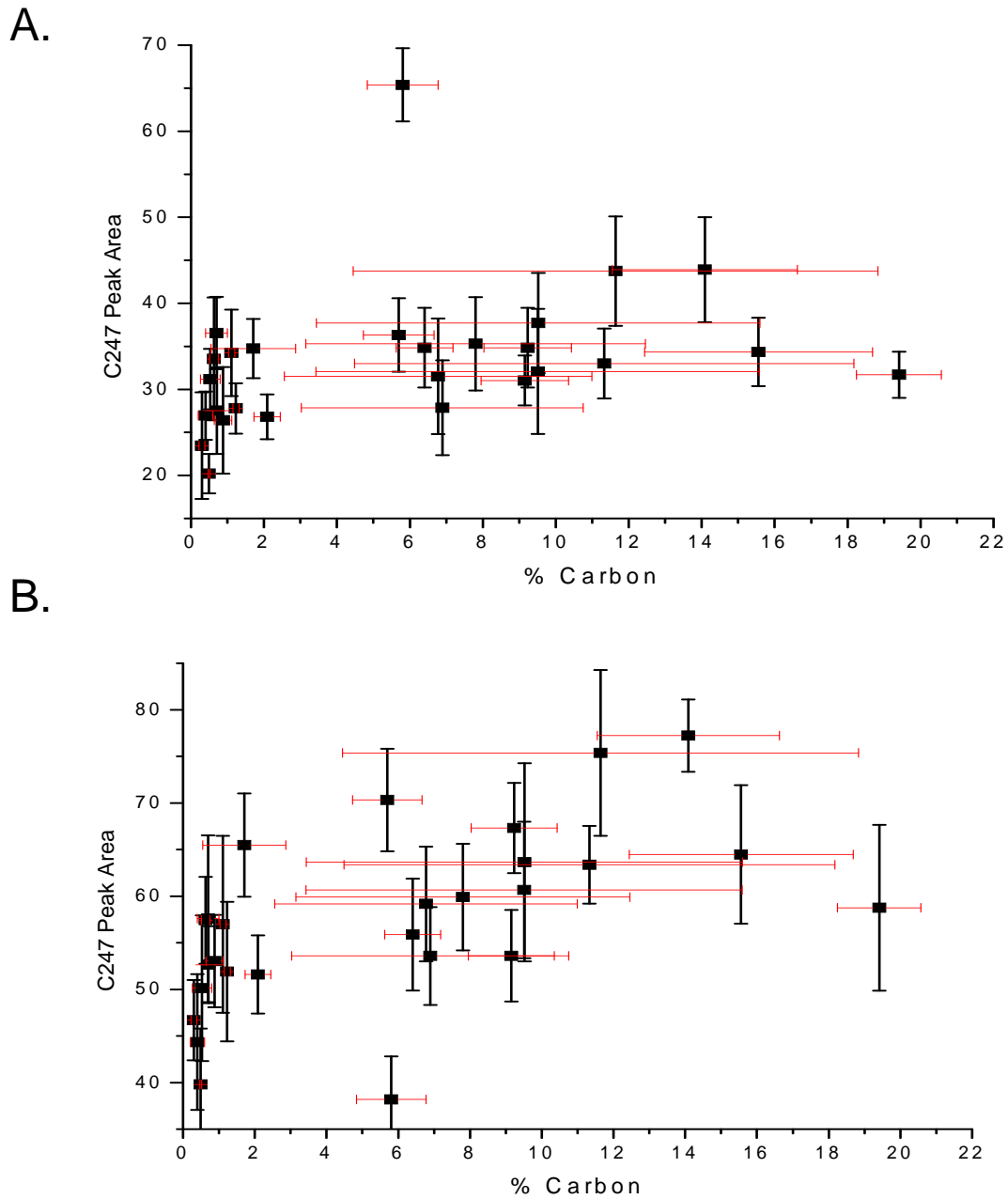


Figure 6-2. LIBS C247 measurements on natural soils as a function of % carbon for A) first shot measurements and B) second shot measurements. The error bars for % carbon represent 1 standard deviation of the average CHN measurements.

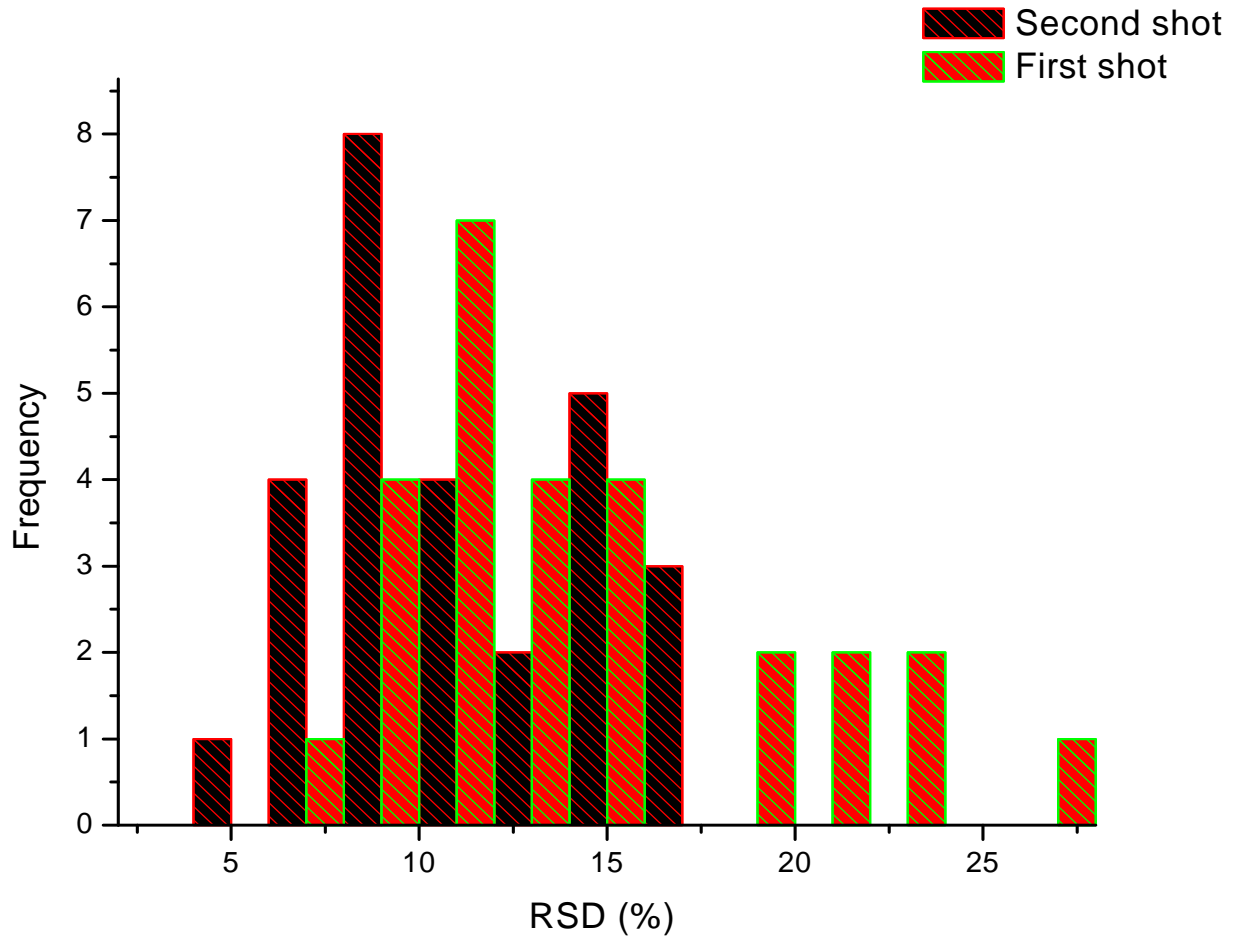


Figure 6-3. A histogram of the RSDs from LIBS C247 measurements using the first shot and the second shot.

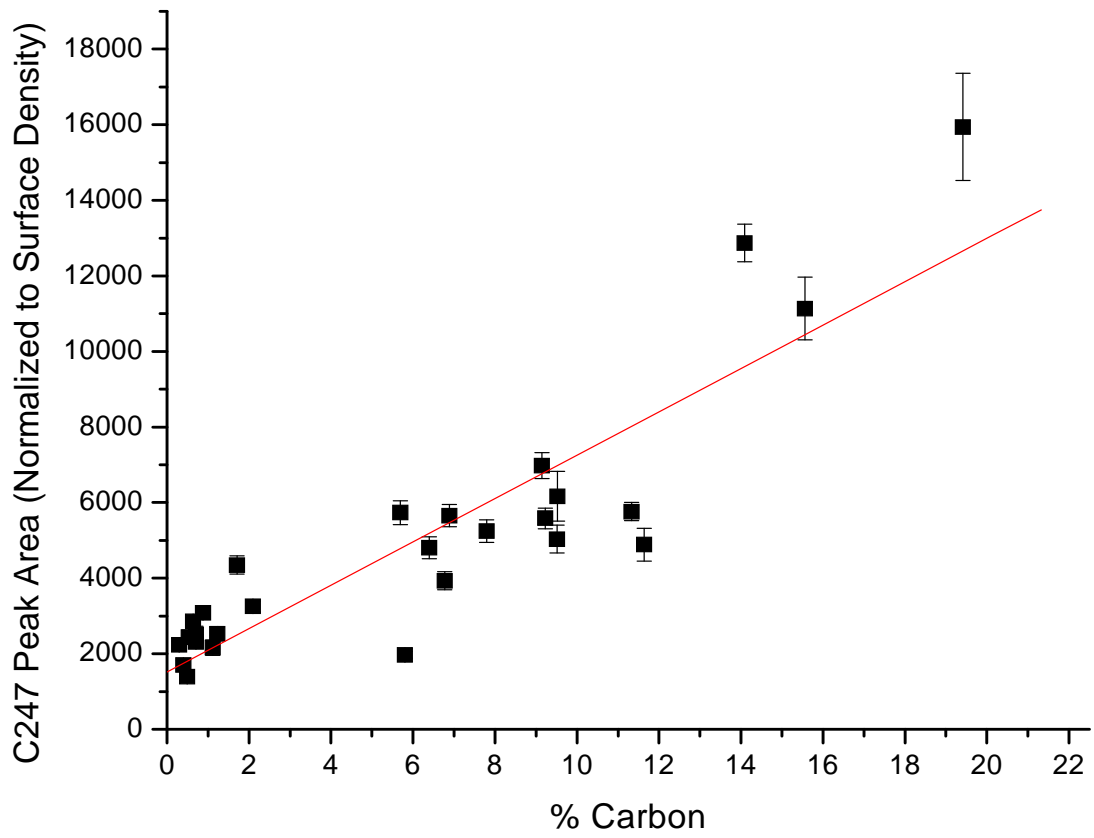


Figure 6-4. Normalizing the C247 peak area by soil surface density increases the correlation between LIBS signal and carbon concentration (error bars are ± 1 standard deviation).

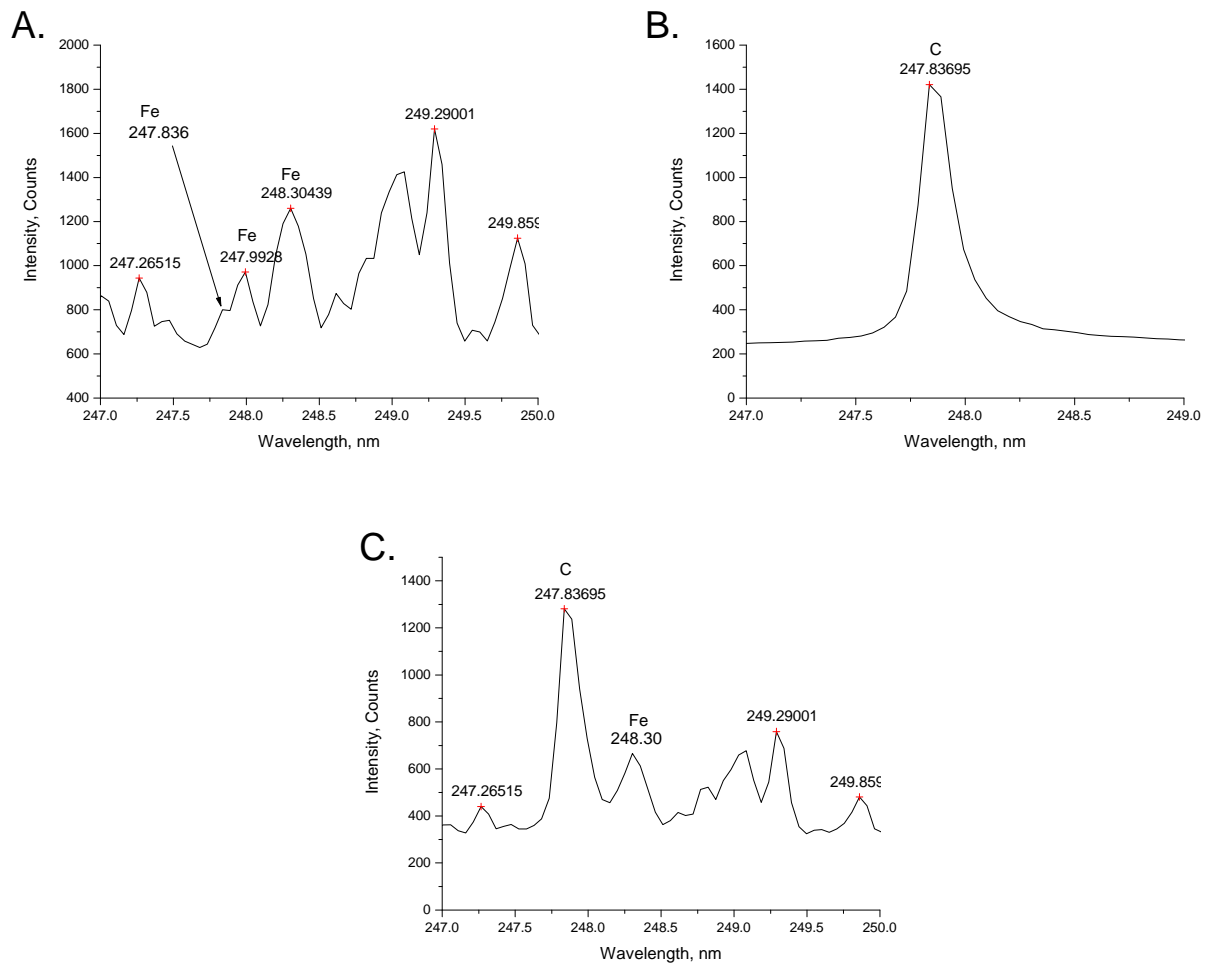


Figure 6-5. Extent of the iron spectral interference. A) Pure iron foil. B) Pure graphite and C) An iron and graphite mixture.

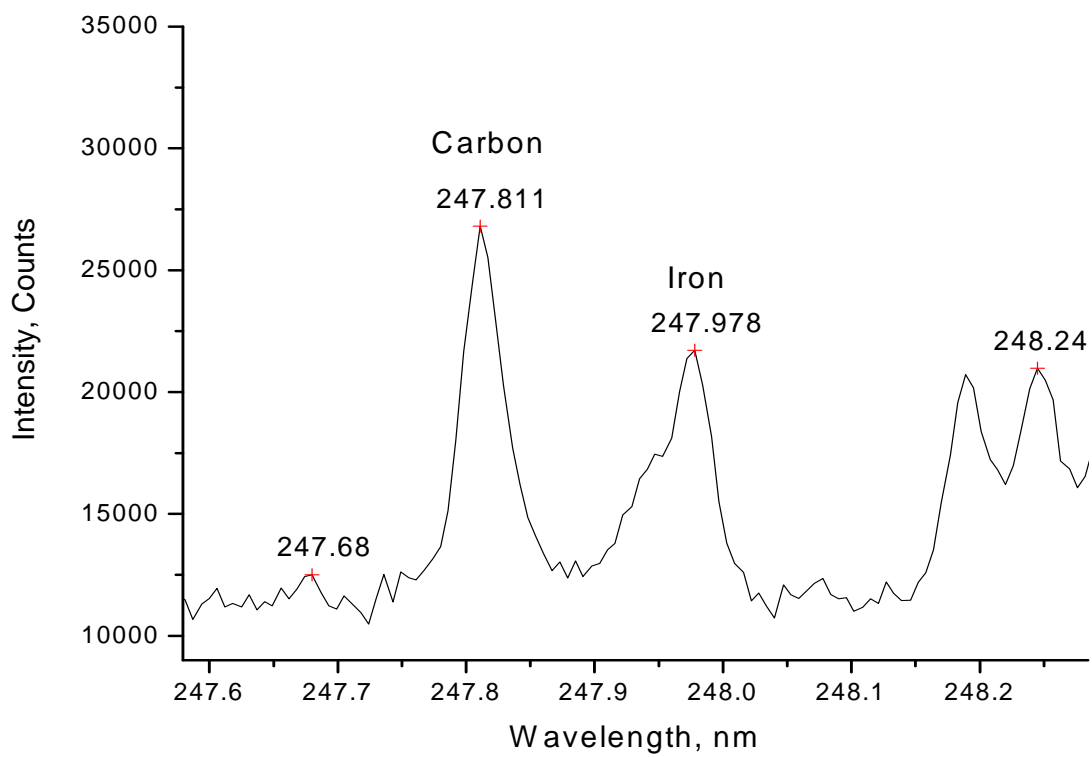


Figure 6-6. A soil spectrum produced using the Acton SpectraPro spectrometer showing the resolved carbon and iron lines.

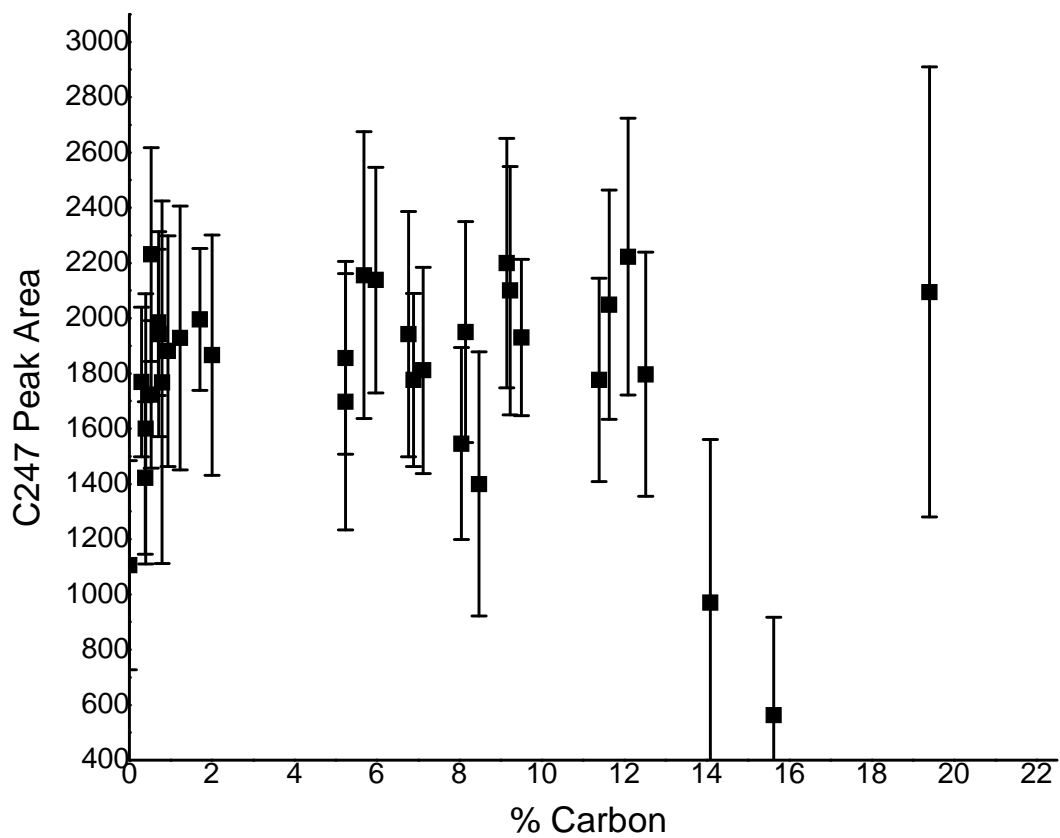


Figure 6-7. The LIBS C247 peak area as a function of carbon concentration for measurements produced using a high resolution spectrometer (error bars are ± 1 standard deviation).

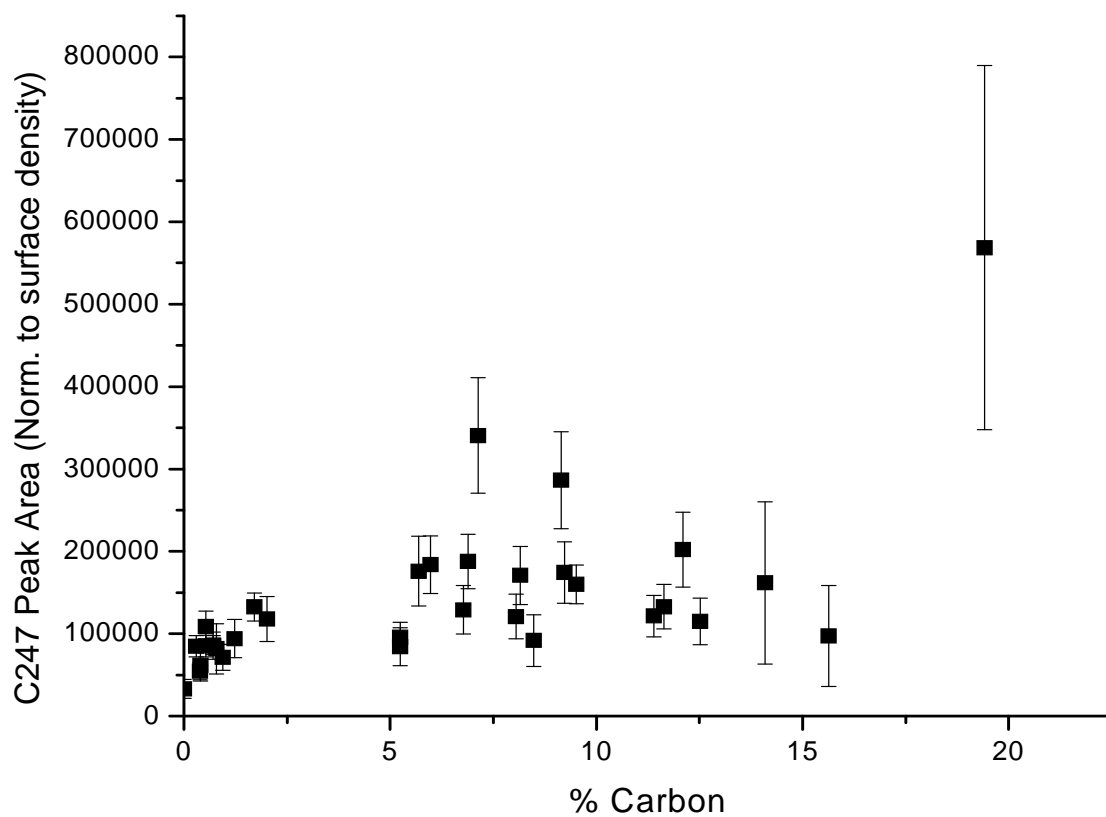


Figure 6-8. A plot of the C247 peak area normalized by surface density vs. carbon content for measurements produced using a high resolution spectrometer (error bars are ± 1 standard deviation).

CHAPTER 7 CONCLUSION AND FUTURE WORK

Natural soils are arguably the most challenging of all samples for quantitative LIBS measurements. There are many variables that must be accounted for that each contributes to detrimental chemical and physical matrix effects. Chemical matrix effects can include spectral interferences from other soil components, speciation of the analyte of interest, water content and the overall chemical composition, which may alter the sample's breakdown threshold. Physical matrix effects include the broad range of different particle sizes, the distribution of the analyte throughout the sample and extensive differences in physical properties such as reflectivity and heat of vaporization on both the macro and micro scale. The initial purpose of this research was to assess the potential of LIBS for quantitative carbon measurements in soil; however, it became readily apparent that a more fundamental approach was necessary before any conclusion concerning quantitative results could be achieved. As such, the majority of this work was devoted to establishing optimal instrumental and sampling parameters exclusively for LIBS measurements on soils. While the ultimate goal of this research was for carbon determination in soils, most of these studies can be extended to any other analyte of interest.

A number of modifications were made to the LIBS instrumental components for the purpose of soil analysis, including the use of a positioning laser to ensure constant LTSD and FTSD for soils of variable heights. A gentle air stream directed over the sample was found to eliminate the interaction of the laser beam with liberated, air-borne particles along the laser axis, thus increasing measurement reproducibility. Careful alignment of the fiber-optic probe, positioned close to the plasma, was found to provide superior emission collection relative to the popular back-side emission collection. A spectrometer delay time of 1 μ s was found to produce the best S/B for the C247 line, as well as the lowest limit of detection for carbon in soil.

Establishing an optimized sampling regime for soils is much more difficult than for most solid samples encountered in LIBS. Due to the highly heterogeneous physical and chemical nature of all soils, combined with the micro-sampling property of LIBS, single shot measurements were not representative of the bulk sample. As such, it was found that a minimum of 20 sample spots must be measured to achieve the minimum, if not always acceptable, RSD. In reality, it might take thousands of sampling shots to produce a precise measurement that is representative of the bulk sample. The particulate nature of the soil samples also greatly affects the LIBS measurements. It was confirmed that the LIBS signal was greatly dependent on the matrix particle size and that the increased homogeneity imparted by samples composed of smaller particles yielded much higher measurement precision. It was also determined that when a single, preparatory laser shot was used to modify the sample surface, the subsequent second laser shot produced increased emission intensity across the entire spectrum. Microscopic images of the soil samples before and after the sampling indicated that surface modification resulted from the removal or break-up of large particles which most likely allowed more sample to interact with the second laser pulse, thus increasing the mass ablated. Under these sampling conditions, the precision of the C247 signal for all 38 soil sample did not exceed 18%.

The optimized sampling regime was applied to natural, dried soil samples to assess the potential of LIBS as a quantitative technique. However, the results revealed no correlation between the uncorrected carbon peak area of all soil samples and their reported carbon concentrations. There are many factors that must be considered before quantification can be ruled out. For instance, all of these soils suffered from very different matrix effects and therefore could not be all be compared together or used to produce one single calibration curve. In

addition to the different matrix effects, other factors independent of the LIBS measurements may have contributed to such poor correlation. For instance, the significant variability in the CHN analyses introduced significant error to the carbon concentrations, which in turn will influence the correlation. In order to minimize this error, for future work, soil samples should be extensively ground prior to dry combustion and analyzed multiple times. Another consideration is whether the mounting tape contributes to the LIBS carbon signal of soil samples, and whether this contribution is relatively constant. Other sample mounting methods that do not involve a carbon based substrate should be explored. For instance, future work could produce LIBS measurements on loose soil samples.

Correlation is likely to increase when soils of very similar chemical and physical compositions are analyzed together, rather than as suite of very different soils. Additional research must focus on identifying the chemical or physical properties that contributed most to the LIBS matrix effects. For instance, this research exploited the particle size dependence of LIBS signal and found an increase in correlation by normalizing the carbon signal to surface density, which is related to the particle size. In addition to particle size other variables may influence the LIBS signal and could be used to categorize soils or to correct the LIBS signal. Examples include the chemical form of carbon, chemical composition, and mineral content. The use of these soil properties would require extensive prior knowledge about each soil sample and collaboration with soil scientists, who often work with fully characterized soils, would be a valuable resource.

Future work should also consider the use of a multivariate analysis of the entire soil spectrum. In the absence of prior knowledge about a specific soil, the LIBS spectrum can provide valuable information concerning the relative concentrations of elemental components.

At the very least, inspection of the entire spectrum can be used to group soils based on major constituents. More advanced multivariate algorithms may be applied to entire spectral regions instead of simply one carbon line and will account for varying peak intensities of other elemental constituents which may be producing specific matrix effects.

The quantification of carbon in natural soils by LIBS was not achieved during this research. While it is possible that this will be accomplished in future work, it is important to reflect on the original motivation of this research: to assess LIBS as a means of *in-situ* carbon determination in natural soils. During this research, every attempt was made to minimize sample preparation and reduce cumbersome instrumentation in order to mimic the LIBS measurements that would be produced using a portable LIBS system. Future work may prove that quantification is achievable on finely ground, pelletized samples and precision drastically increased by taking thousands of measurements. However, once the sample preparation negates *in-situ* analysis and requires extensive laboratory based work, the advantages of LIBS become redundant and more conventional techniques such as dry combustion or wet oxidation may provide more accurate results.

The inability of LIBS to determine carbon in soils at this point does not diminish the importance of the sampling and instrumental studies that were performed using for the purpose of soil measurements. For instance, studies concerning the dependence of LIBS signal on matrix particle size are applicable to nearly all types of particulate samples. In addition to this, qualitative analysis of soils is successfully achieved using the soil sampling characteristics studied here. Indeed, the increase in emission intensity that is observed after a single laser preparatory shot will increase LIBS sensitivity for trace toxic metals such as Hg, As or Pb. A variety of important elements in soil, including Mg, Mn, Na, Fe, Cu can be readily detected in

the LIBS soil spectra produced during this research. In some cases, quantification of these elements may be more easily achieved over carbon. As such, this research has provided a firm foundation for further studies on the characteristics of LIBS on soils and may be extended to a variety of other analytes of interest

LIST OF REFERENCES

- (1) Brech, F.; Cross, L. *Appl. Spectrosc.* **1962**, *16*, 59.
- (2) Rusak, D.A.; Castle, B.C.; Smith, B.W.; Winefordner, J.D. *Trends Anal. Chem.* **1998**, *17*, 453-461.
- (3) SciFinder, version 2006; Chemical Abstracts Service: Columbus, OH, 2006; Accessed June 3, 2006); calculated using ACD/Labs software, version 8.14; ACD/Labs 1994-2006.
- (4) *Laser-Induced Breakdown Spectroscopy (LIBS): Fundamentals and Applications*; Miziolek, A. W.; Palleschi, V.; Schechter, I., Ed.; Cambridge University Press: New York, 2006.
- (5) Weyl, G.M.; Root, R.G.; Baldis, H.A, Hauser, A.A. In *Laser-Induced Plasmas and Applications*; Radziemski, L.J.; Cremers, D.A., Eds.; Marcel Dekker, Inc.: New York and Basel, 1989.
- (6) Lee, Yong-Ill, Song, Kyuseok, Sneddon, Joseph. *Laser Induced Breakdown Spectroscopy*; Nova Science Publishing, Inc.: New York, 2000.
- (7) Sneddon, J.; Lee, Y.; *Curr. Top. Anal. Chem.* **2004**, *4*, 111-117.
- (8) Winefordner, J. D.; Gornushkin, I. B.; Correll, T.; Gibb, E.; Smith, B. W.; Omenetto, N. *J. Anal. At. Spectrom.* **2003**, *19*, 1061-1083.
- (9) Radziemski, L. J. *Spectrochim Acta, Part B.* **2002**, *57B*, 1109-1113.
- (10) Lee, Y.; Sneddon, J *Adv. At. Spectrosc.* **2002**, *5*, 235-288.
- (11) Radziemski, L.J.; Loree, T. R.; Cremers, D. A. *Springer Series in Optical Sciences*, **1983**, *39*, 303-307.
- (12) Gunratne, T.; Kangas, M.; Singh, S.; Gross, A.; Dantus, M.; *Chem. Phys. Lett.* **2006**, *423*, 197-201.
- (13) Le Drogoff, B.; Margot, J.; Vidal, F.; Laville, S.; Chaker, M.; Sabsabi, M.; Johnston, T. W.; Barthelemy, O. *Plasma Sources Sci. Technol.* **2004**, *13*, 223-230.
- (14) Le Drogoff, B.; Chaker, M.; Margot, J.; Sabsabi, M.; Barthelemy, O.; Johnston, T. W.; Laville, S.; Vidal, F. *App. Spectrosc.* **2004**, *58*, 122-129.
- (15) Angel, S. M.; Stratis, D. N.; Eland, K. L.; Lai, T.; Berg, M. A.; Gold, D. M. *Fresenius' J. Anal. Chem.* **2001**, *369*, 320-327.
- (16) Lenk, A.; Witke, T.; Granse, G. *Appl. Surf. Sci.* **1996**, *195*, 96-98.

- (17) Song, K.; Lee, Y.; Sneddon, J. *Appl. Spectrosc. Rev.* **2002**, *37*, 89-117.
- (18) Yamamoto, K.Y.; Cremers, D.A.; Foster, L.E.; Ferris, M.J.; *Appl. Spectrosc.* **1996**, *50*, 222-233.
- (19) Carranza, J.E.; Gibb, E.; Smith, B.W.; Hahn, D.W., Winefordner, J.D. *Appl. Opt.*, **2003**, *42*, 6016-6021.
- (20) Burgio, L.; Melessanaka, K.; Doulgendis, M.; Clark, R.J.H.; Anglos, D.; *Spectrochim. Acta* **2001**, *905*, B56.
- (21) Angelos, D. *Appl. Spectrosc.* **2001**, *55*, 1864.
- (22) Angelos, D.; Balas, C.; Fotakis, C. *Am. Lab.* **1999**, *31*, 60-67.
- (23) Giakoumaki, A.; Melessanaki, K.; Anglos, D. *Anal. Bioanal. Chem.* **2007**, *387*, 749-760.
- (24) Lopez-Moreno, C.; Palanco, S.; Laserna, J.J.; Delucia, F.; Mikirolek, A.W.; Rose, J.; Walters, R.A.; Whitehouse, A.L.; *J. Anal. At. Spectrosc.* **2006**, *21*, 55-60.
- (25) Castle, B.C.; Talabardon, K.; Smith, B.W.; Winefordner, J.D. *Appl. Spectrosc.* **1998**, *52*, 649-657.
- (26) Chaleard, C.; Mauhien, P.; Andre, N.; Uebbing, J.; Lacour, J.L.; Geertsen, C.; *J. Anal. At. Spectrom.* **1997**, *12*, 183-188.
- (27) Panne, U.; Haisch, C.; Clara, M.; Niessner, R.; *Spectrochim. Acta, Part B.* **1998**, *53B*, 1969-1981.
- (28) Gondal, M. A.; Hussain, T. *Talanta* **2007**, *72*, 642-649.
- (29) Rai, V.N.; Yueh, F.Y.; Singh, J.P. *Appl. Opt* **2003**, *42*, 2094-2101.
- (30) Knopp, R.; Scherbaum, F.J.; Kim, J.I. *Fres. J. Anal. Chem.* **1996**, *355*, 16-20.
- (31) Pichahchy, A.E.; Cremers, D.A. *Spectrochim. Acta* **1997**, *25-39*.
- (32) Caceres, J.O.; Tornero Lopez, J.; Telle, H.H.; Gonzalez Urena, A. *Spectrochim. Acta B* **2001**, *56*, 831-838.
- (33) Neuhauser, R.E.; Panne, U.; Niessner, R. *Anal. Chim. Acta* **1999**, *392*, 47-54.
- (34) Carranza, J.E.; Fisher, B.T.; Yoder, G.D.; Hahn, D.A. *Spectrochim. Acta B* **2001**, *56*, 851-864.
- (35) Panne, U.; Neuhauser, R.E.; Theisen, M.; Fink, H.; Niessner, R.; *Spectrochim. Acta B.* **2001**, *56*, 839-850.

- (36) Radzeimski, L.J.; Loree, T.R.; Cremers, D.A.; Hoffman, N.M. *Anal. Chem.* **1987**, 997-981.
- (37) Kaiser, J.; Samek, O.; Reale, L.; Liska, M.; Malina, R.; Ritucci, A.; Poma, A.; Tucci, A.; Flora, F.; Lai, A.; Mancini, L.; Tromba, G.; Zanini, F.; Faenov, A.; Pikuz, T.; Cinque, G. *Microsc. Res.Tech.* **2007**, 70, 147-153.
- (38) Samek, O.; Lambert, J.; Hergenroeder, R.; Liska, M.; Kaiser, J.; Novotny, K.; Kukhlevsky, S. *Laser Phys. Lett.* **2006**, 3, 21-25.
- (39) Sun, Q.; Tran, M.; Smith, B. W.; Winefordner, J. D. *Can. J. Anal. Sci. Spectros.* **1999**, 44, 164-170.
- (40) Morel, S.; Leone, N.; Adam, P.; Amouroux, J. *Appl. Opt.* **2003**, 42, 6184-6191.
- (41) Haisch, C.; Liermann, J.; Panne, U.; Niessner, R.; *Anal. Chem. Acta*, **1997**, 346, 23.
- (42) Marquardt, B.J.; Goode, S.R.; Angel, S.M. *Anal. Chem.* **1996**, 68, 977-981.
- (43) Kraushaar, M.; Noll, R.; Schmitz, H.-U. *Appl. Spectrosc.* **2003**, 57, 1282-1287.
- (44) Eppler, A.S.; Cremers, D. A.; Hickmott, D.; Ferris, M.; Koskelo, A. *Appl. Spectrosc.* **1998**, 50, 1175-1181.
- (45) Barbini, R.; Colao, F.; Fantoni, R.; Palucci, A.; Capitelli, F. *Appl. Phys. A* **1999**, 69, S175 – S178.
- (46) Bublitz, J.; Dolle, C.; Schade, W.; Hartmann, A.;Horn R. *Euro. J. Soil Sci.* **2001**, 52, 505-312.
- (47) Capitelli, F.; Colao, F.; Provenzano, M.R; Fantoni, R.; Brunetti, G.; Senesi, N. *Gerderma* **2002**, 106, 42-65.
- (48) Gornushkin, I.B.; Kim, J.E.; Smith, B.W.; Baker, S.A.; Winefordner, J.D. *Appl. Spectrosc.* **1997**, 51, 1055-1059.
- (49) Hilbk-Kortenbruck, F.; Noll, R.; Wintjens, P.; Falk, H.; Becker, C. *Spectrochim. Acta: Part B* **2001**, 56, 933-945.
- (50) Wisbrun, R.; Schechter, I.; Niessner, N.; Schroder, H.; Kompa, K. *Anal. Chem.* **1994**, 66, 2964-2975.
- (51) Therlault, G.; Bodensteiner, S.; Lieberman, S. *Field Anal. Chem. Tech.* **1998**, 2, 117-125.
- (52) Knight, A.; Scherbarth, N.; Cremers, D.; Ferris, M. *Appl. Spectrosc.* **2000**, 54, 331- 340.
- (53) Arp, Z.; Cremers, D.; Wiens, R.;Wayne, D.; Salle, B.; Maurice, S. *Appl. Spectrosc.* **2004**, 58, 897 – 909.

- (54) Cremers, D.; Ebinger, M.; Breshears, D.; Unkefer, P.; Kammerdiener, S.; Ferris, M.; Catlett, K.; Brown, J. *J. Environ. Qual.* **2001**, *30*, 2202 – 2206.
- (55) Ebinger, M.H.; Breshears, D.D.; Cremers, D.A.; Unkefer, P.J. Earth and Environmental Sciences, Progress Report, 1998 – 2000
- (56) Ebinger, M.; Lee Norfleet, M.; Breshears, D.; Cremers, D.; Unkefer, P.; Kammerdiener, S.; Ferris, M.; Unkefer, P.; Lamb, M.; Goddard, K.; Meyer, C.; *Am. J. Soil Sc.* **2003**, *67*, 1616 – 1619.
- (57) Martin, M.; Wullschleger, S.; Garten, C.; Palumbo, A. *Appl. Opt.* **2003**, *42*, 2072 – 2077.
- (58) Harris, R.; Martin, M.; Labbe, N.; Ebinger, M.; Clegg, S.; Wullschleger, S. Advances in Calibrating Laser-Induced Breakdown Spectroscopy (LIBS) for Measuring Total Soil Carbon. In *Steps Toward Deployment*, Proceedings of the 5th Carbon Capture & Sequestration Conference, Alexandria, Virginia, May 8-11, 2006.
- (59) Freedman, A.; Wormhoudt, J.C. Portable Soil Carbon Monitor, Aerodyne Research, Inc., Billerica, MA, 2006.
- (60) Bruce, J.; Frome, M.; Haites, E.; Janzen, H.; Lal, R.; Paustian, K. Carbon sequestration in soils. In *Carbon Sequestration in Soils Workshop*, Proceedings of the Soil and Water Conservation Society Meeting, Calgary, Alberta, May 21-22, 1998.
- (61) Sulzman, E.W. *The Carbon Cycle* Global Change Instruction Program, 2000, University Corporation for Atmospheric Research: Boulder, CO.
- (70) *Assessment Methods for Soil Carbon*; Lal, R.; Kimble, J.M.; Follett, R.F.; Stewart, B.A., Eds.; Advances in Soil Sciences; Lewis Publishers: Boca Raton, FL, 1998.
- (71) Izzauralde, R.C.; McGill, W.B.; Bryden, A.; Graham, S.; Ward, M.; Dickey, P. In *Management of Carbon Sequestration in Soil*. Advances in Soil Science; Lal, R Kimble, J.; Follett, J.; Stewart, R. Eds.; Lewis Publishers: Boca Raton, FL, 1998; pp 433-446.
- (72) Charles, J.M.; Simmons, M.S. *Analyst* **1986**, *111*, 385-390.
- (73) Schollenberger, C.J. *Soil Sci.* **1927**, *24*, 65-68.
- (74) Tan, K.H. *Soil Sampling, Preparation, and Analysis*; Marcel Dekker, Inc.: New York, 1996.
- (75) Walkley, A.L.; Black, A. *Soil Sci.* **1947**, *63*, 251-263.
- (76) Viscarra Rosel, R.A.; Walvoort, D.J.J.; McBratney, A.B.; Janik, L.J.; Skjemstad, J.O. *Geoderma* **2006**, *131*, 59-75
- (77) Reeves, J.B.; Follett, R.F.; McCarty, G.W.; Kimble, J.M. *Comm. Soil Sci. Plant Anal.* **2006**, *37*, 2307-2325.

- (78) Wight, J.P.; Allen, F.L.; Zanetti, M.Z.; Rials, T.G. *The Science of Conservation Tillage: Continuing the Discoveries*, Proceedings at the 2005 Southern Conservation Tillage Systems Conference, Clemson University, Florence, SC, May 27-29, 2005.
- (79) Grieve, I.C.; Davidson, D.A.; Ostle, N.J.; Bruneau, P.M.C.; Fallik, A.E. *Soil Biol. Biochem.* **2006**, *38*, 229-234.
- (80) Jian-Bing, W.; Du-Ning, X.; Xing-Yi, Z.; Xiu-Zhen, L.; Xiao-Yu, L. *Environ. Monit. Assess.* **2006**, *121*, 597-613.
- (81) Pye, K.; Blott, S.J.; Croft, D.J.; Carter, J.F. *For. Sci. Int.* **2006**, *163*, 59-80.
- (82) Conklin, A.R. In *Introduction to Soil Chemistry*; Winefordner, J.W.; Ed.; Chemical Analysis: A Series of Monographs on Analytical Chemistry and its Applications; Wiley-Interscience: Hoboken, NJ, 2005; Vol. 2.
- (83) 3M, Foam Mounting Tape MSDS, <http://multimedia.mmm.com/mws/mediawebserver>. accessed July 8, 2007.
- (84) Portnov, A.; Rosenwaks, S.; Bar, I. *Appl. Opt.* **2003**, *42*, 2835 – 2842.
- (85) Wormhoudt, J.; Iannarilli, F.J.; Johnes, S.; Annen, K.D.; Freedman, A. *Appl. Spectrosc.* **2005**, *59*, 1098-1102
- (86) Tran, M.; Sun, Q.; Smith, B.; Winefordner, J.D.; *J. Anal. At. Spectrom* **2001**, *16*, 628-632.
- (87) Acquaviva, S.; De Giorgi, M.L. *J. Phys. B* **2002**, *35*, 795-806.
- (88) Harilal, S.S.; Bindu, C.V.; Issac, R.; Nampoori, V.P.N.; Vallabhan, C.P.G. *J. Appl. Phys.* **1997**, *82*, 2140-2146.
- (89) Aguilera, J.A.; Aragon, C.; Campos, J. *Appl. Spectrosc.* **1992**, *46*, 1382 – 1387.
- (90) St-Onge, L.; Sing, R.; Bechard, S.; Sabsasi, M. *Appl. Phys. A* **1999**, *69*, S913 – S916.
- (91) Locke, R.J.; Morris, J.B.; Forch, B.E.; Miziolek, A.W.; *Appl. Opt.* **1990**, *33*, 4987-4992.
- (92) Vivien, C.; Hermann, J.; Perrone, A.; Boulmer-Leborgne, C.; Luches, A.; *J. Phys D* **1998**, *31*, 1263-1272.
- (93) Ralchenko, Yu., Jou, F.-C., Kelleher, D.E., Kramida, A.E., Musgrove, A., Reader, J., Wiese, W.L., and Olsen, K. (2007). *NIST Atomic Spectra Database* (version 3.1.2), [Online]. Available: <http://physics.nist.gov/asd3> [2007, July 12]. National Institute of Standards and Technology, Gaithersburg, MD.
- (94) Gornushkin, I.B.; Anzano, J.M.; King, L.A.; Smith, B.W.; Omenetto, N.; Winefordner, J.D. *Spectrochim. Acta. B* **1999**, *54*, 491-503.

BIOGRAPHICAL SKETCH

Lydia Edwards was born in Shrewsbury, England, in 1981 and is the oldest of four siblings. In 1994 she moved to Woodbridge, Virginia, with her family and attended C.D. Hylton High School from which she graduated *summa cum laude* in 1999. After attending Northern Virginia Community College and working full-time for one year, she moved to Blacksburg, Virginia, to attend Virginia Tech, where she studied chemistry. Lydia graduated from Virginia Tech in May 2003 with a Bachelors of Science in Chemistry. In August 2003 she enrolled in the chemistry graduate program at the University of Florida in Gainesville, Florida and joined the research group of Dr. James D. Winefordner in the analytical chemistry department. In addition to performing graduate research, she also took classes in Forensic Drug Chemistry and Forensic Toxicology. In August 2007 Lydia completed her doctoral research as well as a Master of Science in Forensic Drug Chemistry. In 2008 she will receive a Master of Science in Forensic Toxicology from the UF Department of Veterinary Sciences. Lydia has been married to Daniel Breckenridge since 2006. She has accepted a position in atomic spectroscopy with Bristol-Myers Squibb in New Brunswick, New Jersey.